(12) INTERNATIONAL APPLICATION PUBLISHED UNDER THE PATENT COOPERATION TREATY (PCT)

(19) World Intellectual Property Organization
International Bureau

(43) International Publication Date
04 January 2024 (04.01.2024)

WIPO | PCT

(10) International Publication Number
WO 2024/006765 A2

(51) International Patent Classification:
C12Q 1/689 (2018.01)

(21) International Application Number:
PCT/US2023/069177

(22) International Filing Date:
27 June 2023 (27.06.2023)

(25) Filing Language: English

(26) Publication Language: English

(30) Priority Data:
63/355,931 27 June 2022 (27.06.2022) US

(71) Applicant: **WISCONSIN ALUMNI RESEARCH FOUNDATION** [US/US]; 614 Walnut Street, Madison, Wisconsin 53726 (US).

(72) Inventors: **GOLDBERG, Tony**; 3610 Sunset Drive, Madison, Wisconsin 53705 (US). **OWENS, Leah**; 1105 McKenna Blvd, Madison, Wisconsin 53719 (US).

(74) Agent: **VANHEYNINGEN, Tambryn** et al.; QUARLES & BRADY LLP, 33 East Main Street, Suite 900, Madison, Wisconsin 53703 (US).

(81) Designated States *(unless otherwise indicated, for every kind of national protection available)*: AE, AG, AL, AM, AO, AT, AU, AZ, BA, BB, BG, BH, BN, BR, BW, BY, BZ, CA, CH, CL, CN, CO, CR, CU, CV, CZ, DE, DJ, DK, DM, DO, DZ, EC, EE, EG, ES, FI, GB, GD, GE, GH, GM, GT, HN, HR, HU, ID, IL, IN, IQ, IR, IS, IT, JM, JO, JP, KE, KG, KH, KN, KP, KR, KW, KZ, LA, LC, LK, LR, LS, LU, LY, MA, MD, MG, MK, MN, MU, MW, MX, MY, MZ, NA, NG, NI, NO, NZ, OM, PA, PE, PG, PH, PL, PT, QA, RO, RS, RU, RW, SA, SC, SD, SE, SG, SK, SL, ST, SV, SY, TH, TJ, TM, TN, TR, TT, TZ, UA, UG, US, UZ, VC, VN, WS, ZA, ZM, ZW.

(84) Designated States *(unless otherwise indicated, for every kind of regional protection available)*: ARIPO (BW, CV, GH, GM, KE, LR, LS, MW, MZ, NA, RW, SC, SD, SL, ST, SZ, TZ, UG, ZM, ZW), Eurasian (AM, AZ, BY, KG, KZ, RU, TJ, TM), European (AL, AT, BE, BG, CH, CY, CZ, DE, DK, EE, ES, FI, FR, GB, GR, HR, HU, IE, IS, IT, LT, LU, LV, MC, ME, MK, MT, NL, NO, PL, PT, RO, RS, SE, SI, SK, SM, TR), OAPI (BF, BJ, CF, CG, CI, CM, GA, GN, GQ, GW, KM, ML, MR, NE, SN, TD, TG).

(54) Title: UNIVERSAL METHOD FOR PARASITE AND EUKARYOTIC ENDOSYMBIONT IDENTIFICATION

FIG. 1A

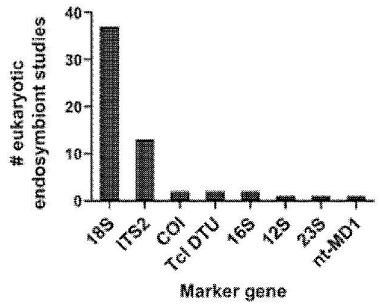

FIG. 1B

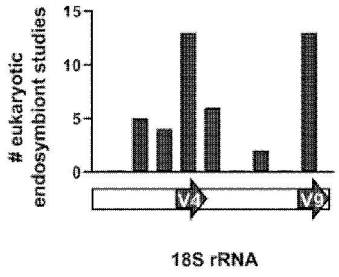

FIG. 1C

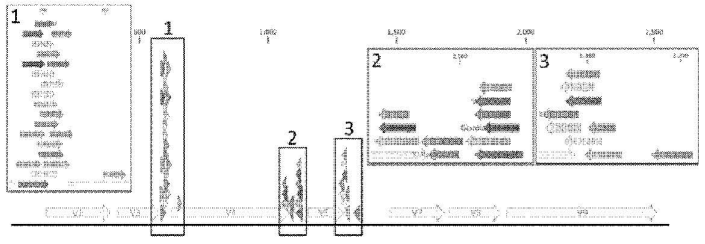

(57) Abstract: The present invention provides methods for detecting eukaryotic endosymbionts in a sample. Primer sets, guide RNAs, and mock communities of eukaryotic endosymbionts for use in these methods are also provided. Further, methods for diagnosing and treating a subject with a parasitic infection are also provided.

[Continued on next page]

WO 2024/006765 A2

Published:

— *without international search report and to be republished upon receipt of that report (Rule 48.2(g))*

— *with sequence listing part of description (Rule 5.2(a))*

UNIVERSAL METHOD FOR PARASITE AND EUKARYOTIC ENDOSYMBIONT IDENTIFICATION

CROSS-REFERENCE TO RELATED APPLICATIONS

This application claims priority to U.S. Provisional Application No. 63/355,931, filed on June 27, 2022, the contents of which are incorporated by reference in their entireties.

STATEMENT REGARDING FEDERALLY SPONSORED RESEARCH

This invention was made with government support under grants AG049395 awarded by the National Institutes of Health. The government has certain rights in the invention.

SEQUENCE LISTING STATMENT

This application includes a sequence listing in XML format titled "960296.04426_ST26.xml", which is 73,899 bytes in size and was created on June 21, 2023. The sequence listing is electronically submitted with this application via Patent Center and is incorporated herein by reference in its entirety.

BACKGROUND

Microbiome research has led to an explosion of knowledge about prokaryotic communities and their influence on host health. However, a parallel revolution for eukaryotic communities has yet to be realized. The field of parasitology, in particular, would benefit from a sequencing-based method for simultaneously characterizing multiple eukaryotic endosymbionts in complex clinical specimens. Currently, parasite diagnostics consist principally of microscopy and single-target assays such as polymerase chain reaction (PCR) and antigen-based tests for known agents. Thus, the parasite diagnostic process is laborious and expensive, and, in the case of microscopy, it relies on the presence of visible organisms or their eggs. Several metabarcoding-based approaches have been developed for parasite detection, but all have serious drawbacks, including lack of parasite taxonomic coverage and high levels of interfering host signal. Accordingly, there remains a need in the art for improved methods for parasite detection.

SUMMARY

In a first aspect, the present invention provides primer sets for amplifying the V4 region of 18S ribosomal RNA (rRNA) genes found in eukaryotic endosymbionts. The primer sets comprise a forward primer comprising a sequence selected from SEQ ID NOs: 1-4 and a reverse primer comprising a sequence selected from SEQ ID NOs: 5-8.

In a second aspect, the present invention provides guide RNAs (gRNAs) that target the V4 region of 18S rRNA genes found in vertebrate organisms. The gRNAs are selected from SEQ ID NOs: 9-14.

In a third aspect, the present invention provides mock communities of eukaryotic endosymbionts comprising 18S rRNA genes, or portions thereof, from a plurality of eukaryotic endosymbionts in equimolar quantities. The plurality of eukaryotic endosymbionts comprises two or more eukaryotic endosymbionts selected from the group consisting of: *Echinorhynchus salmonis* (ES201), *Hymenolopis diminuta* (HD1), *Ascaris suum* (AS1), *Dirofilaria immitis* (DI8), *Trichinella spiralis* (TS3), *Encephalitozoon cuniculi* (EC2), *Entamoeba histolytica* (EH3), *Balamuthia mandrillaris* (BM2), *Naegleria fowleri* (NF12), *Leishmania major* (LM4), *Giardia intestinalis* (GI405), *Plasmodium falciparum* (PF115), *Babesia* sp. (Bab10), *Toxoplasma gondii* (TG3), *Cryptosporidium hominis* (CH109), and *Blastocystis hominis* 1 (ATCC 50177) (BH1).

In a fourth aspect, the present invention provides methods for assessing the ability of a primer set to detect one or more eukaryotic endosymbionts. The methods comprise (a) amplifying a mock community described herein using the primer set; and (b) detecting any resulting amplicons. In these methods, detection of an amplicon associated with a particular eukaryotic endosymbiont (i.e., an amplicon comprising a genomic DNA sequence specific to that eukaryotic endosymbiont) indicates that the primer set is able to detect that particular eukaryotic endosymbiont.

In a fifth aspect, the present invention provides methods for detecting one or more eukaryotic endosymbionts in a sample. The methods comprise (a) extracting DNA from the sample; (b) amplifying the DNA using a primer set described herein to generate amplicons; (c) sequencing the amplicons to generate sequencing reads; and (d) analyzing the sequencing reads. In these methods, the presence of sequencing reads associated with a particular eukaryotic

endosymbiont (i.e., sequencing reads that map to the 18S rRNA gene from that eukaryotic endosymbiont) indicates that that eukaryotic endosymbiont is present in the sample.

In a sixth aspect, the present invention provides methods for diagnosing and treating a subject with a parasitic infection. The methods comprise: (a) obtaining a sample from the subject; (b) extracting DNA from the sample; (c) amplifying the DNA using a primer set described herein to generate amplicons; (e) sequencing the amplicons to generate sequencing reads; (e) analyzing the sequencing reads to detect the presence of a parasite in the sample; and (f) treating the subject for the detected parasite.

In a seventh aspect, the present invention provides kits comprising one or more primer sets described herein and instructions for use. In some embodiments, the kits further comprise a gRNA described herein (i.e., to allow for host DNA depletion) and/or a mock community described herein (i.e., to allow for standardization across experiments and sample types).

BRIEF DESCRIPTION OF THE DRAWINGS

FIGs. 1A-1E show development and evaluation of a new eukaryotic endosymbiont metabarcoding method, termed VESPA (Vertebrate Eukaryotic endoSymbiont and Parasite Analysis). **FIG. 1A -** Histogram of marker genes identified in a literature review of 54 host-associated eukaryotic endosymbiont studies. **FIG. 1B -** Primer sets for amplifying the 18S rRNA gene identified in our literature review, shown as a histogram binned by location along the 18S gene. Hypervariable regions V4 and V9 are demarcated by arrows below the x-axis. **FIG. 1C -** Generalized map of a eukaryotic 18S rRNA gene with hypervariable regions represented as open arrows labeled V2 – V9. Newly designed and published metabarcoding primer sets are shown as colored arrows and the boxed areas 1-3 are expanded as insets. See **Table 5** for full primer names and sequences. **FIG. 1D -** Heat map of published and new 18S V4 primer set coverage across clades exclusively containing parasites of vertebrates. Percent overall complementarity (% coverage) is shown as numbers and as a color scale (color key below heatmap; higher percentage represents lighter color) with taxonomic labels to the left. Red boxes highlight clades with low overall ("problematic") coverage. **FIG. 1E -** Vertebrate endoparasite PCR panel showing amplification (+) or lack of amplification (-) of single-organism genomic DNA templates across new and published primer sets. Total represents the number of successful amplifications per

primer out of 22 possible, shown in left-most "Theoretical" column. Hadz., Hadziavdic. Box highlights a clade with low overall ("problematic") amplification.

FIGs. 2A-2E show testing of metabarcoding methods for amplification bias using a community standard. **FIG. 2A -** Schematic overview of EukMix creation via 18S isolation and cloning. **FIG. 2B -** Equimolar EukMix community standard metabarcoding across primer sets as compared to theoretical input (leftmost bar, blue box) shown as % abundance of reads per organism. The legend is in the same order as the abundance indication. **FIG. 2C -** Equimolar EukMix community standard metabarcoding reads assigned to each component organism shown as mean % abundance of three replicates +/- standard error of the mean (SEM) with theoretical input level of 6.25 % displayed as a horizontal line. ES, *Echinorhynchus salmonis;* HD, *Hymenolepis diminuta;* AS, *Ascaris suum;* DI, *Dirofilaria immitis;* TS, *Trichinella spiralis;* EC, *Encephalitozoon cuniculi;* EH, *Entamoeba histolytica;* BM, *Balamuthia mandrillaris,* NF, *Naegleria fowleri;* LM, *Leishmania major;* GI, *Giardia intestinalis,* PF, *Plasmodium falciparum;* Bab, *Babesia* sp. strain MO1; TG, *Toxoplasma gondii;* CH, *Cryptosporidium hominis;* BH, *Blastocystis hominis.* See **Table 6** for parasite sources and strains. **FIG. 2D -** Mean absolute distance to the theoretical input level for each primer set for three replicates +/- SEM. *P* values are derived from two-tailed Wilcoxon matched-pairs signed rank tests. Owens 29F was significantly different from all other primer sets (shown as bars with asterisks). All comparisons not shown are not significant. **FIG. 2E -** Diversity metrics based on EukMix analysis compared to theoretically equal input (shaded row). Primer set 29F represented the underlying community most accurately by all three metrics (bolded row).

FIGs. 3A-3F show a comparison of VESPA and microscopy using human clinical samples. FIGs. 3A-3C show VESPA metabarcoding data. VESPA data are shown as percent relative abundance of each organism category with all quality-filtered reads included (**FIG. 3A**), with helminth reads only (**FIG. 3B**), or with protozoal reads only (**FIG. 3C**) (archaea, bacteria, host, plants, invertebrates, and fungi are removed in FIG. 3B and FIG. 3C). In FIG. 3A, the numbers above bars are the total percentage of prokaryotic (bacterial + archaeal) reads. **FIG. 3D -** Microscopy versus VESPA. Microscopy findings (M) are shown as a presence/absence (Y = present, N = absent, NA = not assessed) and VESPA metabarcoding (MB) findings are shown as % abundance of quality-filtered reads. Blue cells represent detection by VESPA, green cells by

both VESPA and microscopy, and white cells by neither method. No organisms were identified by microscopy alone. Richness (final 2 rows, shaded cells) is defined as the total number of species detected by the specified method. Prevalence (final 2 columns, shaded cells) is defined as the proportion of the population positive for an organism by the specified method. Note that *Onchocerca* is not detectable in fecal samples by microscopy (asterisk). **FIG. 3E -** Proportional Venn diagrams of findings by microscopy versus VESPA. Individuals identified as positive for the listed organisms by VESPA (blue) or both (green) are shown as numbers in each circle. Overall findings summed over all organisms are shown to the left of the bracket (not to scale). Note that *Onchocerca* is not detectable in fecal samples by microscopy (asterisk). **FIG. 3F -** Richness and prevalence calculations for microscopy (M) and VESPA metabarcoding (MB) findings. Data are shown as mean +/- SEM. *P* values are derived from Wilcoxon matched-pairs signed rank tests, 2-tailed. ns, not significant.

FIGs. 4A-4F show a comparison of VESPA and microscopy using non-human primate clinical samples. FIGs. 4A-4C show VESPA metabarcoding data. VESPA data are shown as percent relative abundance of each organism category with all quality-filtered reads included (**FIG. 4A**), with helminth reads only (**FIG. 4B;** top bar in Fig. 4A), or with protozoal reads only (**FIG. 4C;** second to top bar in Fig. 4A) (archaea, bacteria, host, plants, invertebrates, and fungi are removed in FIG. 4B and FIG. 4C). In FIG. 4A, the numbers above bars are the total percentage of prokaryotic (bacterial + archaeal) reads. In FIG. 4C, the asterisk indicates a microsporidian parasite. **FIG. 4D -** Microscopy versus VESPA. Microscopy findings (M) are shown as a qualitative score (1 least – 3 most) for protozoa, larvae/gram feces for *Strongyloides*, and eggs/gram feces for all other helminths. VESPA findings (MB) are shown as % abundance of quality-filtered reads. Yellow cells represent parasite detection by microscopy, blue cells by VESPA, green cells by both methods, and white cells by neither method. Richness (final 2 rows, shaded cells) is defined as the total number of species detected by the specified method. Prevalence (final 2 columns, shaded cells) is defined as the proportion of the population positive for an organism by the specified method. Note that *Entamoeba histolytica* and *Entamoeba dispar* are a cryptic species complex that cannot be resolved by microscopy (asterisk) and *Piroplasmida* sp. are not detectable in fecal samples by microscopy (double asterisk). **FIG. 4E** - Proportional Venn diagrams of findings by microscopy versus VESPA. Individuals identified as positive for

the listed organisms by microscopy (yellow), VESPA (blue), or both (green) are shown as numbers in each circle. Overall findings summed over all organisms are shown to the left of the bracket (not to scale). Note that *Entamoeba histolytica* and *Entamoeba dispar* are a cryptic species complex that cannot be resolved by microscopy (asterisk) and *Piroplasmida* sp. are not detectable in fecal samples by microscopy (double asterisk). **FIG. 4F -** Richness and prevalence calculations for microscopy (M) and VESPA (MB) findings. Data are shown as mean +/- SEM. *P* values are derived from Wilcoxon matched-pairs signed rank tests, 2-tailed. ns, not significant. NA, not applicable (single data point only).

FIG. 5 shows a comparison of the VESPA primers. Three of the four forward primers are almost entirely overlapping (i.e., 9F, 13F, 2-2bF) and one overlaps with 9 of 18 positions (i.e., 29F). The four reverse primers all contain the same base sequence (i.e., 21b8R) with 4, 5, or 6 additional bases added for compatibility with forward primer melting temperatures (i.e., 21b8R+4, 21b8R+5, and 21b8R+6). Note that the reverse primers are shown in the reverse complement orientation in this figure such that all the primer sequences are going in the same direction.

FIG. 6 demonstrates that certain primer/DNA polymerase combinations work best (i.e., maximize target eukaryotic reads and minimize off-target prokaryotic reads) for amplification of DNA from fecal samples. The percent abundance after quality filtering is shown for target (lighter color green) and off-target (gray) reads.

FIGs. 7A-7B show 18S metabarcoding with peptide nucleic acid (PNA) mammal blocker in nonhuman primate samples. **FIG. 7A -** Percent relative abundance after quality filtering is shown for host reads (Host) and all other reads (Other). Numbers above bars represent percentage abundance of host reads. **FIG. 7B -** Mean relative abundance after quality filtering +/- SEM is shown for host reads (Host) and all other reads (Other). See **Table 12** for source data.

FIGs. 8A-8C show an overview of the CRISPR-Cas9 host digestion method. **FIG. 8A -** Schematic depiction of CRISPR-Cas9 *in vitro* digestion of host amplicons. **FIG. 8B -** Map of representative mammal 18S rRNA gene (green region) from the house mouse (*Mus musculus*; GenBank NR_003278) with locations of 18S amplicon primers (black arrows), newly designed guide RNA (gRNA) sequences (yellow arrows), and published PNA mammal blocker (white arrow). Protospacer adjacent motifs (PAMs) within the host 18S sequence are shown in pink.

gRNAs must bind next to a PAM sequence, and binding determines the location of cleavage by the Cas9 ribonucleoprotein complex. **FIG. 8C** - Schematic of digestion products of mouse 18S V4 amplicons using gRNAs to target various sites. Topmost fragment (no digest) is the full-length host amplicon. Labels to the left are gRNA names. See **Table 13** for gRNA and PAM sequences.

FIG. 9 shows gRNA complementarity to host and eukaryotic endosymbiont groups. Percent coverage of the SILVA 138 Ref NR database is shown with numbers and color scale. Left panel - SILVA TestProbe with the most stringent settings (no mismatches, no N's considered as matches). Right panel - SILVA TestProbe allowing for a single mismatch outside of the conserved seed sequence. Taxonomic groups containing non-target "Host" groups and target "Eukaryotic endosymbiont" groups are shown with representative organism icons to the left of the heatmap. Tetrapoda includes the "Host" groups Amphibia, Aves, Crocodylia, Lepidosauria, Mammalia, and Testudines. Nematoda includes all nematode accessions other than *Trichinella pseudospiralis*. See **Table 13** for gRNA sequences.

FIG. 10 shows *in vitro* CRISPR-Cas9 digests of host and eukaryotic endosymbiont 18S V4 amplicons. Gel electrophoresis images show CRISPR-Cas9 digestion products of 18S V4 DNA amplified from vertebrate hosts (left panel) and eukaryotic endosymbiotic organisms (right panel) with the name of the gRNA in the center. Sources of substrate DNA are shown as organism icons. Black icons represent organisms not cleaved by CRISPR-Cas9 digest with the specified gRNA, and gray icons represent organisms cleaved by CRISPR-Cas9 with the specified gRNA. Organisms used for digest were: Mammalia- *Ursus maritimus* (polar bear), Amphibia- *Lithobates chiricahuensis* (leopard frog), Aves- *Gallus gallus* (chicken), Lepidosauria- *Varanus varius* (monitor lizard), Neopterygii- *Salmo trutta* (brown trout), Amoebazoa- *Entamoeba histolytica,* Excavata- *Trypanosoma brucei,* Microsporidia- *Encephalitozoon cuniculi,* Acanthocephala- *Echinorhynchus salmonis,* Platyhelminthes- *Schistosoma mansoni,* and Nematoda- *Ascaris suum.* Topmost row is a DNA size standard. Note that 18S V4 amplicon length is variable among eukaryotic endosymbionts and that no eukaryotic endosymbiont amplicons were digested using any of the gRNAs tested.

FIGs. 11A-11B show a comparison of host signal reduction with mammal blocking PNA oligo compared to with CRISPR-Cas9 amplicon digestion in 18S V4 metabarcoding. **FIG. 11A -**

Percent abundance of host reads after quality filtering for five DNA samples metabarcoded under four conditions (triplicate mean): no host signal reduction used (None), published mammal-blocking PNA oligo added to amplicon PCR (PNA), CRISPR-Cas9 digest of amplicons (CRISPR-Cas9), and mammal-blocking PNA oligo added to amplicon PCR plus subsequent CRISPR-Cas9 digest of amplicons (PNA + CRISPR-Cas9). Note the scale difference in tissues versus fecal sample. **FIG. 11B -** Results from FIG. 11A displayed as percent change in target (non-host) read abundance as compared to no-treatment control for all non-fecal samples. PNA, published mammal-blocking PNA oligo added to amplicon PCR; CC9, CRISPR-Cas9 digest of amplicons; Both, mammal-blocking PNA oligo added to amplicon PCR plus subsequent CRISPR-Cas9 digest of amplicons. CRISPR-Cas9 treatment is significantly different from PNA (paired t-test: $t = 6.94$, $df = 3$, $P = .0061$) and Both (paired t-test: $t = 8.89$, $df = 3$, $P = 0.0030$). See **Table 14** for source data.

FIGs. 12A-12E show characterization and optimization of CRISPR-Cas9 mediated host signal reduction in 18S V4 metabarcoding. **FIG. 12A -** CRISPR-Cas9 (CC9) reaction optimization. Percent host read abundance (triplicate mean +/- SEM) after quality filtering using varying ribonucleoprotein complex (RNP) to DNA target sequence ratios, where 1X represents a 1:1 ratio. **FIG. 12B -** Identity of high and low molecular weight (MW) CC9 cleavage products. Percent host read abundance (triplicate mean +/- SEM) after quality filtering is shown for high and low MW bands extracted after separation by gel electrophoresis. **FIG. 12C -** Comparison of CC9 digest before and after indexing PCR. Mean percent host read abundance +/- SEM after quality filtering is shown for CC9 digest applied to each amplicon prior to library preparation (Not pooled) or to a single pool of amplicons after library preparation (Pooled). ns, not significant (paired t-test: $t = 1.38$, $df = 30$, $P = 0.18$). **FIG. 12D -** Effect of gRNA sequence on blood sample 18S V4 metabarcoding. Percent host read abundance (triplicate mean +/- SEM) after quality filtering is shown for 18S V4 amplicons that were not treated with any host signal reduction method (None) or digested with CRISPR-Cas9 using the specified gRNA prior to library preparation. See **Table 15** for source data. **FIG. 12E -** Comparison of gRNAs in blood sample metabarcoding. Mean percent host reads abundance +/- SEM after quality filtering is shown for three guide RNAs compared to no digest control. * $P < 0.05$, **** $P < 0.0001$, all

comparisons not shown are insignificant (paired t-test, df = 30 in all comparisons). See **Table 15** for source data.

FIGs. 13A-13B show the effect of host signal reduction method on detection of a known parasite infection. Dog blood infected with *Dirofilaria immitis* microfilariae was used as starting material for DNA extraction and 18S metabarcoding. Amplicons were untreated for host signal reduction (None), amplified with a PNA mammal blocker (PNA), or digested with CRISPR-Cas9 using the specified gRNA (X axis). Percent abundance after quality filtering is shown for all filtered reads (**FIG. 13A**) or reads after removing host sequences (**FIG. 13B**). Numbers above bars represent total percentage host reads (**FIG. 13A**) or total percentage *D. immitis* reads (**FIG. 13B**). Note difference in scale between FIG. 13A and FIG. 13B. See **Table 16** for source data.

FIG. 14 shows the effect of CRISPR-Cas9 host signal reduction on detection of hemoparasite infection in wild non-human primate blood samples. Metabarcoding data are shown as percent read abundance after quality filtering for undigested (left panel) and CRISPR-Cas9 digested (right panel) amplicons using 19 samples. Reads are categorized as host, *Hepatocystis* spp., and all other reads (Other). Numbers above bars represent total % host reads per sample. Legend shows the order of the bars. No *Hepatocystis* spp. positives were detected by metabarcoding in undigested samples. See **Table 17** for source data.

FIG. 15A-15B show the results of performing 18S V9 metabarcoding on non-human primate fecal samples using the Earth Microbiome Project (EMP) protocol. The percent relative abundance of each organism category is shown with all quality-filtered reads included (**FIG. 15A**) and with parasite reads only (**FIG. 15B**) (i.e., archaea, bacteria, environmental sequences, plants, and fungi removed). Note: Sample OI-3 had zero parasite reads and is therefore not included in FIG. 15B. The legends show the order of the bars.

FIG. 16 shows the results of a parasite assessment of non-human primate fecal samples by microscopy and 18S V9 metabarcoding using the EMP protocol. Microscopy findings (M) are shown as a qualitative score (1 least – 3 most) for protozoa, larvae/gram feces for *Strongyloides*, and eggs/gram feces for all other helminths. Metabarcoding findings (MB) are shown as % abundance of quality-filtered reads. Light gray cells represent parasite detection by microscopy, medium gray cells represent parasite detection by metabarcoding, black cells represent parasite detection by both methods, and white cells represent parasite detection by neither method.

Richness (final 2 rows, shaded cells) is defined as the total number of species detected by the specified method.

FIG. 17 shows the results of performing 18S V9 metabarcoding using the EMP protocol on human fecal samples. The percent relative abundance after quality filtering is shown for each organism category detected. Legend shows the order of the bars from top to bottom.

FIG. 18 shows the results of a parasite assessment of human fecal samples by microscopy and 18S V9 metabarcoding using the EMP protocol. Microscopy findings (M) are shown as larvae/gram feces for *Strongyloides* and eggs/gram feces for all other helminths. Metabarcoding findings (MB) are shown as % abundance of quality-filtered reads. Shaded cells represent parasite detection by microscopy and white cells represent parasite detection by neither microscopy nor metabarcoding. Richness (final row, shaded cells) is defined as the total number of species detected by the specified method.

FIG. 19A-19B show a comparison of the results of 18S V4 and 18S V9 metabarcoding of non-human primate fecal samples. The percent relative abundance of each organism category is shown with all quality-filtered reads included (**FIG. 19A**) and with reads from archaea, bacteria, and the host organism as well as uncultured environmental reads removed (**FIG. 19B**). The numbers above the bars in FIG. 19B represent the percentage of reads mapping to helminth organisms. Legends shows the order of the bars from top left to bottom right.

DETAILED DESCRIPTION

The present invention provides methods for detecting eukaryotic endosymbionts in a sample. Primer sets, guide RNAs, and mock communities of eukaryotic endosymbionts for use in these methods are also provided. Further, methods for diagnosing and treating a subject with a parasitic infection are also provided.

The methods of the present invention are methods for metabarcoding eukaryotic endosymbionts, including eukaryotic endoparasites. "Metabarcoding," also referred to as metagenomic barcoding, is a method in which organisms present in a complex sample are identified via amplification and sequencing of a specific portion of a gene that is conserved across the targeted organisms. The resulting sequencing reads are quality-filtered, de-replicated, and compared with reference databases to assign taxonomic identifications. Thus, the

metabarcoding methods allow for the simultaneous identification of many taxa of eukaryotic endosymbionts within the same sample.

As is described in Example 1, the inventors developed their methods after obtaining unsatisfactory results with two published eukaryotic endosymbiont metabarcoding protocols. The published methods did not detect all eukaryotic endosymbionts present in the samples, and the vast majority (> 90 %) of reads produced by these methods were of bacterial or host origin. Like the published metabarcoding protocols, the inventors' method, which they have named VESPA (Vertebrate Eukaryotic endoSymbiont and Parasite Analysis), involves amplifying a target gene and sequencing the resulting amplicons. However, their method utilizes improved polymerase chain reaction (PCR) primers that were designed to amplify the V4 region of the 18S rRNA (18S) gene from all eukaryotic endosymbionts. When tested *in silico*, the inventors' primers amplified DNA from parasites from all 24 clinically relevant parasite clades. In contrast, the primers utilized in the published metabarcoding protocols amplified DNA from an average of only 15.7 of these clades.

To validate their primers *in vitro*, the inventors generated a mock community of eukaryotic endosymbionts. Although there are mock communities of bacteria and yeasts available for standardizing microbiome assays, no equivalent for eukaryotic endosymbionts is commercially available. Thus, the inventors cloned full-length 18S genes from 16 parasitic organisms and combined them in equimolar ratios to create a mock community that is referred to herein as "EukMix". The inventors used this reagent to directly compare the accuracy of their primer sets to that of several high-performing published primer sets. They found that only their primer sets were able to detect all 16 18S genes included in EukMix and that they generated sequencing data that better represented the relative abundances of the underlying eukaryotic endosymbiont community. Additionally, they tested their primer sets against the same published primer sets using fecal samples to assess off-target amplification of bacterial sequences. They found that bacterial read abundance in the data generated using their primers was dramatically lower than in the data generated using the published primers.

In sample types other than feces, most interfering reads are of host origin because primers designed to amplify all eukaryotic endosymbionts will also amplify eukaryotic host DNA. Thus, as is described in Example 3, the inventors developed a method for reducing host signal using

CRISPR-Cas9 *in vitro* digestion. In this method, Cas9 nuclease is targeted to host-specific 18S gene sequences via one of six guide RNAs (gRNAs), and the resulting fragments are purified away by size selection prior to sequencing. Using *in silico* hybridization, they found that their gRNAs did not recognize 18S genes from eukaryotic endosymbionts (with the exception of one nematode worm) but did recognize 18S genes from mammals and other vertebrates. The inventors then tested their gRNAs by performing CRISPR-Cas9 digestion of a panel of genomic DNA isolates, and demonstrated that 18S amplicons from mammals, birds, amphibians, reptiles, and fish are digested by this method while 18S amplicons from eukaryotic endosymbionts remain intact. They compared the efficacy of their method for eukaryotic endosymbiont detection in blood and tissue samples to that of a published protocol that utilizes mammal blocking oligos and found that CRISPR-Cas9 digestion resulted in fewer interfering host reads than the blocking oligo treatment.

Together, this work demonstrates the potential of the inventors' metagenomic barcoding method for identifying eukaryotic endosymbionts in a wide range of host and sample types. Their method is "universal," in that it can detect all eukaryotic endosymbionts simultaneously, whether or not they are visible microscopically. It is also faster, more accurate, more comprehensive, and ultimately has a lower "cost to answer" than any prior method. The inventors envision that this method will be useful for both clinical/veterinary parasite diagnosis and for research on eukaryotic endosymbiont communities in hosts and the environment.

Primers:

In a first aspect, the present invention provides primer sets for amplifying the V4 region of the 18S genes found in eukaryotic endosymbionts. The primer sets comprise a forward primer comprising a sequence selected from SEQ ID NOs: 1-4 and a reverse primer comprising a sequence selected from SEQ ID NOs: 5-8. In Examples 1 and 2, the inventors describe the generation of these primer sets and demonstrate that (1) they can be used to detect parasites from all clinically relevant parasite clades, and (2) that they produce far less off-target amplification than previously published primer sets.

As used herein, a "primer" is a single-stranded DNA oligonucleotide designed to bind to a sequence within or flanking a DNA target sequence via complementary base pairing. DNA polymerases are only capable of adding nucleotides to the 3'-end of an existing nucleic acid.

Thus, the binding of a primer to a DNA template strand creates a site from which DNA polymerase can initiate synthesis of a complementary DNA strand in an amplification reaction. Primers can be chemically synthesized or ordered from commercial vendors.

The primers of the present invention are designed for use in a DNA amplification method. Two primers, i.e., a forward primer and reverse primer, are required for DNA amplification, one for each of the complementary strands of the DNA target sequence. The "forward primer" binds to the anti-sense strand on the 5' end of the target sequence, while the "reverse primer" binds to the sense strand on the 3' end of the target sequence. Thus, the 5' ends of the primers define the termini of the amplified DNA target sequence (i.e., the amplicon). A pair of a forward primer and a reverse primer that is designed to amplify a DNA target sequence is referred to as a "primer set".

In some embodiments, the primers further comprise adapters. Specifically, in some embodiments, the forward primer further comprises a first adapter and the reverse primer further comprises a second adapter. Adapters can be added to primers as demonstrated in the Examples (see, e.g., the VESPA Protocol in Example 1).

As used herein, an "adapter" is a DNA sequence designed to interact with a specific sequencing platform to facilitate a sequencing reaction. For example, in the Illumina sequencing workflow, the adapters contain complementary sequences that allow the DNA fragments to bind to the flow cell. The optimal length of an adapter will vary depending on the sequencing platform used. One of ordinary skill will understand that adapter sequences may be as short as 20 nucleotides or substantially longer. Examples of suitable adapter sequences are disclosed herein as SEQ ID NO: 66 and SEQ ID NO: 67. In some embodiments, the sequencing adapters comprise unique molecular identifier (UMI) sequences, which comprise a sequence label (e.g., a random DNA sequence) that is unique to each DNA molecule to enable its quantification and identification. In some embodiments, the sequencing adapters comprise "barcode" sequences, which are used to label all DNA molecules from a particular sample or source (e.g., DNA from a particular tissue, subject, organism, or environment). The inclusion of barcodes in the adapters allows multiple sequencing libraries to be sequenced simultaneously during a single run, thereby reducing sequencing costs.

Guide RNAs:

In a second aspect, the present invention provides guide RNAs (gRNAs) that target the V4 region of 18S rRNA genes found in vertebrate organisms. These gRNAs are disclosed as SEQ ID NOs: 9-14. In Example 3, the inventors describe the generation of these gRNAs and demonstrate that they can be used to specifically deplete vertebrate 18S sequences via CRISPR-Cas9 digestion. Thus, these gRNAs can be used to increase the efficacy of eukaryotic endosymbiont detection methods by depleting DNA sequences from the host organism.

A "guide RNA (gRNA)" is a single-stranded RNA oligonucleotide that recruits an RNA-guided nuclease to a specific genomic sequence via complementary base pairing.

In some embodiments, the gRNAs are chemically modified. For example, the gRNAs may be chemically modified to decrease a cell's ability to degrade them. Chemically modified gRNAs may include one or more of the following exemplary modifications or others available to those skilled in the art: 2′-fluoro (2′—F), 2′-O-methyl (2′-O—Me), S-constrained ethyl (cEt), 2′-O-methyl (M), 2′-O-methyl-3′-phosphorothioate (MS), and 2′-O-methyl-3′-thiophosphonoacetate (MSP).

The sequences of ribosomal RNA (rRNA) genes, including 16S rRNA, 18S rRNA, and 23S rRNA, are commonly used to identify microorganisms present within a sample since they are found across nearly all forms of life. As is noted above, the primers and gRNAs described herein are designed to target a portion of the small subunit 18S rRNA (18S) gene, which is one of the most commonly used markers for taxonomic identification in eukaryotes.

In Example 3, the inventors demonstrate that the six disclosed gRNAs hybridize to over 50% of mammalian 18S rRNA gene amplicons but fail to hybridize to eukaryotic endosymbiont 18S rRNA gene amplicons. As used herein, the term "amplicon" refers to an amplification product. Thus, an "18S rRNA gene amplicon" is an amplification product generated using an 18S rRNA gene or portion thereof as the DNA template.

The six gRNAs have different specificities. While arb321 (SEQ ID NO: 9) and arb326 (SEQ ID NO: 10) only hybridize to mammalian sequences; arb615 (SEQ ID NO: 11), CA149 (SEQ ID NO: 13), and CA172 (SEQ ID NO: 14) hybridize to mammal, bird, and fish sequences; and PT7.1 (SEQ ID NO: 12) hybridizes to sequences from all tested vertebrates. Thus, for effective vertebrate host DNA depletion, the gRNA should be selected based on the host from which a sample is derived.

As used herein, the term "hybridize" refers to the process in which two complementary single-stranded polynucleotides bind together to form a double-stranded molecule. The term "complementary" refers to the ability of a polynucleotide to bind to (i.e., hybridize with) another nucleic acid molecule through the formation of hydrogen bonds between specific nucleotides (i.e., A with T or U and G with C). Whereas PCR primers can still bind to partially complementary sequences to prime DNA synthesis under some conditions, gRNAs must exactly match an 8-10 base seed sequence within the target sequence to be able to bind to the active site of the nuclease. The target sequence must additionally contain a 3-5 base protospacer adjacent motif (PAM) to be recognized and cleaved by the nuclease, which further increases target specificity and limits the number of possible sites for gRNA targeting.

Mock communities:

In a third aspect, the present invention provides mock communities of eukaryotic endosymbionts. The mock communities comprise 18S rRNA genes, or portions thereof, from a plurality of eukaryotic endosymbionts in equimolar quantities. The plurality of eukaryotic endosymbionts comprises two or more eukaryotic endosymbionts selected from the group consisting of: *Echinorhynchus salmonis* (ES201), *Hymenolopis diminuta* (HD1), *Ascaris suum* (AS1), *Dirofilaria immitis* (DI8), *Trichinella spiralis* (TS3), *Encephalitozoon cuniculi* (EC2), *Entamoeba histolytica* (EH3), *Balamuthia mandrillaris* (BM2), *Naegleria fowleri* (NF12), *Leishmania major* (LM4), *Giardia intestinalis* (GI405), *Plasmodium falciparum* (PF115), *Babesia* sp. (Bab10), *Toxoplasma gondii* (TG3), *Cryptosporidium hominis* (CH109), and *Blastocystis hominis* 1 (ATCC 50177) (BH1).

As used herein, a "mock community" is a mixture of polynucleotides that was created *in vitro* to simulate the polynucleotides that would be isolated from a community of eukaryotic endosymbionts. The mock communities of the present invention may comprise nucleic acids from about 2-50 different eukaryotic endosymbionts, preferably from about 5-20 eukaryotic endosymbionts. In the Examples, the inventors combined nucleic acids from 16 different eukaryotic endosymbionts (i.e., ES201, HD1, AS1, DI8, TS3, EC2, EH3, BM2, NF12, LM4, GI405, PF115, Bab10, TG3, CH109, and BH1) to form the mock community referred to herein as "EukMix". These 16 eukaryotic endosymbionts were selected such that they cover the taxonomic range of clinically important parasitic organisms (i.e., protozoan, worm, and

microsporidian). Thus, in some embodiments, the mock community comprises polynucleotides from these 16 specific eukaryotic endosymbionts.

EukMix, which is depicted schematically in **FIG. 2A**, comprises an equimolar mix of 16 different plasmids, each of which contain the full-length 18S rRNA gene from one of the 16 eukaryotic endosymbionts noted above. Thus, in some embodiments, each 18S rRNA gene or portion thereof included in the mock community is provided as part of a plasmid. A "plasmid" is a small circular DNA molecule that can replicate independently from chromosomal DNA.

The mock communities disclosed herein can be used to assess the ability of a primer set to detect one or more eukaryotic endosymbionts, as described in the following section. Additionally, the mock communities disclosed herein can be used as a positive control (i.e., to allow for standardization across experiments and sample types) in the methods for detecting eukaryotic endosymbionts and the methods for treating parasitic infections discussed below.

Methods for assessing primers:

In a fourth aspect, the present invention provides methods for assessing the ability of a primer set to detect one or more eukaryotic endosymbionts. The methods comprise (a) amplifying a mock community described herein using the primer set; and (b) detecting any resulting amplicons. In these methods, detection of an amplicon associated with a particular eukaryotic endosymbiont (i.e., an amplicon comprising a genomic DNA sequence specific to that eukaryotic endosymbiont) indicates that the primer set is able to detect that particular eukaryotic endosymbiont.

Notably, in embodiments in which a known amount of template DNA is used, these methods can also be used to assess the quantitative potential of the assay (i.e., by comparing the number of copies of template DNA to the number of reads produced therefrom).

The term "amplification" refers to a template-dependent process that results in an increase in the concentration of a DNA molecule relative to its initial concentration. A "template-dependent process" is a process in which the sequence of the newly synthesized DNA molecule is dictated by the rules of complementary base pairing. The amplification step of the present methods can be performed using any amplification method known in the art. Exemplary amplification methods include polymerase chain reaction (PCR), loop-mediated isothermal amplification (LAMP), strand displacement amplification (SDA), ligase chain reaction (LCR),

and transcription-mediated-amplification (TMA). However, in preferred embodiments, the amplification step is performed using PCR.

PCR is an *in vitro* method used to selectively amplify a specific DNA target sequence in a sample. PCR employs two main reagents: primers and a DNA polymerase. In PCR, a repeated series of reaction steps (i.e., template denaturation, primer annealing, and extension of the annealed primers by DNA polymerase) results in exponential amplification of the target sequence. See Saiki et al., 1985, Science 230:1350 for a detailed description of PCR.

PCR is commonly performed using a "reaction mixture" that comprises template DNA (typically 1-1000 ng) and at least about 25 pmol of each primer. The reaction mixture must also include deoxynucleotide triphosphates (dNTPs) and a DNA polymerase. For example, a typical reaction mixture might include: 2 µl of template DNA, 25 pmol of each primer, 2.5 µl of a suitable buffer, 0.4 µl of 1.25 µM dNTP, 2.5 units of DNA polymerase, and deionized water to a total volume of 25 µl. The reaction mixture may include additional reagents such as a GC enhancer to increase amplification specificity. In the methods of the present invention, the template DNA is eukaryotic endosymbiont genomic DNA and the primers comprise a forward primer selected from SEQ ID NOs: 1-4 and a reverse primer selected from SEQ ID NOs: 5-8. The template DNA may also be derived from a sample obtained from a subject.

A "DNA polymerase" is an enzyme that catalyzes the polymerization of DNA. The polymerase initiates synthesis starting at the 3'-end of the primers annealed to the target sequence, and proceeds in the 5'-direction along the template DNA. Known DNA polymerases for use in PCR methods include, without limitation, *E. coli* DNA polymerase I, T7 DNA polymerase, Thermus thermophilus (Tth) DNA polymerase, *Bacillus stearothermophilus* DNA polymerase, *Thermococcus litoralis* DNA polymerase, *Thermus aquaticus* (Taq) DNA polymerase, and *Pyrococcus furiosus* (Pfu) DNA polymerase. Many suitable Taq polymerases are commercially available including, for example, HotStarTaq™ DNA Polymerase, Platinum™ II Taq Hot-Start DNA Polymerase, AmpliTaq™ DNA Polymerase, FastStart™ Taq DNA Polymerase, and TaKaRa Ex Taq™ DNA Polymerase. In the Examples, the inventors determined that the Platinum™ II Taq Hot-Start DNA Polymerase worked better than several other polymerases for amplification of eukaryotic endosymbiont 18S rRNA gene sequences from

fecal samples. Thus, in some embodiments, the polymerase is Platinum™ II Taq Hot-Start DNA Polymerase.

PCR is performed using a programmable thermal cycler. The length and temperature of each step of a PCR cycle, as well as the number of cycles, are adjusted according to the stringency requirements of the particular reaction. Annealing temperature and timing are determined both by the efficiency with which a primer is expected to anneal to the template DNA and by the degree of mismatch (i.e., between the primer and template DNA) that can be tolerated. The ability to optimize the stringency of primer annealing conditions is well within the knowledge of one of ordinary skill in the art. An annealing temperature of between 30° C and 72° C is typically used. An initial denaturation of the template molecules is normally performed for a period of time (e.g., for 4 minutes) at between 92° C and 99° C, followed by 20-40 cycles consisting of a denaturation step (94-99° C for 15 seconds to 1 minute), annealing step (temperature determined as discussed above; 30 seconds-2 minutes), and extension step (72° C for 1 minute). An optional final extension step is generally carried out for 4 minutes at 72° C, and may be followed by an indefinite (0-24 hour) hold at 4° C.

Following amplification, any resulting amplicon is detected. Detection may be performed using any method known in the art. Suitable methods for detecting an amplicon include, without limitation, gel electrophoresis, sequencing (e.g., Sanger sequencing, single-molecule sequencing, high-throughput sequencing, pyrosequencing), restriction fragment length polymorphism (RFLP) analysis, and quantitative PCR (qPCR).

Methods for detecting eukaryotic endosymbionts:

In a fifth aspect, the present invention provides methods for detecting one or more eukaryotic endosymbionts in a sample. The methods comprise (a) extracting DNA from the sample; (b) amplifying the DNA using a primer set described herein to generate amplicons; (c) sequencing the amplicons to generate sequencing reads; and (d) analyzing the sequencing reads. In these methods, the presence of sequencing reads associated with a particular eukaryotic endosymbiont (i.e., sequencing reads that map to the 18S rRNA gene from that eukaryotic endosymbiont) indicates that the eukaryotic endosymbiont is present in the sample.

The methods of the present invention allow for detection of eukaryotic endosymbionts. As used herein, the term “eukaryotic endosymbionts” includes all non-fungal eukaryotes residing

within vertebrate hosts. This term includes both microscopic eukaryotes (e.g., microsporidia, protozoa, algal parasites) and macroscopic metazoans (e.g., helminths, pentastomes). The prefix "endo" is meant include endoparasites and commensals, while excluding ectoparasites (e.g., mites, ticks, fleas).

As noted above, the term eukaryotic endosymbiont encompasses eukaryotic endoparasites. A "parasite" is an organism that lives in or on an organism of another species (its host) and derives benefits at the other organism's expense. Eukaryotic endoparasites include protozoans, helminths (worms), and microsporidians. Thus, in some embodiments, the methods of the present invention are used to detect parasites or diagnose parasitic diseases.

In step (a) of the present methods, DNA is extracted from the sample. "DNA extraction" is a process in which DNA is separated from cell membranes, proteins, and other cellular components using physical and/or chemical methods. DNA can be extracted using various methods that are well known in the art, including those that rely on organic extraction, ethanol precipitation, silica-binding chemistry, cellulose-binding chemistry, and ion exchange chemistry. Many reagents and kits for DNA extraction are commercially available.

In step (b), the DNA is amplified using a primer set described herein. As is discussed above, any method of DNA amplification may be used with the present methods. However, in preferred embodiments, the DNA is amplified via PCR.

In step (c), the amplicons are sequenced to generate sequencing reads. DNA sequencing is the process of determining the order of nucleotides in a DNA molecule. Any DNA sequencing method may be used with the present invention. Suitable methods include, for example, Sanger sequencing, Illumina sequencing, single molecule real time (SMRT) sequencing, Nanopore DNA sequencing, massively parallel signature sequencing (MPSS), Polony sequencing, 454 pyrosequencing, combinatorial probe anchor synthesis (cPAS), Ion Torrent semiconductor sequencing, DNA nanoball sequencing, and SOLiD sequencing.

For methods that utilize a high-throughput sequencing method, the amplicons must be converted into a sequencing library for sequencing. A "sequencing library" is a pool of DNA fragments that include adapters. Thus, in these embodiments, the methods may further comprise (a) fragmenting the amplicons, and/or (b) adding adapters to the amplicons. Methods of generating sequencing libraries are well known in the art. Adapters must be included in or added

to the amplicons to allow them to interact with a high-throughput sequencing platform. In some embodiments, adapters are included in the primers disclosed herein such that the adapters are added to the amplicons during the DNA amplification step. In other embodiments, adapters are ligated to the amplicons following the DNA amplification step using a ligase enzyme.

In step (d), the sequencing reads are analyzed. DNA sequencing produces sequencing reads, i.e., sequences of the DNA fragments present in the sequencing library as determined by the sequencer. To analyze the sequencing reads, they are first cleaned up (e.g., trimmed, filtered for quality, de-noised to limit the impact of sequencing errors, de-replicated to reduce file size). Without further analysis, the resulting sequences lack genomic context. Thus, to determine the source of a read (i.e., organism from which the sequenced DNA fragment was derived), it must be mapped to a reference database. Methods for mapping sequencing reads to reference databases are available in the form of free tools, including mothur, QIIME, and various R packages.

Any type of sample may be tested for the presence of eukaryotic endosymbionts using the methods of the present invention. Suitable samples include, but are not limited to, clinical samples (e.g., blood, serum, plasma, mucus, urine, feces, saliva, tissue), environmental samples (e.g., soil, plant, water), food samples (e.g., meat, dairy, produce), and the like.

Methods for treating parasitic infections:

In a sixth aspect, the present invention provides methods for diagnosing and treating a subject with a parasitic infection. The methods comprise: (a) obtaining a sample from the subject; (b) extracting DNA from the sample; (c) amplifying the DNA using a primer set described herein to generate amplicons; (d) sequencing the amplicons to generate sequencing reads; (e) analyzing the sequencing reads to detect the presence of a parasite in the sample; and (f) treating the subject for the detected parasite.

As used herein, a "parasitic infection" is an illness caused by a parasite. Symptoms of parasitic infections may include fever, fatigue, intestinal symptoms, skin rashes, or neurological symptoms. Parasites are commonly acquired by eating contaminated food or undercooked meat, drinking contaminated water, touching contaminated surfaces, and bug bites.

In these methods, the sample is a biological sample obtained from a subject. Exemplary subject samples include stool, peripheral blood, sera, plasma, ascites, urine, cerebrospinal fluid,

sputum, saliva, bone marrow, synovial fluid, aqueous humor, amniotic fluid, cerumen, breast milk, bronchoalveolar lavage fluid, semen, prostatic fluid, Cowper's fluid or pre-ejaculatory fluid, female ejaculate, sweat, fecal matter, hair, tears, cyst fluid, pleural and peritoneal fluid, pericardial fluid, lymph, chyme, chyle, bile, interstitial fluid, menses, pus, sebum, vomit, vaginal secretions, mammary secretions, mucosal secretion, stool, stool water, pancreatic juice, lavage fluids from sinus cavities, bronchopulmonary aspirates, blastocoel cavity fluid, umbilical cord blood, a skin swab sample, a throat swab sample, a genital swab sample, and an anal swab sample. However, in preferred embodiments, the sample is a blood sample or fecal sample. In some embodiments, the sample is suspected of containing a parasite.

In the Examples, the inventors found that a primer set comprising the forward primer of SEQ ID NO: 3 and the reverse primer of SEQ ID NO: 6 works best for amplifying18S gene sequences from fecal samples. Thus, in some embodiments, the sample is a fecal sample and the primer set comprises the forward primer of SEQ ID NO: 3 and the reverse primer of SEQ ID NO: 6.

The "subject" that is diagnosed and treated using these methods may be any vertebrate animal, including fish, birds, mammals, amphibians, and reptiles. Examples of suitable mammals include, but are not limited to, humans, cows, horses, sheep, pigs, goats, rabbits, dogs, cats, bats, mice, and rats. In certain embodiments, the methods may be performed on lab animals (e.g., mice, rats) for research purposes. In other embodiments, the methods are used to treat commercially important farm animals (e.g., cows, horses, pigs, rabbits, goats, sheep, chickens) or companion animals (e.g., cats, dogs). In some embodiments, the subject is suspected of having a parasitic infection. In preferred embodiments, the subject is a human.

In step (f) of the methods, the subject is treated for the detected parasite. As used herein, "treating" or "treatment" describes the management and care of a subject for the purpose of combating a parasitic infection. Treatments include methods or medications that prevent the onset of the symptoms or complications, alleviate the symptoms or complications, or eliminate the parasitic infection. Suitable treatments for parasitic infections include antiparasitic, antifungal, and antibiotic drugs. Specific examples of antiparasitic drugs include albendazole, mebendazole, metronidazole, and tinidazole. Other treatments for parasitic infections include physical interventions such as fluid aspiration, surgical removal of parasites, or resection of

affected tissues. Treatment often includes prevention of re-infection using approaches such as vector control, environmental treatment, prophylactic drug administration, and behavioral modification.

Depletion of host DNA:

In many samples, sequencing reads of host origin crowd out reads from eukaryotic endosymbionts. Thus, in some embodiments, the methods of the present invention further comprise adding an RNA-guided nuclease and a gRNA described herein to digest host DNA (or amplicons generated therefrom) prior to sequencing. The RNA-guided nuclease and gRNA may be added (1) to DNA extracted from the sample prior to the amplification step, or (2) to the amplicons produced via the amplification step prior to the sequencing library preparation step, or (3) to the sequencing library prior to the sequencing step. In this additional step, the RNA-guided nuclease is targeted to non-parasitic 18S gene sequences via the gRNA(s), and the resulting fragments are purified away by size selection prior to sequencing. Because these gRNAs specifically target non-parasitic 18S sequences and leave eukaryotic endosymbiont 18S sequences intact, this additional step can be used to increase the efficacy of eukaryotic endosymbiont detection by depleting host DNA present in the sample. In Example 3, the inventors demonstrate that the gRNAs disclosed herein are capable of digesting 18S sequences from mammals, birds, amphibians, reptiles, and fish. Thus, this additional step may be used to deplete host DNA from any vertebrate organism. This extra step may be added to any of the methods provided herein in advance of the amplification step.

As used herein, a "RNA-guided nuclease" is a nuclease that cleaves DNA/RNA and is targeted to specific DNA/RNA sequences via a gRNA. An RNA-guided nuclease can be an endonuclease or an exonuclease and can be naturally occurring or engineered. Examples of RNA-guided nucleases include Cas9, Cpf1, Cas3, Cas8a-c, Cas10, Cas13, Cas14, Cse1, Csy1, Csn2, Cas4, Csm2, Cm5, Csf1, C2c2, CasX, CasY, Cas14, and NgAgo. The RNA-guided nuclease can be from any bacterial or archaeal species. For example, in some embodiments, the RNA-guided nuclease is from *Streptococcus pyogenes, Staphylococcus aureus, Neisseria meningitidis, Streptococcus thermophiles, Treponema denticola, Francisella tularensis, Pasteurella multocida, Campylobacter jejuni, Campylobacter lari, Mycoplasma gallisepticum, Nitratifractor salsuginis, Parvibaculum lavamentivorans, Roseburia intestinalis, Neisseria*

cinerea, Gluconacetobacter diazotrophicus, Azospirillum, Sphaerochaeta globus, Flavobacterium columnare, Fluviicola taffensis, Bacteroides coprophilus, Mycoplasma mobile, Lactobacillus farciminis, Streptococcus pasteurianus, Lactobacillus johnsonii, Staphylococcus pseudintermedius, Filifactor alocis, Legionella pneumophila, Suterella wadsworthensis Corynebacter diphtheria, Acidaminococcus, Lachnospiraceae bacterium, or *Prevotella.*

Advantages:

In Example 1, the inventors determined (via an *in silico* analysis) that their primers amplify the 18S gene from eukaryotic endosymbionts in all 24 clinically relevant parasite clades, i.e., Acanthocephala, Cestoda, Trematoda, Ascaridida, Oxyurida, Rhabditida, Spirurida, Dorylaimia, Microsporidia, Dermocystidium, Entamoeba, Centramoebida, Leishmania, Trypanosoma, Giardia, Trichomonadea, Plasmodium, Babesia, Eimeria, Sarcocystis, Toxoplasma, Cryptosporidium, Balantidium, and Blastocystis (see **FIG. 1D**). Thus, in some embodiments, the methods of the present invention are capable of detecting eukaryotic endosymbionts from these 24 clinically relevant clades.

Additionally, in Example 1, the inventors demonstrate that their method produces less than 50% off-target reads (see **FIG. 3A** and **FIG. 4A**). Thus, in some embodiments, less than 50% of the sequencing reads produced by the methods of the present invention are off-target reads. As used herein, the term "off-target reads" refers to sequencing reads produced from DNA from organisms other than eukaryotic endosymbionts (e.g., bacterial DNA and vertebrate DNA).

Kits:

In a seventh aspect, the present invention provides kits comprising one or more primer sets described herein and instructions for use. In some embodiments, the kits further comprise a gRNA described herein (i.e., to allow for host DNA depletion) and/or a mock community described herein (i.e., to allow for standardization across experiments and sample types).

Additionally, the kits may include additional reagents for use in a DNA extraction reaction, an amplification reaction (e.g., a DNA polymerase, dNTPs, amplification buffer), or a DNA sequencing reaction (e.g., adapters). As noted above, the adapters may be part of the primers or put another way the primers may include sequencing adapter or barcoding portions when supplied as part of the kit to allow for easy use of the kit and to minimize steps in the methods.

The present disclosure is not limited to the specific details of construction, arrangement of components, or method steps set forth herein. The compositions and methods disclosed herein are capable of being made, practiced, used, carried out and/or formed in various ways that will be apparent to one of skill in the art in light of the disclosure that follows. The phraseology and terminology used herein is for the purpose of description only and should not be regarded as limiting to the scope of the claims. Ordinal indicators, such as first, second, and third, as used in the description and the claims to refer to various structures or method steps, are not meant to be construed to indicate any specific structures or steps, or any particular order or configuration to such structures or steps. All methods described herein can be performed in any suitable order unless otherwise indicated herein or otherwise clearly contradicted by context. The use of any and all examples, or exemplary language (e.g., "such as") provided herein, is intended merely to facilitate the disclosure and does not imply any limitation on the scope of the disclosure unless otherwise claimed. No language in the specification, and no structures shown in the drawings, should be construed as indicating that any non-claimed element is essential to the practice of the disclosed subject matter. The use herein of the terms “including,” “comprising,” or “having,” and variations thereof, is meant to encompass the elements listed thereafter and equivalents thereof, as well as additional elements. Embodiments recited as “including,” “comprising,” or “having” certain elements are also contemplated as “consisting essentially of” and “consisting of” those certain elements.

Recitation of ranges of values herein are merely intended to serve as a shorthand method of referring individually to each separate value falling within the range, unless otherwise indicated herein, and each separate value is incorporated into the specification as if it were individually recited herein. For example, if a concentration range is stated as 1% to 50%, it is intended that values such as 2% to 40%, 10% to 30%, or 1% to 3%, etc., are expressly enumerated in this specification. These are only examples of what is specifically intended, and all possible combinations of numerical values between and including the lowest value and the highest value enumerated are to be considered to be expressly stated in this disclosure. Use of the word “about” to describe a particular recited amount or range of amounts is meant to indicate that values very near to the recited amount are included in that amount, such as values that could or naturally would be accounted for due to manufacturing tolerances, instrument and human

error in forming measurements, and the like. All percentages referring to amounts are by weight unless indicated otherwise.

No admission is made that any reference, including any non-patent or patent document cited in this specification, constitutes prior art. In particular, it will be understood that, unless otherwise stated, reference to any document herein does not constitute an admission that any of these documents forms part of the common general knowledge in the art in the United States or in any other country. Any discussion of the references states what their authors assert, and the applicant reserves the right to challenge the accuracy and pertinence of any of the documents cited herein. All references cited herein are fully incorporated by reference, unless explicitly indicated otherwise. The present disclosure shall control in the event there are any disparities between any definitions and/or description found in the cited references.

The following examples are meant only to be illustrative and are not meant as limitations on the scope of the invention or of the appended claims.

EXAMPLES

Example 1:

In the following example, the inventors describe the development of an improved sequencing-based method for detecting eukaryotic endosymbionts. They demonstrate that this method can be used to recognize all major groups of vertebrate endoparasites while amplifying relatively few off-target sequences.

Introduction:

Microbiomes are multi-kingdom assemblages of microorganisms and their entire "theater of activity" including signaling molecules and metabolites[1]. Such communities have emergent properties arising from cross-species and cross-kingdom interactions[2]. One of the most salient examples is the human gut, wherein bacterial community dynamics have direct effects on health[3] and can be manipulated to improve disease outcomes in clinical settings[4]. Evidence is mounting that assemblages of host-associated eukaryotes also form communities with important consequences for host health[5], although they are far less studied compared to their bacterial, archaeal, and fungal counterparts[6]. Even terminology to describe host-associated eukaryotes is lacking. "Eukaryotic microbiome/microbiota"[7] does not include host-associated macro-

organisms such as helminths, "nemabiome"[8] is limited to nematodes, and "parasites"[9] excludes commensal/beneficial organisms and includes ectoparasites. Herein we use the term "eukaryotic endosymbionts" to refer to both microscopic eukaryotes (microsporidia, protozoa, algal parasites) and macroscopic metazoans (helminths, pentastomes). In this context, we use the prefix "endo" to include endoparasites and commensals, while excluding ectoparasites (mites, ticks, fleas). We exclude fungi because of their fundamentally different life histories[10] and the fact that established methods already exist for assessing the "mycobiome"[11]. However, we include microsporidia, because their life cycles are considered more similar to protozoa than to fungi[12].

Well-established methods exist to study eukaryotic endosymbiotic organisms. Microscopic observation has been an essential tool since van Leeuwenhoek first described *Giardia* in the seventeenth century[13]. Combined with subsequent advances in staining and enrichment techniques, microscopy is still a gold standard method[14], although it requires specialized training[15] and has inherent resolution limits (i.e., some species cannot be distinguished solely based on morphology, a phenomenon known as "cryptic species complexes"[16]). For example, the genus *Entamoeba* contains pathogenic *E. histolytica* and benign *E. dispar* which appear identical under the microscope[17]. More recently developed molecular assays (e.g., PCR and DNA sequencing of amplicons) have enabled finer taxonomic differentiation, including strain-level identification of species complexes[18]. Although extremely useful, such assays usually have high DNA sequence specificity and are therefore not suitable for characterizing diverse assemblages of eukaryotic endosymbionts.

Methods for characterizing bacterial and fungal assemblages are standardized and based on massively parallel sequencing of amplified marker genes, or metagenomic barcoding (henceforth metabarcoding)[19]. For bacteria, the 16S ribosomal RNA (16S rRNA, or just 16S) locus[20] and for fungi, the internal transcribed spacer (ITS) locus[21] are proven targets for metabarcoding. By contrast, "universal" targets and protocols for metabarcoding of eukaryotic endosymbionts are not standardized[6]. For example, some published methods utilize PCR primer sets originally designed for free-living eukaryotic microbes[22-25], some target metazoans only[26,27], while others focus exclusively on helminths[8,28-30] or gut-associated organisms[31-33]. There is also a conspicuous absence of published comparisons to "gold standard" methods such as

microscopy[34]. Moreover, no commercially available reagents exist for assessing the accuracy of eukaryotic endosymbiont metabarcoding-based methods. Community standards (mixtures of organisms or their genetic material in known composition and quantity) have been important for standardizing microbiome protocols and are commercially available[35]. Unfortunately, no such standard exists for eukaryotes other than fungi.

Here we present VESPA (Vertebrate Eukaryotic endoSymbiont and Parasite Analysis), a new methodology for eukaryotic endosymbiont metabarcoding that resolves the issues described above. We compare VESPA to published methods *in silico* and using a new community standard comprised of cloned DNA from eukaryotic endosymbiont lineages across the Tree of Life. We then compare our new method to the "gold standard" of microscopy using clinical samples. Our results show that VESPA and our community standard constitute a major advance that should enable "microbiome-like" insights into the structure and function of vertebrate-associated eukaryotic endosymbiont communities.

Rationale:

Our goal at the outset of this work was to establish a eukaryotic endosymbiont metabarcoding pipeline as an alternative to standard methods of microscopy and group-specific PCR for use in ongoing studies. Several eukaryotic endosymbiont metabarcoding studies had already been published, so we chose one such protocol and validated it in our lab. To validate the protocol, we used DNA isolated from a set of non-human primate fecal samples, which had been previously characterized by microscopy as part of a completed study (n = 10). By microscopic examination, all 10 samples contained at least 1 protozoan organism (total population richness = 5) and 9 of 10 contained at least one helminth (total population richness = 8). We used the Earth Microbiome Project (EMP; mSystems 3(3), 2018) protocol to amplify the hypervariable 9 region (V9 hereafter) of the 18S small subunit ribosomal RNA gene (18S hereafter) and sequence the resulting amplicon libraries. Specifically, we used the forward primer 1391f (GTACACACCGCCCGTC; SEQ ID NO: 80) and the reverse primer EukBr (TGATCCTTCTGCAGGTTCACCTAC; SEQ ID NO: 81). The majority of the reads obtained using the EMP protocol (total mean reads after quality filter = 33,513 per sample, range: 4,222 – 126,119) were identified as from bacteria or archaea (prokaryotic read mean = 96.1 % per sample, range: 84. 5 % – 99.7 %; **FIG. 15A**). The finding of off-target 16S prokaryotic reads was

not unexpected based on published results. Nonetheless, this result was not ideal because, in such high numbers, these off-target reads can introduce bias and mask the presence of rarer organisms. In total, six parasitic/commensal protozoans were identified including three subtypes of *Blastocystis* (**FIG. 15B**) and the average protozoan richness per sample was similar between the two methods (average richness by microscopy = 3.0, average richness by metabarcoding = 3.2; **FIG. 16**, top panel). Unexpectedly, for helminths, despite an average sample richness by microscopy of 1.5, no helminths were detected by metabarcoding (**FIG. 16**, bottom panel).

To further investigate the preponderance of prokaryotic sequences and lack of helminth coverage, we performed 18S V9 metabarcoding using the EMP protocol on a more common sample type, human fecal samples (n = 11), which were previously characterized for soil-transmitted helminths (total population richness = 5) as part of a concluded study. Similarly, the majority of the reads obtained (total mean reads after quality filter = 11,018 per sample, range: 2,320 – 20,053) were bacterial or archaeal in origin (prokaryotic read mean = 71.5 % per sample, range: 39.3 % - 96.9 %) and very few helminth reads were detected **(FIG. 17)**. Several annotated sequence variants (ASVs) were identified in the QIIME2 pipeline as Rhabditiform nematodes but were later re-classified as archaeal sequences based on BLAST analysis. No correctly classified helminth reads were numerous enough to pass the quality-filtering threshold of 0.01% total reads per sample, in contrast to microscopy findings in which helminth prevalence was 0.7 and mean richness was 1.5 (range: 1 - 3, **FIG. 18**).

It was possible that the high number of off-target reads was masking the presence of less-abundant target reads (i.e., helminths), so we hypothesized that a different method that results in fewer prokaryote reads would yield more target identifications. We chose a set of 18S hypervariable region 4 (V4 hereafter) primers, i.e., forward primer E572F and reverse primer E1009R (see **Table 5** for primer sequences) that had been used in studies on fecal samples with no reports of issues with prokaryotic reads and performed metabarcoding using this protocol alongside the EMP protocol for comparison. As starting material, we used non-human primate fecal samples (n = 5) that were known to contain both protozoan and helminth parasites. Because it was possible that our previous sequencing depth was not sufficient to detect less abundant organisms, we sequenced more deeply than in previous experiments (total mean reads after quality filter = 64,081 per sample, range: 8,201 – 109,545). Generally, V9 primer data tended to

include more archaeal sequences and V4 primer data more bacterial sequences, but in both cases the majority of reads were identified as off-target amplification of prokaryotic origin (V4 prokaryotic read mean = 72.0 % per sample, range: 50.5 % - 94.2 %; V9 prokaryotic read mean = 75.4 % per sample, range: 57.4 % - 91. 5 %; **FIG. 19A**). After filtering out the reads from prokaryotes, uncultured environmental sequences, and the host organism, the remaining reads were dominated by fungal, plant, and protozoal sequences with very few helminth reads (V4 helminth read mean = .26 % per sample, range: 0 % - 0.96 % per sample, prevalence = 0.4; V9 helminth read mean = .62 % per sample, range: 0 % - 2.48 % per sample, prevalence = 0.6; **FIG. 19B**), despite our expectation that all samples would contain at least one helminth.

In view of the unsatisfying results generated using these published methods, we performed an extensive literature review to identify additional methods for eukaryotic endosymbiont metabarcoding and we ultimately designed our own method.

Results:

Here we compile and evaluate published methods for metabarcoding vertebrate-associated eukaryotic endosymbionts and choose a marker gene and region for amplification. We then compare the relevant subset of published methods to a new method of our own design in a progressive series of experiments. We begin with *in silico* PCR, proceed to amplification of single parasite DNA templates, and then conduct metabarcoding using an engineered mock community standard. We finally apply the best-performing protocol to clinical samples from humans and non-human primates and compare results to those obtained with microscopy.

Methods review and new method design

In a literature review consisting of 54 papers that used amplicon sequencing (metabarcoding) to characterize eukaryotic assemblages in vertebrate hosts, we identified eight marker genes, including 16S (n = 1), nt-MD1 (n = 1), 12S (n = 1), mitochondrial 16S (n = 1), 28S (n = 1), mini-exon Tcl DTU (n = 2), CO1 (n = 2), ITS-2 (n = 13), and 18S (n = 37; **FIG. 1A**). Of these publications, 25 targeted specific sub-groups (e.g., nematodes or trypanosomes) and 29 used a pan-parasite/commensal approach. Based on the widespread incorporation of small subunit ribosomal RNA 18S gene (18S hereafter) sequences into databases, the standardized use of the counterpart prokaryotic 16S gene for bacterial metabarcoding, and evidence that non-protein coding genes outperform protein-coding genes as metabarcoding markers[36], we chose to

pursue 18S as our marker gene.

18S contains hypervariable regions V1 - V9, and the regions that were most commonly targeted in the studies reviewed were V4 (n = 13) and V9 (n = 13; **FIG. 1B**). The 18S V4 region has the highest entropy within the size limits of MiSeq v2 chemistry[37] and therefore the highest taxonomic resolution for this commonly used metabarcoding platform, so we chose to target this region. We identified a total of 22 published sets of V4 primers. Additionally, we created new 18S V4 primers designed to target all eukaryotic endosymbionts, consisting of 4 candidate forward primers and one reverse primer (see methods section for details on primer design, **Table 5** for primer sequences, and **FIG. 1C** for a map of primer binding sites).

Testing metabarcoding methods for taxonomic coverage using in silico PCR

Testing all 22 published 18S V4 primer sets *in silico* yielded an average eukaryotic endosymbiont coverage of 64.9 % (**Table 1,** bolded columns). No primer set recognized both *Plasmodium* and *Giardia*, and 9 of 19 did not recognize either (**Table 1,** final two columns). We found significant off-target coverage (> 5 %) of bacterial and/or archaeal groups for 4 of 22 sets (**Table 1,** asterisks), and the primer set with the highest overall eukaryotic coverage (96.3 %; Hugerth 2014 "563/1132") also had the highest coverage of archaea and bacteria (47.9 % and 72.0 % respectively; **Table 1**). Primer sets with > 5 % off-target coverage were not analyzed further.

In silico PCR including our 4 new primer sets alongside the remaining 18 published 18S V4 sets yielded coverage data spanning a wide range (5.8 % to 98.0 %; **Table 2**). Across target groups (normalizing by eligible accessions), our newly designed primers had the highest mean percent coverage, at 95.2 % - 96.8 %, and the best complementarity as evidenced by the lowest score in a rank sum analysis (**Table 2**, final column).

Table 1. *In silico* taxonomic coverage for published 18S V4 primer sets

		Off-target groups		**Eukaryotic endosymbiont groups**		Specific examples	
	n =	20,197	381,535	4,229	15,265	198	23
Reference ID	Primers	Archaea	Bacteria	**Helminths**	**Protozoa**	*Plasmodium*	*Giardia*
Bates 2012	515f/1119r	0	0	**80.4**	**95.9**	94.8	0
Bower 2004*	18SEUK581F/1134R	46.2*	8.2*	**0.4**	**82.4**	0	72.7
Bradley 2016	TAReuk454F1/V4r	0	0	**48.9**	**67.1**	97.9	0
Cavalier-Smith 2009, Brate 2010	3NDf/V4_euk_R2	0	0	**50.8**	**22.8**	0	0
Cavalier-Smith 2009, Brate 2010	3NDf/V4_euk_R1	0	0	**5.8**	**21.1**	0	0
Cavalier-Smith 2009, Giesen 2010	3NDf/1132mod	0.3	0	**80.7**	**94.2**	0	0
Comeau 2011	E572F/E1009R	0	0	**65.3**	**44.5**	0	0
DeMone 2020**	18SV4_F/-R	0	0	**86.4**	**62.3**	42.8	0
Hadziavdic 2014	F-566/R-1200	0	0	**76.4**	**81**	99.6	0
Hadziavdic 2014	F-574/R-952	0	0	**48.3**	**62.9**	61.3	0
Hugerth 2014*	574/1132	12.5*	0	**80**	**94.2**	0	0
Hugerth 2014	616/1132	3.3	0.2	**93.1**	**75.8**	0	45.5
Hugerth 2014*	563/1132	47.9*	72*	**96.1**	**96.4**	0	100
Krogsgaard 2018**	G31/G43/G61	0	0	**78.5**	**67**	94.8	0
Machida 2012	18S#1/#2RC	0	0	**78.1**	**45.2**	97.9	0
Sikder 2020*	MMSF/R	17.5*	0	**79.3**	**42.7**	0	0
Stoeck 2010	TAReuk454F1/R3	0	0	**49.1**	**78.4**	97.9	0
Wood 2013	Nem18SFlong/R	0	0	**32.2**	**25.2**	2.6	0
Zhan 2013	Uni18S/R	0	0	**72.8**	**64**	0	100

Numbers shown are % coverage allowing for 1 mismatch with a 2-base pair 3' window using the SILVA 138.1 SSU rRNA NR Ref database; n, number of total eligible accessions; * removed from further analysis due to high prokaryotic complementarity; ** multiple primer sets were combined for analysis.

Table 2. *In silico* taxonomic coverage of helminths and protozoa for published and newly designed 18S V4 primer sets

Short ID	Primers	**Mean**	n = 3,097 Helminths	n = 2,913 Protozoa	Rank Helminths	Rank Protozoa	**Rank sum**
Owens- 29F	29F/21b8R	**96.8%**	95.5%	98.0%	1	1	**2**
Owens- 2-2b	2-2F/21b8R	**96.4%**	94.9%	97.9%	2	2	**4**
Owens- 13F	13F/21b8R	**96.4%**	94.9%	97.9%	2	2	**4**
Owens- 9F	9F/21b8R	**95.2%**	94.4%	96.0%	4	4	**8**
Bates	515f/1119r	**88.2%**	80.4%	95.9%	8	5	**13**
Hugerth	616/1132	**84.5%**	93.1%	75.8%	5	8	**13**
Krogsgaard**	G3/G4/G6	**81.0%**	93.0%	69.0%	6	9	**15**
Hadziavdic- 566	F-566-R-1200	**78.7%**	76.4%	81.0%	10	6	**16**
DeMone**	18SV4F/R/GR	**75.3%**	86.4%	64.1%	7	11	**18**
Stoeck	TAReukF1/R3	**63.8%**	49.1%	78.4%	13	7	**20**
Machida	18S#1/18S#2	**61.7%**	78.1%	45.2%	9	14	**23**
Bradley	TAReukF1/V4r	**58.0%**	48.9%	67.1%	14	10	**24**
Hadziavdic- 574	F-574/R-952	**55.6%**	48.3%	62.9%	15	12	**27**
Comeau	E572F/E1009R	**54.9%**	65.3%	44.5%	11	15	**26**
C-S/Giesen*	3NDf/1132	**47.5%**	40.7%	54.2%	16	13	**29**
C-S/Brate- 2*	3NDf/V4eukR2	**36.8%**	50.8%	22.8%	12	17	**29**
Wood*	Nem18SFl/Rl	**28.7%**	32.2%	25.2%	17	16	**33**
Zhan*	Uni18S/UniR	**14.0%**	5.7%	22.3%	19	18	**37**
C-S/Brate- 1*	3NDf/V4eukR1	**13.5%**	5.8%	21.1%	18	19	**37**

Shaded rows, primers designed in this study; %, % coverage calculated allowing for 1 mismatch with a 2-base pair 3' window using the SILVA 138 SSU rRNA NR Ref database; n, number of eligible accessions; Mean, mean coverage of all parasite/commensal groups; * < 50 % overall mean target complementarity; ** multiple primer sets combined for analysis.

In silico coverage analysis using finer-resolution groups (**FIG. 1D**) showed that our new primers consistently amplified (defined as coverage of 50 % or higher) all 24 clades of eukaryotes tested whereas no other primer sets did. Particularly problematic were *Giardia* (recognized by our primers and one other set in which a second reverse primer must be used to specifically amplify *Giardia*), *Microsporidia* (recognized by our primers and two other sets), and *Trichomonadea* (recognized by our primers and three other sets; **FIG. 1D,** red boxes). All methods that amplified an overall mean < 50 % of target sequences (n=5; **Table 2**, asterisks) or that required > 1 primer set (n=2; **Table 2**, double asterisks) were not analyzed further.

Testing metabarcoding methods for on-target amplification using purified DNA

In PCR amplification of genomic DNA (gDNA) from 22 individual eukaryotic endosymbiont organisms (**Table 6**), all four sets of candidate primers amplified more organisms than did any of the published primer sets (Owens 29F: 22 of 22, Owens 2-2bF: 21 of 22, Owens 13F: 20 of 22, Owens 9F: 20 of 22), followed by the Bates (19 of 22), Hadziavdic (18 of 22), and Stoeck (16 of 22) sets (**FIG. 1E**). Furthermore, two of the new sets were the only primers to successfully amplify 18S V4 from *Giardia* gDNA (Owens 29F and Owens 2-2bF), as expected based on *in silico* data (**FIG. 1E,** row 17).

Testing metabarcoding methods for amplification bias using a community standard

Community standards are not available for eukaryotic endosymbionts, so we collected protozoa (n = 10), helminths (n = 5), and a microsporidian (n = 1) (**Table 7**) from various sources (e.g., specimen repositories, veterinary post-mortem examinations). We then isolated 18S genes from these samples and mixed them at an equimolar ratio to create a community standard, which we named "EukMix" (**FIG. 2A**). Metabarcoding EukMix as input with previously published and newly designed primers allowed us to directly compare empirical read abundances for each organism to their predicted (equal) abundances (**FIG. 2B**). The abundances of six organisms were underestimated by every primer set, and the abundances of three organisms were overestimated by every primer set (**Table 3**), but the absolute mean difference from theoretically equal abundance was lowest with newly designed primer set Owens 29F (**FIG. 2C**), which also yielded abundance data statistically significantly closer to actual input levels than any other set tested (**FIG. 2D**). Primer set Owens 29F consistently reconstructed the EukMix community most accurately (i.e., evenly), as determined by standard diversity and

evenness measures (Pielou's species evenness, Simpson's diversity index, and Shannon diversity; **FIG. 2E**).

Table 3. Equimolar EukMix metabarcoding accuracy metrics

		Mean distance from the theoretical by primer set					Estimated abundance pattern
		Owens 29F	Owens 2-2bF	Stoeck TAREuk	Hadziavdic F-566	Bates 515f	
1	*Echinorhynchus salmonis*	-1.12%	-1.36%	1.71%	1.48%	4.77%	mixed
2	*Hymenolepis diminuta*	4.09%	4.75%	0.39%	5.51%	5.88%	over
3	*Ascaris suum*	2.48%	7.13%	9.48%	8.08%	11.28%	over
4	*Dirofilaria immitis*	0.66%	-1.91%	2.14%	4.39%	0.15%	mixed
5	*Trichinella spiralis*	-0.57%	-3.40%	-6.22%	-5.91%	-5.84%	under
6	*Encephalitozoon cuniculi*	-0.14%	-0.92%	3.56%	1.72%	4.12%	mixed
7	*Entamoeba histolytica*	-1.75%	-1.34%	-4.67%	-1.56%	-2.86%	under
8	*Balamuthia mandrillaris*	0.00%	4.11%	11.05%	3.26%	-1.18%	mixed
9	*Naegleria fowleri*	1.03%	2.03%	0.98%	-5.41%	-3.86%	mixed
10	*Leishmania major*	-1.41%	-1.84%	-6.25%	-6.15%	-4.72%	under
11	*Giardia intestinalis*	-2.69%	-3.09%	-5.58%	-1.43%	-2.57%	under
12	*Plasmodium falciparum*	-1.02%	-5.32%	-4.84%	-3.39%	-6.18%	under
13	*Babesia* sp. strain MO1	-0.98%	-4.12%	-6.22%	-5.78%	-6.04%	under
14	*Toxoplasma gondii*	-0.80%	-4.93%	1.27%	-1.73%	0.18%	mixed
15	*Cryptosporidium hominis*	1.48%	4.23%	4.72%	10.62%	6.40%	over
16	*Blastocystis hominis*	0.73%	2.59%	-1.53%	-3.71%	0.45%	mixed

VESPA compared to microscopy

Human VESPA analysis of 12 human clinical samples yielded high-quality data (**Table 4**) including low proportions of off-target prokaryotic reads (**FIG. 3A**) and host reads (host read mean = 2.97 % per sample, range: 0.11 % - 17.4 %) and correspondingly high proportions of endosymbiont reads (**FIG. 3B, FIG. 3C**).

Table 4. VESPA MiSeq run metrics

Library ID	Sample type	Raw reads	Reads post-quality filter	% lost in filter
Human01	Human fecal	62,512	56,602	9.45%
Human02	Human fecal	32,755	30,195	7.82%
Human03	Human fecal	223,911	206,999	7.55%
Human04	Human fecal	43,371	39,228	9.55%
Human05	Human fecal	116,016	106,130	8.52%
Human06	Human fecal	24,095	22,204	7.85%
Human07	Human fecal	55,882	50,772	9.14%
Human08	Human fecal	80,184	72,324	9.80%
Human09	Human fecal	35,824	32,808	8.42%
Human10	Human fecal	30,176	27,645	8.39%
Human11	Human fecal	78,021	72,165	7.51%
Human12	Human fecal	123,564	112,774	8.73%
NHP1	Nonhuman primate fecal	37,377	35,637	4.65%
NHP2	Nonhuman primate fecal	98,953	92,910	6.11%
NHP3	Nonhuman primate fecal	287,932	269,181	6.51%
NHP4	Nonhuman primate fecal	56,002	52,080	7.00%
NHP5	Nonhuman primate fecal	28,351	26,874	5.21%
NHP6	Nonhuman primate fecal	104,900	97,907	6.67%
NHP7	Nonhuman primate fecal	28,409	26,415	7.02%
NHP8	Nonhuman primate fecal	25,764	23,788	7.67%
NHP9	Nonhuman primate fecal	29,434	27,018	8.21%
NHP10	Nonhuman primate fecal	58,005	53,206	8.27%
NHP11	Nonhuman primate fecal	44,422	39,862	10.26%
NHP12	Nonhuman primate fecal	36,887	33,991	7.85%
NHP13	Nonhuman primate fecal	55,101	49,958	9.33%

NHP14	Nonhuman primate fecal	34,701	31,934	7.97%
NHP15	Nonhuman primate fecal	64,954	60,237	7.26%
NHP16	Nonhuman primate fecal	50,839	47,371	6.82%
NHP17	Nonhuman primate fecal	75,005	68,826	8.24%
NHP18	Nonhuman primate fecal	76,770	70,964	7.56%
NHP19	Nonhuman primate fecal	46,543	44,239	4.95%
NHP20	Nonhuman primate fecal	40,031	37,507	6.31%
NHP21	Nonhuman primate fecal	39,344	36,571	7.05%
NHP22	Nonhuman primate fecal	29,797	27,118	8.99%
NHP23	Nonhuman primate fecal	36,615	33,891	7.44%
NHP24	Nonhuman primate fecal	84,056	76,577	8.90%
NHP25	Nonhuman primate fecal	27,672	26,198	5.33%
NHP26	Nonhuman primate fecal	32,150	28,996	9.81%
NHP27	Nonhuman primate fecal	157,483	144,045	8.53%
NHP28	Nonhuman primate fecal	31,830	29,320	7.88%
NHP29	Nonhuman primate fecal	41,127	37,816	8.05%
NHP30	Nonhuman primate fecal	60,491	55,710	7.90%
NHP31	Nonhuman primate fecal	74,435	67,968	8.69%
NHP32	Nonhuman primate fecal	59,136	54,146	8.44%
NHP33	Nonhuman primate fecal	35,473	32,346	8.82%
NHP34	Nonhuman primate fecal	39,545	36,508	7.68%
NHP35	Nonhuman primate fecal	33,505	31,048	7.33%
NHP36	Nonhuman primate fecal	44,082	41,003	6.98%
NHP37	Nonhuman primate fecal	59,451	54,867	7.71%
NHP38	Nonhuman primate fecal	14,879	13,872	6.77%
NHP39	Nonhuman primate fecal	71,275	64,595	9.37%
NHP40	Nonhuman primate fecal	62,042	57,199	7.81%

VESPA successfully identified all three helminth and seven protozoan taxa identified with microscopy (**FIG. 3D**) and found these taxa in more individuals than did microscopy, with 61.4 % of positive samples identified solely by VESPA (**FIG. 3E**). Conversely, no positives were identified by microscopy alone. Four additional taxa were found exclusively by VESPA, including one helminth, *Trichuris trichuria* (1 positive of 12 samples), and three protozoa, *Entamoeba hartmanni* (10 positives of 12 samples), *Enteromonas hominis* (3 positives of 12

samples), and *Pentatrichomonas hominis* (1 positive of 12 samples). Three of 12 patients were known by taxon-specific PCR to be infected with *Onchocerca,* which is not visible microscopically in feces, and all 3 were positive by VESPA. Overall, taxonomic richness was statistically significantly higher by VESPA than by microscopy for both helminths (mean richness = 0.5 by microscopy, 1.92 by VESPA, Wilcoxon matched-pairs signed rank test, 2-tailed, $P = 0.001$) and protozoa (mean richness = 2.33 by microscopy, 5.67 by VESPA, Wilcoxon matched-pairs signed rank test, 2-tailed, $P = 0.0005$; **FIG. 3F,** left panel). Prevalence was also higher by VESPA for helminths (mean prevalence = 0.25 by microscopy, 0.60 by VESPA, Wilcoxon matched-pairs signed rank test, 2-tailed, $P = 0.25$) and protozoa (mean prevalence = 0.23 by microscopy, 0.54 by VESPA, Wilcoxon matched-pairs signed rank test, 2-tailed, $P = 0.002$; **FIG. 3F,** right panel).

Non-human primate VESPA analysis of 40 non-human primate clinical samples yielded high-quality sequencing reads (**Table 4**) with low proportions of off-target prokaryotic reads (**FIG. 4A**) and host sequence reads (host read mean = 3.2 % per sample, range: 0 % - 18.49 %) and correspondingly high proportions of endosymbiont reads (**FIG. 4B, FIG. 4C**).

VESPA successfully identified all eight helminth and six protozoan taxa identified with microscopy (**FIG. 4D**) and found these taxa in more individuals than did microscopy, with 47.08 % of positive samples identified by VESPA only (**FIG. 4E**). One positive out of 29 total for a helminth (*Physaloptera* sp. 1) and 2 positives out of 28 total for a protozoan (*Balantidium coli)* were identified by microscopy only. Six additional taxa were found exclusively by VESPA: *Entamoeba chattoni* (16 positives of 40 samples), *Endolimax nana* (19 positives of 40 samples), *Enteromonas* sp. (6 positives of 40 samples), *Piroplasmida* sp. (2 positives of 40 samples), *Blastocystis* sp. (38 positives of 40 samples), and *Enterocytozoon bieneusi* (3 positives of 40 samples; **FIG. 4D, FIG. 4E**). *Piroplasmida* are intraerythrocytic parasites not visible in fecal samples and were found in 2 of 40 samples with VESPA. Thirty-one samples were positive for the *Entamoeba histolytica/dispar* species complex by microscopy and the same 31 samples were found to be positive by VESPA but could be further taxonomically resolved as *Entamoeba dispar* in all cases. Richness was higher by VESPA than by microscopy for helminths (mean richness = 1.73 by microscopy, 2.13 by VESPA, Wilcoxon matched-pairs signed rank test, 2-tailed, $P = 0.0009$), protozoa (mean richness = 2.8 by microscopy, 5.5 by VESPA, Wilcoxon

matched-pairs signed rank test, 2-tailed, $P < 0.0001$), and microsporidia (mean richness = 0 by microscopy, 0.08 by VESPA, Wilcoxon matched-pairs signed rank test, 2-tailed, $P = 0.25$; **FIG. 4F,** left panel). Prevalence was also higher by VESPA than by microscopy for all three parasite groups (helminth mean prevalence = 0.22 by microscopy, 0.26 by VESPA, Wilcoxon matched-pairs signed rank test, 2-tailed, $P = 0.33$; protozoa mean prevalence = 0.22 by microscopy, 0.43 by VESPA, Wilcoxon matched-pairs signed rank test, 2-tailed, $P = 0.002$; microsporidia mean prevalence = 0 by microscopy, 0.8 by VESPA, Wilcoxon matched-pairs signed rank test, 2-tailed, $P = 0.25$; **FIG. 4F,** right panel).

Discussion:

To identify a single method for the "universal" identification of vertebrate-associated eukaryotic endosymbionts in community assemblages, we analyzed published approaches and found a wide range of amplification targets and protocols. From this literature review, we chose to focus on the 18S V4 locus and designed new primers to recognize all known groups of eukaryotic endosymbionts. We then tested published primers and our newly designed primers in a series of experiments *in silico* and *in vitro* to determine which protocols, if any, could accurately reconstruct eukaryotic endosymbiont communities. Our results clearly show that metabarcoding using newly designed primer set 29F recognizes the greatest range of endosymbionts of interest with the least off-target amplification and PCR bias of any method tested. We named our new method VESPA (Vertebrate Eukaryotic endoSymbiont and Parasite Analysis).

VESPA recognized more eukaryotic endosymbiont groups *in silico* than did other published methods tested, including methods that used multiple primer sets to increase coverage. Multiple primer sets, usually involving multiple independent PCR amplifications, are a feasible strategy for increasing coverage[32,33]. However, this approach adds reagent costs and presents technical challenges related to sequencing and bioinformatics[38,39]. Our single primer set approach should therefore reduce barriers to entry for adopting our new method. We then corroborated these *in silico* results with amplification of purified targets and similarly found that our primer sets amplified the greatest range of single organisms *in vitro*.

To examine the performance of published methods and VESPA, we directly compared assays by using an equimolar community standard, EukMix, as input for metabarcoding. Results

from VESPA reflected the underlying composition of the community standard more accurately than did results from other assays. The EukMix community standard should be useful for quality control in laboratories choosing to adopt our method, and for standardization and validation, much as community standards containing bacteria and fungi have enabled standardization of microbiome protocols[35,40]. We note that the relationship between sequencing reads and organism abundance or biomass is complicated by wide variation in 18S copy number among eukaryotic endosymbionts[34,41]. Copy number corrections have been applied in studies of other systems[42,43], and such corrections could prove useful for investigations where quantifying organism abundance or biomass are the desired outputs.

Compared to microscopic examination, VESPA detected protozoa, microsporidia, and helminths in more individuals, identified additional organisms, resolved a cryptic species complex, and identified organisms not visible in fecal samples. We suspect that the greater sensitivity of VESPA results from the nature of molecular amplification – namely, that PCR can detect a theoretical minimum of one molecule of target DNA[44]. Microscopy-negative samples that were PCR positive by VESPA may not have contained intact organisms or their eggs or may even have been positive by virtue of the presence of small amounts of cell-free DNA[45]. In this light, we caution that our method will likely be most useful for applications where the presence of eukaryotic endosymbiont DNA is itself taxonomically informative, regardless of whether that DNA represents an intact or viable organism.

Because of the labor-intensive nature of microscopy and its dependence on trained experts, VESPA will also be useful for studies which are large-scale or performed in multiple laboratories, where labor costs and inter-observer variability would otherwise be impractical. In this light, we note that microscopy identified three positive samples not identified by VESPA in non-human primates. We suspect that these findings may represent microscopy false positives, especially because these two taxa (*Physaloptera* and *Balantidium*) are notoriously difficult to identify morphologically[46,47].

Our contribution with this work is a publicly available protocol for metabarcoding eukaryotic endosymbiont communities that outperforms published methods by every measure examined. VESPA is intentionally designed to have broad applicability, from microbial ecology to parasitology to clinical diagnostics. Although we tested VESPA using Illumina sequencing

technology, it should be readily adaptable to other amplicon sequencing technologies available now and in the future. VESPA is compatible with existing bacterial and fungal pipelines, with metabarcoding of all three taxa run on the same sequencing platform. Addition of VESPA to established protocols for characterizing bacterial microbiomes and mycobiomes could have far reaching benefits. For example, it has been suggested that studies of the human gut microbiome should routinely incorporate analyses of eukaryotic diversity in order to capture overall microbial community function[5]. VESPA can provide this missing eukaryotic component and thereby enable cross-kingdom characterization of microbial ecosystem structure and function, opening new avenues for basic and applied research.

Materials and Methods:

Methods review and new method design

Literature searches were performed in January 2021 and updated in January 2023. Search terms or combinations of search terms including "Metagenomics," "Metagenomic barcoding," "Metabarcoding," "Targeted amplicon deep sequencing," "Eukaryotic microbiome," "Gastrointestinal," "Gut," "Parasite," and "18S" were used to query PubMed, Web of Science, and Google Scholar. Results were manually evaluated for relevance and details were compiled in an excel spreadsheet. We identified 96 studies including reviews and methods papers, 54 of which were primary research on vertebrate-associated eukaryotes. We chose to focus on 18S because in previous metabarcoding studies, non-coding genes outperformed coding genes[36,48], 18S has islands of conserved sequence interspersed with areas of high entropy (hypervariable regions), allowing broad priming for coverage and diverse amplicons for resolution[49], and database coverage for 18S is higher than for other loci[50]. Of the 9 hypervariable 18S regions, V4 has the highest taxonomic resolution[37], so we focused on this region and identified 22 sets of published V4 primers (**Table 5**).

Table 5. 18S primers used in this study

Primer Name	Reference	F/R/B	Sequence (5′ – 3′)	SEQ ID NO:	Region
E572F	Comeau 2011	F	CYGCGGTAATTCCAGCTC	15	V4
E1009R	Comeau 2011	R	AYGGTATCTRATCRTCTTYG	16	V4
PNA mammal block	Mann 2020	B	TCTTAATCATGGCCTCAGTT	17	V4
515f	Bates 2012	F	GTGCCAGCMGCCGCGGTAA	18	V4
1119r	Bates 2012	R	GGTGCCCTTCCGTCA	19	V4
18S-EUK581-F	Bower 2004	F	GTGCCAGCAGCCGCG	20	V4
18S-EUK1134-R	Bower 2004	R	TTTAAGTTTCAGCCTTGCG	21	V4
TAReuk454FWD1	Stoeck 2010	F	CCAGCASCYGCGGTAATTCC	22	V4
TAReukREV3	Stoeck 2010	R	ACTTTCGTTCTTGATYRA	23	V4
V4r	Bradley 2016	R	ACTTTCGTTCTTGAT	24	V4
3NDf	Cavalier-Smith 2009	F	GGCAAGTCTGGTGCCAG	25	V4
V4_euk_R1	Brate 2010	R	GACTACGACGGTATCTRATCRTCTTCG	26	V4
V4_euk_R2	Brate 2010	R	ACGGTATCTRATCRTCTTCG	27	V4
18SV4_F	DeMone 2020	F	GCCGCGGTAATTCCAGCTC	28	V4
18SV4_R	DeMone 2020	R	ATYYTTGGCAAATGCTTTCGC	29	V4
Giardia 18SV4_R	DeMone 2020	R	ATACGGTGGTGTCTGATCGC	30	V4
F-566	Hadziavdic 2014	F	CAGCAGCCGCGGTAATTCC	31	V4
R-1200	Hadziavdic 2014	R	CCCGTGTTGAGTCAAATTAAGC	32	V4
F-574	Hadziavdic 2014	F	GCGGTAATTCCAGCTCCAA	33	V4
R-952	Hadziavdic 2014	R	TTGGCAAATGCTTTCGC	34	V4
616	Hugerth 2014	F	TTAAARVGYTCGTAGTYG	35	V4
574	Hugerth 2014	F	CGGTAAYTCCAGCTCYV	36	V4

563	Hugerth 2014	F	GCCAGCAVCYGCGGTAAY	37	V4
1132	Hugerth 2014	R	CCGTCAATTHCTTYAART	38	V4
G3F1	Krogsgaard 2018	F	GCCAGCAGCCGCGGTAATTC	39	V4
G3R1	Krogsgaard 2018	R	ACATTCTTGGCAAATGCTTTCGCAG	40	V4
G4F3	Krogsgaard 2018	F	AGCCGCGGTAATTCCAGCTC	41	V4
G4R3	Krogsgaard 2018	R	GGTGGTGCCCTTCCGTCAAT	42	V4
G6F1	Krogsgaard 2018	F	TGGAGGGCAAGTCTGGTGCC	43	V4
G6R1	Krogsgaard 2018	R	TACGGTATCTGATCGTCTTCGATCCC	44	V4
18S#1	Machida 2012	F	CTGGTGCCAGCAGCCGCGGYAA	45	V4
Machida 2012	Machida 2012	R	TCCGTCAATTYCTTTAAGTT	46	V4
MMSF	Sikder 2020	F	GGTGCCAGCAGCCGCGGTA	47	V4
MMSR	Sikder 2020	R	CTTTAAGTTTCAGCTTTGC	48	V4
Nem18SlongF	Wood 2013	F	CAGGGCAAGTCTGGTGCCAGCAGC	49	V4
Nem18SlongR	Wood 2013	R	GACTTTCGTTCTTGATTAATGAA	50	V4
9F	This study	F	CTGGTGCCAGCAGCCGCGG	1	V4
13F	This study	F	TGGTGCCAGCAGCCGCGG	2	V4
29F	This study	F	AGCAGCCGCGGTAATTCC	3	V4
2-2bF	This study	F	TGGTGCCAGCASCCGCG	4	V4
21b8R+4	This study	R	TCCGTCAATTYCTTNAASTTTC*	6	V4
EukA_F	Medlin 1988	F	AACCTGGTTGATCCTGCCAGT	51	5' terminus
EukB_R	Medlin 1988	R	TGATCCTTCTGCAGGTTCACCTAC	52	3' terminus
1520_R	Lopez-Garcia 2003	R	CYGCAGGTTCACCTAC	53	3' terminus
V3Mod_F	This study (modified from Flaherty 2018)	F	CCGGAGAGRGAGCMTKAG	54	5' terminus
EukBshort_R	This study (modified from Medlin 1988)	R	CCTTCCGCAGGTTCACCTAC	55	3' terminus

WO 2024/006765 PCT/US2023/069177

LAOEukF	This study	F	CTGGTTGATCCTGCCAGTAKT	56	5' terminus
LAOEuk2F	This study	F	CTGGTTGATCCTGCCAGT	57	5' terminus
LAO18SF	This study	F	CGCGAANGGCTCATTANAWCAGC	58	5' terminus
LAOGiarF	This study	F	ACGGCTCAGGACAACGGTT	59	5' terminus
LAO1498R	This study	R	GGTTCACCTACGGANACCTTGTTA	60	3' terminus
LAOECR	This study	R	TCGTCTTCTCAGCGCCGGT	61	3' terminus
LAOEntCrypF	This study	F	GATTAAGCCATGCATGTSTAAG	62	5' terminus
LAO380F	This study	F	GGTTCGACTCCGGAGAG	63	5' terminus
LAOTW2F	This study	F	TGGATAACTGTAATRACTCT	64	5' terminus
LAOTW3R	This study	R	GACCTYACTAAACCATTCAATC	65	3' terminus

F, Forward primer; R, Reverse primer; B, Blocking primer

*The N shown in bold in SEQ ID NO: 5 may be I, A, T, C, or G. While the 21b8R primer used in this example contained an I (5-deoxyinosine) at this position, we achieved similar results with a 1:1:1:1 mix of 21b8R variants comprising an A, T, C, or G at this position. Note: 5-deoxyinosine is a "universal" base that can base pair with A, T, C, or G.

5

WO 2024/006765 PCT/US2023/069177

We also designed new 18S V4 primers with the goal of amplifying all eukaryotic endosymbiont groups with little to no prokaryotic complementarity. We began by creating a database of parasite/commensal 18S rRNA sequences containing representatives from all phylogenetic lineages containing at least one vertebrate-associated eukaryotic endosymbiont. We downloaded sequences from all known groups of endoparasites/endosymbionts from NCBI Genbank[51] or the SILVA 138.1 Small Subunit rRNA Non-Redundant Reference Database (n = 510,508 total accessions[50,52]; SILVA Ref NR hereafter) at a depth of one species per genus, beginning with the Centers for Disease Control's "Alphabetical Index of Parasitic Diseases" [53]. To ensure broad coverage of commensals, zoonoses, and novel organisms we added non-pathogenic protozoans of humans[54], parasites/commensals of great apes[55], and parasites of veterinary importance[56]. We then used MUSCLE[57] implemented in MEGA 11[58] to align the resulting 658 full-length 18S sequences, which covered a broad range of pathogenicity, vertebrate hosts, and tissue tropisms. To identify candidate conserved regions, we utilized the Arb software suite[59], and the ecoPrimers function in OBItools[60], with manual inspection and adjustment as needed. We then extracted every 16 - 20-mer candidate sequence within those regions and tested them for taxonomic coverage against SILVA Ref NR using the SILVA TestProbe and TestPrime tools[61]. Candidate primers with high overall complementarity were manually adjusted for maximum coverage.

We aimed to avoid degeneracy as it has been shown to create bias in 18S V4 amplification[37] and succeeded in the forward primer. Degeneracy was required in the reverse primer, although not in the four terminal 3′ nucleotides. Furthermore, of the three degenerate positions in the reverse primer, no targeted groups required all three degeneracies, and most required just one. To increase homogeneity and avoid potential biases against rare sequences, we used 5-deoxyinosine in the four-fold degenerate position instead of N, thereby limiting our reverse primer mixture to four distinct oligonucleotides[62]. (Note: Inosine is considered a 'universal base' or a 'degenerate base' because it has the ability to pair indiscriminately with each of the four standard nucleotide bases, adenine (A), cytosine (C), guanine (G), and thymine (T), via two hydrogen bonds.)

The forward region identified for priming had higher GC content than the reverse region, so we forewent the standard guidelines for GC content and melting temperature differences in

order to prioritize coverage, with the knowledge that we could later add locked nucleic acids (LNAs) to modify the melting temperature if needed[63]. In the end, this modification was not necessary because the DNA polymerase for PCR (described below) tolerates a wide melting temperature range and has a universal annealing temperature regardless of primer sequence. In total we designed four forward primers and one reverse primer (**Table 5)** for further testing.

Testing metabarcoding methods for taxonomic coverage using in silico PCR

For the initial analysis of published protocols for taxonomic coverage, we used locus-specific sequences (i.e., not including linkers, adapters, or barcode elements) from all 22 18S V4 primer sets identified in our literature search (**Table 5**). *In silico* PCR of SILVA Ref NR was performed using the TestPrime tool allowing for a single mismatch and a mismatch-free two base pair 3′ window. For this analysis, "helminth" accessions included Acanthocephala (n = 66), Nematoda (n = 2,170), and Platyhelminthes (n = 1,993) and "protozoa" accessions included Amoebozoa (n = 1,148), Discoba (n = 1,032), Excavata (n = 389), Alveolata (n = 9,140), and Stramenopiles (n = 3,556). In two cases where multiple primer sets were used in combination (Krosgaard - three sets and DeMone - two sets), we tested each set individually and conservatively estimated coverage by reporting only the highest percentage for each taxon. Primer sets with > 5 % coverage of off-target prokaryote groups (archaea and bacteria) were not analyzed further (n = 4 sets).

In silico PCR was then used to evaluate the published primer sets remaining (n = 18) alongside our new candidate primers (n = 4; **Table 5**). At this stage, we filtered target sequences to contain only parasites of vertebrates because the inclusion of environmental/free-living organisms can distort parasite coverage metrics. Specifically, we split clades that contained both free-living organisms and parasites of invertebrate hosts (e.g., *Rhabditida* and *Entamoeba*) into higher-resolution, curated groups. We included free-living, opportunistic parasites of clinical importance, including *Balamuthia mandrillaris* and *Naegleria fowleri*, and we excluded sequences whose label in the SILVA database was incorrect (i.e., the taxonomy string associated with the record did not match the phylogenetic placement in the guide tree; n = 14). Coverage metrics were normalized to eligible accession numbers, which were similar across primer sets because of similar priming locations in the V4 region. We compared taxonomic coverage for primer sets using the TestPrime tool[61] and SILVA Ref NR[50,52] allowing for a single mismatch

with a mismatch-free two base pair 3′ window. Primers with ≤ 50 % overall mean coverage of target groups and methods that required more than a single primer set were not considered further.

Testing metabarcoding methods for on-target amplification using purified DNA

We assessed amplification success of the remaining 4 newly designed and 8 published primer sets across parasite groups using 22 genomic DNA (gDNA) isolates from single vertebrate endoparasites as template for PCR. Samples were obtained from reputable reagent repositories and expert parasitologists (for sample details, including sources, see **Table 6**) either as purified DNA or whole organisms. gDNA from whole worms and pelleted protozoal cultures were extracted using the DNeasy Blood and Tissue Kit (Qiagen, Hilden, Germany) using 0.2 g of starting material, eluted in Qiagen buffer AE, and stored at -20 °C. PCR conditions were as follows: 1 X Platinum II Hot Start PCR MasterMix (ThermoFisher, Waltham, Massachusetts, USA), 0.2 µM forward primer with Nextera adapter, 0.2 µM reverse primer with Nextera adapter, ThermoFisher 0.2 X Platinum II GC Enhancer, 0.8 ng/µl gDNA in a total 12.5 µl reaction; 94 °C for 2 minutes, 30 cycles of [94 °C for 15 seconds, 60 °C for 15 seconds, 68 °C for 15seconds], and hold at 4 °C. Products were electrophoresed on a 1.5 % agarose gel with SYBR gold DNA dye (ThermoFisher) and a 1 kb DNA size standard. Amplification was scored by band presence on an agarose gel upon visualization under UV illumination with a GelDoc XR imager (BioRad, Hercules, California, USA).

Table 6. Parasite specimens and sources

Organism	**Sample type**	**Source**	**Catalog #**
Echinorhynchus salmonis	Whole adult worms	UW Madison School of Veterinary Medicine, Dr. Tony	NA
Hymenolepis diminuta	Whole adult worms	UW Madison School of Veterinary Medicine, Dr. Timothy	NA
Taenia hydatigena	Cysts	Wisconsin Veterinary Diagnostic Lab	NA
Bertiella studeri	Proglottids	UW Madison School of Veterinary Medicine, Dr. Tony	NA
Schistosoma mansoni Strain NMRI	DNA	BEI Resources	NR-28911
Ascaris suum	Whole adult worms	Wisconsin Veterinary Diagnostic Lab	NA

Dictyocaulus viviparous	Whole adult worms	Wisconsin Veterinary Diagnostic Lab	NA
Dirofilaria immitis Strain Missouri 2005	DNA	BEI Resources	NR-44348
Trichinella spiralis	DNA	USDA Animal Parasitic Diseases Laboratory	NA
Encephalitozoon cuniculi	DNA	BEI Resources	NR-13510
Entamoeba histolytica Strain HK-9	DNA	BEI Resources	NR-175
Balamuthia mandrillaris CDC: V188	Axenic culture	BEI Resources	NR-46452
Acanthamoeba sp. Strain CDC: 12741:1	DNA	BEI Resources	NR-45611
Naegleria fowleri Strain CDC: V414	Axenic culture	BEI Resources	NR-46494
Leishmania major Strain NIH SD	DNA	BEI Resources	NR-48764
Trypanosoma cruzi Strain G	DNA	BEI Resources	NR-50238
Giardia lamblia Strain WB clone C6	DNA	BEI Resources	NR-15894
Plasmodium falciparum Strain D6	DNA	BEI Resources	MRA-398
Babesia sp. Strain MO1	DNA	BEI Resources	NR-50663
Toxoplasma gondii	DNA	UW Madison Department of Medical Microbiology and Immunology, Dr. Laura Knoll	NR-33509
Cryptosporidium hominis	DNA	BEI Resources	NR-2520
Blastocystis hominis Strain BT1	DNA	ATCC (American Type Culture Collection)	50608

NA, not applicable.

Testing metabarcoding methods for amplification bias using a community standard

Preliminary metabarcoding experiments using mixes of gDNA from single parasites demonstrated a non-linear relationship between DNA input and sequence read abundance, likely due to rRNA copy number variation[64]. We addressed this issue by extracting, amplifying, and cloning parasite DNA from 16 vouchered parasite specimens from verified sources or identified by experts (**Table 6**). 18S rDNA sequences were amplified with full-length universal or group-specific primers (see **Table 5** and **Table 7**) using Qiagen HotStar Plus Taq DNA polymerase

according to manufacturer's instructions. Products were verified for size on an agarose gel and Sanger sequenced. Correct 18S sequences were cloned into a pCR4-TOPO vector using a TOPO TA Cloning Kit for Sequencing (Invitrogen, Waltham, Massachusetts, USA) and Invitrogen One Shot competent cells according to manufacturer's instructions. Colonies were screened by PCR and Sanger sequencing. Plasmid DNA (plDNA) extracted from verified transformants was mixed at equimolar ratios to create the equimolar EukMix community standard reagent. This strategy assures equal 18S copy number input among organisms, which, in the case of amplicon sequencing, enables assessment of primer bias and potential of the assays to yield quantitative data[65].

Table 7. Equimolar EukMix components and full-length 18S cloning primers

	Organism	FWD primer*	REV primer*
1	*Echinorhynchus salmonis*	EukA_F	EukB_R
2	*Hymenolepis diminuta*	LAOTW2F	LAOTW3R
3	*Ascaris suum*	LAO18SF	LAO1498R
4	*Dirofilaria immitis*	LAO18SF	LAO1498R
5	*Trichinella spiralis*	V3mod_F	EukBshort_R
6	*Encephalitozoon cuniculi*	V3mod_F	LAOECR
7	*Entamoeba histolytica*	LAOEuk2F	EukB_R
8	*Balamuthia mandrillaris*	EukA_F	EukB_R
9	*Naegleria fowleri*	LAO380F	LAO1498R
10	*Giardia intestinalis*	LAO380F	EukB_R
11	*Leishmania major*	LAOEukF	EukB_R
12	*Plasmodium falciparum*	EukA_F	EukB_R
13	*Babesia* sp. strain MO1	EukA_F	EukB_R
14	*Toxoplasma gondii*	EukA_F	EukB_R
15	*Cryptosporidium hominis*	EukA_F	LAO1498R
16	*Blastocystis hominis*	LAOEukF	LAO1498R

*See Table 5 for primer sequences and references

Metabarcoding using new and published primer sets was performed in triplicate with community standard as starting material using the procedure described below. Resulting sequencing reads were filtered for quality using a cutoff of Q = 30 and mapped to a database containing full-length 18S sequences of clones comprising the EukMix mock community using a mapping stringency of 99 % similarity and 99 % length fraction in CLC genomics workbench

v.10.2 (Qiagen). The resulting abundances for each community standard component were used to calculate evenness metrics in R v.3.6.3, and GraphPad Prism v.8.4.3 was used for graphing data and for statistical analyses.

VESPA compared to microscopy

Sample collection: Clinical samples used in this work were excess material from concluded studies that had been previously evaluated for eukaryotic endosymbionts using microscopy. Human fecal samples had been collected from communities on the southern Venezuelan border with Brazil[66]. Non-human primate fecal samples were collected from semi-free ranging Nigerian red capped mangabeys (*Cercocebus torquatus*) in a sanctuary[67]. Appropriate IRB approvals (IVIC IRB #DIR-0609/1542/2015) and IACUC protocols were obtained by each collaborator and all samples were completely de-identified prior to use.

Microscopy: Microscopic analyses of non-human primate and human feces were performed as previously described[68]. Briefly, one gram of formalin preserved feces was concentrated via formalin-ethyl acetate sedimentation[67] and the sediment was examined in its entirety at ×10 objective light magnification for gastrointestinal parasites by an expert parasitologist. Additionally, one drop of sediment from each sample was examined at ×40 objective light magnification for identification of protozoa.

Genomic DNA isolation: Human fecal samples were processed to remove bacteria and debris as previously described[69]. Briefly, feces were diluted in PBS (0.2 *M* phosphate-buffered saline, pH 7.2), homogenized, filtered through sterile four-ply cotton gauze, pelleted for 5 min at 300 x *g*, resuspended in molecular grade water and layered on top of a 1.5 *M* sucrose solution. After centrifugation for 10 min at 1,700 x *g* the interphase was collected and the process was repeated with a 0.75 *M* sucrose gradient. The resulting pellet was collected, washed in PBS, and resuspended in 2 ml of molecular-grade water. 0.2 ml of the resulting sample was used as starting material for phenol: chloroform: isoamyl alcohol (25: 24: 1) DNA extraction, eluted in IDTE buffer and stored at -20 °C.

Non-human primate fecal samples in 1:1 RNAlater nucleic acid preservation solution (ThermoFisher) were thawed on ice and homogenized by vortexing prior to transferring 0.2 g of homogenate to bead beating tubes (for a total of 0.1 g fecal material) for extraction using the

Qiagen DNeasy PowerLyzer PowerSoil kit. gDNA was eluted in Qiagen C6 buffer and stored at -20 °C.

Metabarcoding: See **VESPA Protocol** for step-by-step instructions. For compatibility of sequencing libraries across primer sets and amplicon library types, we created a 2-step Illumina Nextera-based protocol that does not require custom sequencing primers to be added to the sequencing cartridge. Primers for the first (amplicon) PCR consist of a locus-specific sequence (see **VESPA Protocol** and **Table 5** for locus-specific primer sequences) with Nextera adapter sequences attached at the 5′ end: F-TCGTCGGCAGCGTCAGATGTGTATAAGAGACAG (SEQ ID NO: 66) and R- GTCTCGTGGGCTCGGAGATGTGTATAAGAGACAG (SEQ ID NO: 67). A second, limited cycle (indexing) PCR was then used to add Nextera indexing primers to both ends. Note that Platinum II MasterMix (ThermoFisher) has a universal annealing temperature of 60 °C regardless of primer melting temperature. PCRs were run in triplicate with the following conditions: ThermoFisher 1 X Platinum II Hot Start PCR MasterMix, 0.2 µM forward primer with Nextera adapter, 0.2 µM reverse primer with Nextera adapter, 0.2 X ThermoFisher Platinum II GC Enhancer, 0.8 ng/µl gDNA in a total 12.5 µl reaction; 94 °C for 2 minutes, 30 cycles of [94 °C for 15 seconds, 60 °C for 15 seconds, 68 °C for 15seconds], and hold at 4 °C. Triplicate reactions were then pooled and amplicons were cleaned using Ampure XP beads (Beckman Coulter, Brea, California, USA) then used as template for indexing PCR as follows: 1 X KAPA HiFi HotStart ReadyMix (Roche, Basel, Switzerland), 1 X Nextera Unique Dual Index primers (Illumina, San Diego, California, USA), 1 µl of clean amplicons in a total 12.5 µl reaction; 95 °C for 3 minutes, 10 cycles of [95 °C for 30 seconds, 55 °C for 30 seconds, 72 °C for 30 seconds], 72 °C for 5 minutes, and hold at 4 °C. Indexed libraries were cleaned using Ampure XP beads (Beckman Coulter) assessed for concentration on a Qubit fluorometer (ThermoFisher), and pooled for sequencing on an Illumina MiSeq with 300 x 300 cycle chemistry using default index and sequencing read primers and 10 – 20 % PhiX.

Data processing and Bioinformatics: We processed reads from our final two VESPA data sets with both QIIME 2[70] and DADA2 v.1.16.0[71] in the R environment v.3.6.3 and found that, while results were similar, DADA2 was more user-friendly (i.e., did not require installation of new software, required less steps, and was implementable within a familiar computing environment). Read files were converted to vectors and filtered for quality using the

filterAndTrim command with default settings plus modifiers to remove primers (trimLeft = c(18,20)), residual PhiX reads (rm.phix = TRUE), and short sequences (minLen = 100). Error rate for forward and reverse reads were calculated using the learnErrors command, data were dereplicated using the derepFastq command, and sequence variants were inferred using the dada command. Read pairs were merged using the mergePairs command with justConcatenate = TRUE and chimeras were removed using the removeBimeraDenovo command with default parameters. Taxonomy assignments were made using the assignTaxonomy command and the PR2 version 4.14.0 database, which contains 18S and 16S sequences at species-level resolution. For comparison we also tested 2 other taxonomy databases: v132 which includes all eukaryotic organisms from the SILVA v132 database and v128 which includes all eukaryotic organisms from the SILVA v128 database plus corrected species labels for *Blastocystis* and additional *Entamoeba* sequences. However, we found that the PR2 database returned higher numbers of fully assigned ASVs. Any ASVs not assigned taxonomy using the PR2 database were queried against the full NCBI nucleotide database on September 3rd, 2022 using MegaBLAST[72] with default parameters.

Data Availability

Sequence data that support the findings of this study have been deposited in the National Center for Biotechnology Information (NCBI) Sequence Read Archive with BioProject ID PRJNA944233 and BioSample accessions SAMN33744948 to SAMN33744999.

VESPA Protocol:

Contents

1 - Starting material

- Starting material can be fresh, freshly frozen (no buffer), or stored ~1:1 in RNA later.
- Sample types tested: feces, vomit, stomach contents, intestine tissue, intestine contents, environmental, entamoeba cysts, whole helminths, and tapeworm proglottids/cysts.

2 - gDNA extraction

- Use Qiagen DNeasy PowerLyzer PowerSoil Kit (catalog #12855-5) according to manufacturer's instructions.
- Weigh out up to .20 g of input feces or .25 g of input for all other sample types.
- Elute in 100 µl C6 buffer (included in kit) and store at -20 °C.

3 - 18S V4 Amplicon PCR

- Set up amplicon PCR reactions *in triplicate.*
- Use Invitrogen Platinum II Hot Start 2X PCR Master Mix (Catalog # 14000012) with the reaction conditions (**Table 8**) and cycling conditions (**Table 9**) shown below.
- Use a forward primer selected from SEQ ID NOs: 1-4 and a reverse primer selected from SEQ ID NOs: 5-8. Include Nextera adapter sequences, as demonstrated below.

Table 8. Reaction conditions for 18S V4 amplicon PCR

Reaction component	Final Conc.	1 x 12.5 µl rxn. (µl)
2X Platinum II HotStart PCR Master Mix*	1X	6.0
10 µM Forward primer	0.2 µM	0.25
10 µM Reverse primer	0.2 µM	0.25
Platinum II GC Enhancer*	NA	2.5
Nuclease-free water*	NA	2.5
~10 ng/µl gDNA	0.8 ng/µl	1.0
		12.5 µl

*Included in Master Mix Kit

Table 9. Cycling conditions for 18S V4 amplicon PCR

Step	Temp °C	Time	Cycles

Activation	94	2 min	1
Denaturation	94	15 sec	30
Annealing	60	15 sec	
Extension	68	15 sec	
Final hold	4	hold	

Primers (Nextera adapter sequence - locus-specific primer sequence)

Forward: 29F

TCGTCGGCAGCGTCAGATGTGTATAAGAGACAGAGCAGCCGCGGTAATTCC

(SEQ ID NO: 66 - SEQ ID NO: 3)

Reverse: 21b8R+4

GTCTCGTGGGCTCGGAGATGTGTATAAGAGACAGTCCGTCAATTYCTTNAASTTTC

(SEQ ID NO: 67 - SEQ ID NO: 6)

4 – Amplicon cleanup

- Use Beckman Coulter Ampure XP beads (catalog #A63880) and magnetic particle separator (MPC).
- Always make 75% ethanol immediately prior to use.

1- Shake Ampure XP beads at room temperature for > 30 minutes prior to use.

2- Pool all 3 PCR reactions into a single plate or tube and mix by pipetting (~37.5 µl).

3- Remove 7.5 µl and store at -20 °C if you would like to visualize bands on a gel (~30 µl).

4- Add AMPure XP beads for 0.8X RATIO (e.g., 24 µl beads per 30 µl product).

5- Gently pipette up and down 15 times.

6- Incubate at room temperature for 5 minutes.

7- Put tubes on MPC and incubate at room temperature for 2 minutes.

8- Remove and discard supernatant.

9- With tubes on MPC, add 175 µl of 75% ethanol.

10- Wait >1 minute.

11- Remove and discard supernatant.

12- Add 175 µl of 75% ethanol.

13- Wait >1 minute.

14- Remove and discard supernatant.

15- Remove all ethanol with P20 tips.

16- With tubes on MPC, let the pellet air-dry for 5 minutes.

17- Add 47 µl of Tris pH 8.5.

18- Remove tubes from MPC and gently pipette up and down to resuspend beads.

19- Incubate at room temperature for 2 minutes.

20- Put tubes on MPV and incubate at room temperature for 2 minutes.

21- Carefully transfer 45 µl of supernatant to a new PCR tubes or plate.

5 - Indexing PCR

- Set up indexing PCR reactions on ice.
- Use Roche KAPA HiFi HotStart ReadyMix (catalog #KK2601) and IDT for Illumina Nextera DNA Unique Dual Indexes (catalog #20027215) with the reaction conditions (**Table 10**) and cycling conditions (**Table 11**) shown below.

Table 10. Reaction conditions for indexing PCR

Reaction component	1 x 12.5 µl rxn. (µl)
2X KAPA HiFi HotStart ReadyMix	6.0
Nextera Unique Dual Index	2.5
Nuclease-free water	3.0
Clean amplicons in Tris pH 8.5	1.0
	12.5 µl

Table 11. Cycling conditions for indexing PCR

Step	Temp °C	Time	Cycles
Activation	95 °C	3 min	1
Denaturation	95 °C	30 sec	10
Annealing	55 °C	30 sec	
Extension	72 °C	30 sec	
Final extension	72 °C	5 min	1

Final hold	4 °C	hold	

6 – Library cleanup

- Use Beckman Coulter Ampure XP beads (catalog #A63880) and magnetic particle separator (MPC).
- Always make 75% Ethanol immediately prior to use.

1- Shake Ampure XP beads at room temperature for > 30 minutes prior to use.
2- Add AMPure XP beads for 0.8X RATIO (e.g., 9.6 µl beads per 12.5 µl PCR product).
3- Gently pipette up and down 15 times.
4- Incubate at room temperature for 5 minutes.
5- Put tubes on MPC and incubate at room temperature for 2 minutes.
6- Remove and discard supernatant.
7- With tubes on MPC, add 175 µl of 75% ethanol.
8- Wait >1 minute.
9- Remove and discard supernatant.
10- Add 175 µl of 75% ethanol.
11- Wait >1 minute.
12- Remove and discard supernatant.
13- Remove all ethanol with P20 tips.
14- With tubes on MPC, let the pellet air-dry for 5 minutes.
15- Add 22 µl of Tris pH 8.5.
16- Remove tubes from MPC and gently pipette up and down to resuspend beads.
17- Incubate at room temperature for 2 minutes.
18- Put tubes on MPV and incubate at room temperature for 2 minutes.
19- Carefully transfer 20 µl of supernatant to a new PCR tubes or plate.

7 – Quantification and size determination

- Use Invitrogen Qubit Fluorimeter and dsDNA High-Sensitivity Assay Kit (catalog #Q33230) and Agilent Bioanalyzer and Agilent High Sensitivity DNA Kit (catalog #5067-4626) according to manufacturer's instructions.

- Measure the concentration of each library using a Qubit fluorometer and 3 µl of each library.
- Measure the size of each library or a representative subset of libraries using an Agilent Bioanalyzer and 1 µl of a 1 ng/µl dilution (in Tris pH 8.5) of the library for a total of 1 ng.

8 - Pooling and sequencing

- Requirements for core facility submission/in-house sequencing will determine pooling specifics.
- Run on an Illumina MiSeq instrument, 300 x 300 cycle chemistry, and add 10 – 20% PhiX.

References:

1. Whipps JML, K.; Cooke, R.C. Mycoparasitism and plant disease control. In: Burge MN, ed. *Fungi in biological control systems*. Manchester University Press; 1988:161-187:chap 9.

2. Konopka A. What is microbial community ecology? *Isme J.* Nov 2009;3(11):1223-30. doi:10.1038/ismej.2009.88

3. Gilbert JA, Blaser MJ, Caporaso JG, Jansson JK, Lynch SV, Knight R. Current understanding of the human microbiome. *Nat Med.* Apr 10 2018;24(4):392-400. doi:10.1038/nm.4517

4. Pepper JW, Rosenfeld S. The emerging medical ecology of the human gut microbiome. *Trends Ecol Evol.* Jul 2012;27(7):381-4. doi:10.1016/j.tree.2012.03.002

5. Clemente JC, Ursell LK, Parfrey LW, Knight R. The impact of the gut microbiota on human health: an integrative view. *Cell.* Mar 16 2012;148(6):1258-70. doi:10.1016/j.cell.2012.01.035

6. Laforest-Lapointe I, Arrieta MC. Microbial eukaryotes: a missing link in gut microbiome studies. *mSystems.* Mar-Apr 2018;3(2)doi:10.1128/mSystems.00201-17

7. Kodio A, Menu E, Ranque S. Eukaryotic and prokaryotic microbiota interactions. *Microorganisms.* Dec 17 2020;8(12)doi:10.3390/microorganisms8122018

8. Avramenko RW, Redman EM, Lewis R, Yazwinski TA, Wasmuth JD, Gilleard JS. Exploring the gastrointestinal "Nemabiome": deep amplicon sequencing to quantify the species composition of parasitic nematode communities. *Plos One*. Dec 2 2015;10(12)

9. Matijasic M, Mestrovic T, Paljetak HC, Peric M, Baresic A, Verbanac D. Gut microbiota beyond bacteria-mycobiome, virome, archaeome, and eukaryotic parasites in IBD. *Int J Mol Sci*. Apr 11 2020;21(8)doi:10.3390/ijms21082668

10. Kohler JR, Hube B, Puccia R, Casadevall A, Perfect JR. Fungi that infect humans. *Microbiol Spectr*. Jun 2017;5(3)doi:10.1128/microbiolspec.FUNK-0014-2016

11. Tedersoo L, Bahram M, Zinger L, et al. Best practices in metabarcoding of fungi: from experimental design to results. *Mol Ecol*. May 2022;31(10):2769-2795. doi:10.1111/mec.16460

12. Vossbrinck CR, Debrunner-Vossbrinck BA. Molecular phylogeny of the Microsporidia: ecological, ultrastructural and taxonomic considerations. *Folia Parasitol (Praha)*. May 2005;52(1-2):131-42; discussion 130. doi:10.14411/fp.2005.017

13. Dobell C. The discovery of the intestinal protozoa of man. *Proc R Soc Med*. 1920;13(Sect Hist Med):1-15.

14. Momcilovic S, Cantacessi C, Arsic-Arsenijevic V, Otranto D, Tasic-Otasevic S. Rapid diagnosis of parasitic diseases: current scenario and future needs. *Clin Microbiol Infect*. Mar 2019;25(3):290-309. doi:10.1016/j.cmi.2018.04.028

15. Ricciardi A, Ndao M. Diagnosis of parasitic infections: what's going on? *J Biomol Screen*. Jan 2015;20(1):6-21. doi:10.1177/1087057114548065

16. Nadler SA, GP DEL. Integrating molecular and morphological approaches for characterizing parasite cryptic species: implications for parasitology. *Parasitology*. Nov 2011;138(13):1688-709. doi:10.1017/S003118201000168X

17. Jackson TF. *Entamoeba histolytica* and *Entamoeba dispar* are distinct species; clinical, epidemiological and serological evidence. *Int J Parasitol*. Jan 1998;28(1):181-6. doi:10.1016/s0020-7519(97)00177-x

18. Fotedar R, Stark D, Beebe N, Marriott D, Ellis J, Harkness J. PCR detection of *Entamoeba histolytica*, *Entamoeba dispar*, and *Entamoeba moshkovskii* in stool samples from Sydney, Australia. *J Clin Microbiol*. Mar 2007;45(3):1035-7. doi:10.1128/JCM.02144-06

19. Cristescu ME. From barcoding single individuals to metabarcoding biological communities: towards an integrative approach to the study of global biodiversity. *Trends Ecol Evol*. Oct 2014;29(10):566-71. doi:10.1016/j.tree.2014.08.001

20. D'Amore R, Ijaz UZ, Schirmer M, et al. A comprehensive benchmarking study of protocols and sequencing platforms for 16S rRNA community profiling. *BMC Genomics*. Jan 14 2016;17:55. doi:10.1186/s12864-015-2194-9

21. Nilsson RH, Anslan S, Bahram M, Wurzbacher C, Baldrian P, Tedersoo L. Mycobiome diversity: high-throughput sequencing and identification of fungi. *Nat Rev Microbiol*. Jan 2019;17(2):95-109. doi:10.1038/s41579-018-0116-y

22. Amaral-Zettler LA, McCliment EA, Ducklow HW, Huse SM. A method for studying protistan diversity using massively parallel sequencing of V9 hypervariable regions of small-subunit ribosomal RNA genes. *PLoS One*. Jul 27 2009;4(7):e6372. doi:10.1371/journal.pone.0006372

23. Parfrey LW, Walters WA, Lauber CL, et al. Communities of microbial eukaryotes in the mammalian gut within the context of environmental eukaryotic diversity. *Frontiers in Microbiology*. Jun 19 2014;5

24. Mann AE, Mazel F, Lemay MA, et al. Biodiversity of protists and nematodes in the wild nonhuman primate gut. *Isme J*. Feb 2020;14(2):609-622. doi:10.1038/s41396-019-0551-4

25. Maritz JM, Rogers KH, Rock TM, et al. An 18S rRNA workflow for characterizing protists in sewage, with a focus on zoonotic trichomonads. *Microb Ecol*. Nov 2017;74(4):923-936. doi:10.1007/s00248-017-0996-9

26. Jarman SN, McInnes JC, Faux C, et al. Adelie penguin population diet monitoring by analysis of food DNA in scats. *Plos One*. Dec 16 2013;8(12)doi:ARTN e8222710.1371/journal.pone.0082227

27. Bhadury P, Austen MC. Barcoding marine nematodes: an improved set of nematode 18S rRNA primers to overcome eukaryotic co-interference. *Hydrobiologia*. Mar 2010;641(1):245-251. doi:10.1007/s10750-009-0088-z

28. Avramenko RW, Bras A, Redman EM, et al. High species diversity of trichostrongyle parasite communities within and between Western Canadian commercial and conservation bison

herds revealed by nemabiome metabarcoding. *Parasites & Vectors*. May 15 2018;11doi:ARTN 29910.1186/s13071-018-2880-y

29. Avramenko RW, Redman EM, Lewis R, et al. The use of nemabiome metabarcoding to explore gastro-intestinal nematode species diversity and anthelmintic treatment effectiveness in beef calves. *International Journal for Parasitology*. Nov 2017;47(13):893-902. doi:10.1016/j.ijpara.2017.06.006

30. Poissant J, Gavriliuc S, Bellaw J, et al. A repeatable and quantitative DNA metabarcoding assay to characterize mixed strongyle infections in horses. *Int J Parasitol*. Feb 2021;51(2-3):183-192. doi:10.1016/j.ijpara.2020.09.003

31. Dollive S, Peterfreund GL, Sherrill-Mix S, et al. A tool kit for quantifying eukaryotic rRNA gene sequences from human microbiome samples. *Genome Biol*. Jul 3 2012;13(7):R60. doi:10.1186/gb-2012-13-7-r60

32. Krogsgaard LR, Andersen LO, Johannesen TB, et al. Characteristics of the bacterial microbiome in association with common intestinal parasites in irritable bowel syndrome. *Clin Transl Gastroenterol*. Jun 19 2018;9(6):161. doi:10.1038/s41424-018-0027-2

33. Gogarten JF, Calvignac-Spencer S, Nunn CL, et al. Metabarcoding of eukaryotic parasite communities describes diverse parasite assemblages spanning the primate phylogeny. *Mol Ecol Resour*. Jan 2020;20(1):204-215. doi:10.1111/1755-0998.13101

34. Lamb PD, Hunter E, Pinnegar JK, Creer S, Davies RG, Taylor MI. How quantitative is metabarcoding: A meta-analytical approach. *Molecular Ecology*. 2019;28(2):420-430.

35. Sergaki C, Anwar S, Fritzsche M, et al. Developing whole cell standards for the microbiome field. *Microbiome*. Aug 9 2022;10(1):123. doi:10.1186/s40168-022-01313-z

36. Marquina D, Andersson AF, Ronquist F. New mitochondrial primers for metabarcoding of insects, designed and evaluated using *in silico* methods. *Mol Ecol Resour*. Jan 2019;19(1):90-104. doi:10.1111/1755-0998.12942

37. Bradley IM, Pinto AJ, Guest JS. Design and evaluation of Illumina MiSeq-compatible, 18S rRNA gene-specific primers for improved characterization of mixed phototrophic communities. *Applied and Environmental Microbiology*. Oct 2016;82(19):5878-5891. doi:10.1128/Aem.01630-16

38. Beermann AJ, Werner MT, Elbrecht V, Zizka VMA, Leese F. DNA metabarcoding improves the detection of multiple stressor responses of stream invertebrates to increased salinity, fine sediment deposition and reduced flow velocity. *Sci Total Environ.* Jan 1 2021;750:141969. doi:10.1016/j.scitotenv.2020.141969

39. Bohmann K, Elbrecht V, Caroe C, et al. Strategies for sample labelling and library preparation in DNA metabarcoding studies. *Mol Ecol Resour*. May 2022;22(4):1231-1246. doi:10.1111/1755-0998.13512

40. Song F, Kuehl JV, Chandran A, Arkin AP. A simple, cost-effective, and automation-friendly direct PCR approach for bacterial community analysis. *mSystems*. Oct 26 2021;6(5):e0022421. doi:10.1128/mSystems.00224-21

41. Albaina A, Aguirre M, Abad D, Santos M, Estonba A. 18S rRNA V9 metabarcoding for diet characterization: a critical evaluation with two sympatric zooplanktivorous fish species. *Ecol Evol*. Mar 2016;6(6):1809-24. doi:10.1002/ece3.1986

42. Krehenwinkel H, Wolf M, Lim JY, Rominger AJ, Simison WB, Gillespie RG. Estimating and mitigating amplification bias in qualitative and quantitative arthropod metabarcoding. *Sci Rep*. Dec 15 2017;7(1):17668. doi:10.1038/s41598-017-17333-x

43. Deagle BE, Thomas AC, McInnes JC, et al. Counting with DNA in metabarcoding studies: how should we convert sequence reads to dietary data? *Mol Ecol*. Jan 2019;28(2):391-406. doi:10.1111/mec.14734

44. Yu Z, Ito SI, Wong MK, et al. Comparison of species-specific qPCR and metabarcoding methods to detect small pelagic fish distribution from open ocean environmental DNA. *PLoS One*. 2022;17(9):e0273670. doi:10.1371/journal.pone.0273670

45. Weerakoon KG, McManus DP. Cell-Free DNA as a diagnostic tool for human parasitic infections. *Trends Parasitol*. May 2016;32(5):378-391. doi:10.1016/j.pt.2016.01.006

46. Maldonado A, Simoes RO, Luiz JS, Costa-Neto SF, Vilela RV. A new species of *Physaloptera* (Nematoda: Spirurida) from *Proechimys gardneri* (Rodentia: Echimyidae) from the Amazon rainforest and molecular phylogenetic analyses of the genus. *J Helminthol*. Jul 24 2019;94:e68. doi:10.1017/S0022149X19000610

47. Abraham JS, Sripoorna S, Maurya S, Makhija S, Gupta R, Toteja R. Techniques and tools for species identification in ciliates: a review. *Int J Syst Evol Microbiol*. Apr 2019;69(4):877-894. doi:10.1099/ijsem.0.003176

48. Macheriotou L, Guilini K, Bezerra TN, et al. Metabarcoding free-living marine nematodes using curated 18S and CO1 reference sequence databases for species-level taxonomic assignments. *Ecol Evol*. Feb 2019;9(3):1211-1226. doi:10.1002/ece3.4814

49. Hadziavdic K, Lekang K, Lanzen A, Jonassen I, Thompson EM, Troedsson C. Characterization of the 18S rRNA gene for designing universal eukaryote specific primers. *Plos One*. Feb 7 2014;9(2)doi:ARTN e8762410.1371/journal.pone.0087624

50. Quast C, Pruesse E, Yilmaz P, et al. The SILVA ribosomal RNA gene database project: improved data processing and web-based tools. *Nucleic Acids Res*. Jan 2013;41(Database issue):D590-6. doi:10.1093/nar/gks1219

51. Benson DA, Cavanaugh M, Clark K, et al. GenBank. *Nucleic Acids Res*. Jan 4 2018;46(D1):D41-D47. doi:10.1093/nar/gkx1094

52. Yilmaz P, Parfrey LW, Yarza P, et al. The SILVA and "All-species Living Tree Project (LTP)" taxonomic frameworks. *Nucleic Acids Res*. Jan 2014;42(Database issue):D643-8. doi:10.1093/nar/gkt1209

53. Centers for Disease Control GH, Division of Parasitic Diseases and Malaria. Alphabetical Index of Parasitic Diseases. www.cdc.gov/parasites/az/index.html

54. Lukes J, Stensvold CR, Jirku-Pomajbikova K, Parfrey LW. Are human intestinal eukaryotes beneficial or commensals? *Plos Pathogens*. Aug 2015;11(8)doi:ARTN e1005039 10.1371/journal.ppat.1005039

55. Modrý DP, B. Petrželková, K. Hasegawa, H. *Parasites of apes an atlas of coproscopic diagnostics*. vol 78. Frankfurt Contributions to Natural History / Frankfurter Beiträge zur Naturkunde. Edition Chimaira; 2018:198.

56. Taylor MA, Coop RL, Wall R. *Veterinary parasitology*. 4th edition. ed. John Wiley and Sons, Inc.; 2016:p.

57. Edgar RC. MUSCLE: multiple sequence alignment with high accuracy and high throughput. *Nucleic Acids Res*. 2004;32(5):1792-7. doi:10.1093/nar/gkh340

58. Tamura K, Stecher G, Kumar S. MEGA11: Molecular Evolutionary Genetics Analysis version 11. *Mol Biol Evol.* Jun 25 2021;38(7):3022-3027. doi:10.1093/molbev/msab120

59. Ludwig W, Strunk O, Westram R, et al. ARB: a software environment for sequence data. *Nucleic Acids Res.* 2004;32(4):1363-71. doi:10.1093/nar/gkh293

60. Riaz T, Shehzad W, Viari A, Pompanon F, Taberlet P, Coissac E. ecoPrimers: inference of new DNA barcode markers from whole genome sequence analysis. *Nucleic Acids Res.* Nov 2011;39(21):e145. doi:10.1093/nar/gkr732

61. Klindworth A, Pruesse E, Schweer T, et al. Evaluation of general 16S ribosomal RNA gene PCR primers for classical and next-generation sequencing-based diversity studies. *Nucleic Acids Res.* Jan 7 2013;41(1):e1. doi:10.1093/nar/gks808

62. Loakes D. Survey and summary: The applications of universal DNA base analogues. *Nucleic Acids Res.* Jun 15 2001;29(12):2437-47. doi:10.1093/nar/29.12.2437

63. Levin JD, Fiala D, Samala MF, Kahn JD, Peterson RJ. Position-dependent effects of locked nucleic acid (LNA) on DNA sequencing and PCR primers. *Nucleic Acids Res.* 2006;34(20):e142. doi:10.1093/nar/gkl756

64. Wang C, Zhang T, Wang Y, Katz LA, Gao F, Song W. Disentangling sources of variation in SSU rDNA sequences from single cell analyses of ciliates: impact of copy number variation and experimental error. *Proc Biol Sci.* Jul 26 2017;284(1859)doi:10.1098/rspb.2017.0425

65. Piñol J, Senar MA, Symondson WO. The choice of universal primers and the chatacteristics of the species mixtuer determine when DNA metabarcoding can be quantitative. *Molecular Ecology Notes.* 2018;28:407-419.

66. Clemente JC, Pehrsson EC, Blaser MJ, et al. The microbiome of uncontacted Amerindians. *Sci Adv.* Apr 3 2015;1(3)doi:10.1126/sciadv.1500183

67. Friant S, Ziegler TE, Goldberg TL. Changes in physiological stress and behaviour in semi-free-ranging red-capped mangabeys (*Cercocebus torquatus*) following antiparasitic treatment. *Proceedings of the Royal Society B-Biological Sciences.* Jul 27 2016;283(1835)

68. Friant S, Ziegler TE, Goldberg TL. Primate reinfection with gastrointestinal parasites: behavioural and physiological predictors of parasite acquisition. *Anim Behav.* Jul 2016;117:105-113. doi:10.1016/j.anbehav.2016.04.006

69. Walderich B, Müller L, Bracha R, Knobloch J, Burchard GD. A new method for isolation and differentiation of native *Entamoeba histolytica* and *E. dispar* cysts from fecal samples. *Parasitol Res*. 1997;83(7):719-21. doi:10.1007/s004360050326

70. Caporaso JG, Kuczynski J, Stombaugh J, et al. QIIME allows analysis of high-throughput community sequencing data. *Nat Methods*. May 2010;7(5):335-6. doi:10.1038/nmeth.f.303

71. Callahan BJ, McMurdie PJ, Rosen MJ, Han AW, Johnson AJ, Holmes SP. DADA2: High-resolution sample inference from Illumina amplicon data. *Nat Methods*. Jul 2016;13(7):581-3. doi:10.1038/nmeth.3869

72. Morgulis A, Coulouris G, Raytselis Y, Madden TL, Agarwala R, Schaffer AA. Database indexing for production MegaBLAST searches. *Bioinformatics*. Aug 15 2008;24(16):1757-64. doi:10.1093/bioinformatics/btn322

Example 2:

In the following Example, the inventors describe the generation of additional reverse primers that can be used in their method for detecting eukaryotic endosymbionts (i.e., VESPA).

We originally designed four forward primers (i.e., 9F, 13F, 29F, and 2-2bF) and one reverse primer (i.e., 21b8R; TCAATTYCTTNAASTTTC (SEQ ID NO: 5)) for PCR amplification of the V4 region of the 18S gene. However, our forward primers have a higher melting temperature than the initial 21b8R reverse primer. Thus, to increase its PCR compatibility with the forward primers, the 21b8R primer was lengthened to increase its melting temperature. Specifically, we designed three additional reverse primers comprising the same core sequence of 18 nucleotides as the 21b8R primer but with 4, 5, or 6 additional nucleotides added to the 3' end. These additional reverse primers are thus referred to as 21b8R+4 (TCCGTCAATTYCTTNAASTTTC; SEQ ID NO: 6), 21b8R+5 (TTCCGTCAATTYCTTNAASTTTC; SEQ ID NO: 7), and 21b8R+6 (CTTCCGTCAATTYCTTNAASTTTC; SEQ ID NO: 8). Note: The N shown in bold in SEQ ID NOs: 5-8 may be I, A, T, C, or G. While the reverse primers tested in this example contained an I (5-deoxyinosine) at this position, we achieved similar results with 1:1:1:1 mixtures of reverse primer variants comprising an A, T, C, or G at this position.

Amongst the forward and reverse primers, each have slightly different specificities based on *in silico* analysis (**FIG. 5**). The four forward primers comprise overlapping but distinct

sequences, and one of the four primers comprises a single degenerate base.

In 32 published studies in which amplicon sequencing was used to identify parasites, 14 different PCR enzymes were used for the initial amplification. In preliminary tests using two different polymerases, the results varied significantly depending on the polymerase used. Thus, we next set out to determine which combination of the four forward primers, four reverse primers, and PCR polymerases would produce the best results when applied to blood and fecal samples. Specifically, we wanted to know which combination resulted in the best amplification efficiency (band size on gel), read number (total reads after quality filtering), and ratio of on-target to off-target reads (% bacterial/archaeal reads vs other). To this end, we used one blood and one fecal sample as starting material for DNA extraction and amplified the resulting DNA via PCR with various combinations of the PCR primers and eight different polymerases. After PCR, half of the reaction volume was run on an agarose gel to visualize amplification products and the other half was used for library preparation and sequencing. The resulting data were quality-filtered and assigned to taxonomic groups.

We found that amplification with all combinations of the primers and with 6 of the 8 tested polymerases resulted in consistent PCR bands and those products were used for library preparation and sequencing. For blood samples, all primer combinations and 5 of the 6 polymerases gave comparable results. For fecal samples, 1 forward primer (29F) and 1 polymerase (Platinum II HotStart) were clearly superior in terms of high read number and low off-target read abundance (**FIG. 6**). The +4 and +5 reverse primers performed equally well with this sample. However, we determined that the +4 reverse primer picks up slightly more protozoan parasites by performing an *in silico* analysis. Thus, the use of the Platinum™ II Taq Hot-Start DNA Polymerase (Invitrogen) and the primer combination 29F (SEQ ID NO: 3)/21b8R+4 (SEQ ID NO: 6) may be best suited for a universal protocol that is compatible across sample types. Based on these results, the reverse primer 21b8R+4 was selected to perform the experiments described in Example 1.

Example 3:

In the following example, the inventors describe a method for reducing host signal for sequencing-based detection of eukaryotic endosymbionts using CRISPR-Cas9 digestion.

Introduction:

Metagenomic barcoding (metabarcoding) provides a high throughput alternative to traditional methods for reconstructing communities of host-associated organisms (1). Substantial progress has been made in methods for metabarcoding bacteria and archaea (i.e., the "microbiome") (2) and fungi (i.e., the "mycobiome") (3), but similar progress has lagged for eukaryotic endosymbionts (defined here as all non-fungal eukaryotes residing within vertebrate hosts, spanning the continuum of parasites to commensals and including micro- and macro-organisms) (4). One critical reason for this lag is that eukaryotic endosymbionts share highly similar DNA sequences with their eukaryotic hosts but usually at much lower concentration, leading to host signal interference (5, 6). Polymerase chain reaction (PCR) primers designed to broadly recognize eukaryotic endosymbionts (especially metazoans, such as helminths) also often bind to and amplify host DNA (i.e., non-specific, or off-target amplification) (7, 8). Primers that recognize both host and target sequences generally detect only 10^{-3} ng parasite DNA for every ng host DNA present (9). For example, spleen tissue from mice experimentally infected via tail vein injection with *Leishmania donovoni* harbored an average of 200 promastigotes per 0.2 mg spleen tissue, resulting in an average ng parasite DNA: ng host DNA ratio of 10^{-5} (10, 11). One "brute force" solution to this problem is ultra-deep sequencing – in other words, sequencing amplicons to great enough depth to compensate for host signal overabundance – but this approach is inefficient, costly, and biased against detecting low-abundance organisms (8, 12). Using metabarcoding to reconstruct eukaryotic endosymbiont assemblages from feces is commonplace, but feces is so dominated by bacterial DNA that it can also interfere with detection of eukaryotes, even using primers that appear to be eukaryote-specific (13, 14).

A reliable and efficient eukaryotic endosymbiont metabarcoding method should include a host-blocking element to enrich resulting sequences for eukaryotic endosymbiont reads in any sample type with high host DNA content (15). We refer to this process as "host signal reduction" (HSR). Published HSR methods, including restriction enzyme digestion (16), peptide nucleic acid (PNA) clamps (17), blocking oligonucleotides (18), and nested blocking primers (19). Each of these methods have advantages and disadvantages. The restriction enzyme approach, in which primers are designed such that only host amplicons contain a restriction enzyme recognition site allowing for selective cleavage of off-target amplicons prior to sequencing (20), is effective, but suitable restriction sites with flanking PCR primer sites are rare or sometimes non-existent.

Selective inhibition of off-target amplification during PCR is the most commonly published host signal reduction technique (21) and can be achieved using PNA clamps or various blocking oligonucleotides (22, 23). Such methods have been used in published eukaryotic endosymbiont metabarcoding studies (24-26), but efficacy can be low, particularly in samples with high host biomass (5). Nested blocking primers were recently published for plant systems (19) but have yet to be adapted for eukaryotic endosymbiont metabarcoding and may suffer the same drawbacks as PNA clamps and blocking oligos.

CRISPR-Cas9 (CC9) mediated removal of highly abundant off-target nucleic acids is regularly used in other sequencing-based approaches, such as chromatin structure studies (27), cancer screening (28), and plant microbiome profiling (29). CC9 is a promising HSR method for eukaryotic endosymbiont metabarcoding because CRISPR-Cas9 nuclease activity is highly specific (30), reagents are readily available and relatively inexpensive, and the reaction components are modular such that different hosts or read types (e.g., dietary or environmental sequences) can be eliminated depending on experimental requirements. To our knowledge, however, CC9 has not been applied to HSR in the context of eukaryotic endosymbiont metabarcoding.

Here we assess the most commonly published HSR protocol for eukaryotic endosymbiont metabarcoding, the use of a PNA blocker, and demonstrate the need for a more effective approach. We design such a method based on a recombinant *Streptococcus pyogenes* CC9 system, in which vertebrate sequences are selectively targeted for cleavage and removal by host-specific guide RNAs (gRNAs) while leaving amplicons of interest intact for sequencing and analysis. Using *in silico* analyses, *in vitro* digests, and samples from experimentally infected animals, we show that our method is more effective than published HSR methods across various sample types. Finally, we compare the efficacy of eukaryotic endosymbiont metabarcoding for detection of known parasite infections and show that CC9 host signal reduction is necessary to detect hemoparasites in blood samples from naturally infected hosts.

Results:

High host read abundance in 18S V4 metabarcoding data using a PNA clamp

18S V4 metabarcoding (24, 42) using DNA extracted from chimpanzee samples as input (n = 28) and including the mammal-blocking PNA clamp in every amplification (24) yielded a

wide range of host signal relative abundances (**FIG. 7A**). The percent abundance of host reads obtained was low in fecal samples (overall mean < 1 %) but high in all other sample types tested, including blood, plasma, serum, brain, liver, lung, spleen (overall mean = 93.5 %; **Table 12**). Of non-fecal samples, plasma samples contained the lowest relative abundance of host reads (mean = 78.6 %) and spleen samples contained the highest (mean = 99.9 %; **FIG. 7B**).

Table 12. Descriptive statistics of read data obtained from 18S V4 metabarcoding with PNA mammal blocker applied to nonhuman primate fecal, blood, and tissue samples

		% host reads after quality filtering			
Sample	n	Mean	SEM	Min	Max
Feces	6	0.0078	0.0042	0.0000	0.0290
Blood	2	0.8954	0.0644	0.8044	0.9864
Plasma	2	0.7865	0.0410	0.7286	0.8445
Serum	10	0.9018	0.0297	0.6806	0.9928
Brain	2	0.9912	0.0056	0.9832	0.9992
Liver	2	0.9998	0.0000	0.9998	0.9999
Lung	2	0.9732	0.0074	0.9627	0.9837
Spleen	2	0.9999	0.0000	0.9999	0.9999

Guide RNA design for universal eukaryotic endosymbiont enrichment

We designed six candidate vertebrate host-specific gRNAs targeting 18S V4 (**FIG. 8A**), including one fortuitously identical to the published 18S V4 mammal-blocking PNA oligo used above (arb321; **Table 13**) (24). Host DNA sequences targeted by the gRNAs all include a protospacer adjacent motif (PAM) "NGG" required by the *Streptococcus pyogenes* Cas9 enzyme. Target sites are located centrally in 18S V4 (**FIG. 8B**) such that the digestion products can be differentiated from uncleaved amplicons based on size (**FIG. 8C**).

Using *in silico* hybridization to the SILVA 138 RefNR database (35) we found all six candidates to have similar mammalian complementarity (**FIG. 9**), with each hybridizing to 50 % or more of mammalian sequences (mean = 66.4 %) with no mismatches and 60 % or more when allowing for a single mismatch (mean = 76.4 %). gRNAs arb321 and arb326 were effective for mammalian hosts, but several gRNAs additionally recognized non-mammalian vertebrate groups, making them useful for a wider variety of hosts: arb615, CA149, and CA172 recognized

mammal, bird, and fish sequences, while PT7.1 recognized all vertebrates (**Table 13**). All six gRNA oligos failed to hybridize to any parasite/endosymbiont group, with the sole exception of *Trichinella pseudospiralis* (mean = 17.8 %; **FIG. 9**) due to high 18S sequence similarity between *Trichinella* and mammals (mean = 45.5 % DNA identity for all gRNA target regions combined in *Trichinella pseudospiralis* AY851258; **Table 14**).

Table 13. gRNA sequences and characteristics

ID	Target/gRNA Seq	SEQ ID NO:	Orientation	PAM Seq	GC %	Seed seq	Host specificity**
arb321*	AACTGAGGCCATGATTAAGA*	9	sense	GGG	45	TTAAGA	Mammals
arb326	AGGCCATGATTAAGAGGGA	10	sense	CGG	40	GAGGGA	Mammals
arb615	GCAGCTAGGAATAATGGAAT	11	sense	AGG	55	TGGAAT	Mammals, Birds, Fish
PT7.1	ATTCTTGGACCGGCGCAAGA	12	sense	CGG	40	GCAAGA	Vertebrates
CA149	CTCAGCTAAGAGCATCGAGG	13	antisense	GGG	60	ATCGAGG	Mammals, Birds, Fish
CA172	TCTTAGCTGAGTGTCCCGCG	14	sense	GGG	55	CCCGCG	Mammals, Birds, Fish

gRNA, guide RNA; seq, sequence; PAM, protospacer adjacent motif; * sequence identical to V4 mammal blocking PNA oligo used in Mann et al. 2020; ** specificity to host groups determined by SILVA TestProbe *in silico* hybridization data.

Table 14. 18S V4 region comparison and percent DNA identity between gRNAs, mouse, and *Trichinella pseudospiralis* sequences

gRNA	Target/gRNA Seq	Mouse Seq NR_003278*	Mouse % ID	Trichinella Seq AY851258**	TP % ID
arb321	AACTGAGGCCATGA**TTAAGA** (SEQ ID NO: 9)	AACTGAGGCCATGA**TTAAGA** (SEQ ID NO: 9)	100 %	ACCGGAGATAAGTA**TTGAAA** (SEQ ID NO: 68)	55 %
arb326	AGGCCATGATTAA**GAGGGA** (SEQ ID NO: 10)	AGGCCATGATTAA**GAGGGA** (SEQ ID NO: 10)	100 %	AGATAAGTATTGAA**AGGAA** (SEQ ID NO: 69)	58 %
arb615	GCAGCTAGGAATAA**TGGAAT** (SEQ ID NO: 11)	GCAGCTAGGAATAA**TGGAAT** (SEQ ID NO: 11)	100 %	GGTGCATGGAATAATA**GAAT** (SEQ ID NO: 70)	75 %
PT7.1	ATTCTTGGACCGGC**GCAAGA** (SEQ ID NO: 12)	ATTCTTGGACCGGC**GCAAGA** (SEQ ID NO: 12)	100 %	ATTCTTGGATCGCA**GCAAGA** (SEQ ID NO: 71)	85 %
CA149	CTCAGCTAAGAGC**ATCGAGG** (SEQ ID NO: 13)	CTCAGCTAAGAGC**ATCGAGG** (SEQ ID NO: 13)	100 %	NA	0 %
CA172	TCTTAGCTGAGTGT**CCCGCG** (SEQ ID NO: 14)	TCTTAGCTGAGTGT**CCCGCG** (SEQ ID NO: 14)	100 %	NA	0 %
		Mean	100 %	Mean	45.5 %

CRISPR-Cas9 in vitro digestion selectively cleaves target organisms

In vitro digests of 18S V4 amplicons from single representative vertebrate hosts and eukaryotic endosymbionts corresponded to SILVA TestProbe predicted coverages (**FIG. 9**) and fragment sizes (**FIG. 8B**). For example, CC9 digestion with the "mammal" arb321 gRNA resulted in cleavage of mammal samples, but not amphibian, reptile, bird, or fish samples, whereas digestion with the "vertebrate" PT7.1 gRNA resulted in cleavage of all 5 host samples including mammal, amphibian, reptile, bird, and fish (**FIG. 10**, left panel). All eukaryotic endosymbiont amplicons, including protozoans (n = 2), microsporidians (n = 1), and helminths (n = 3) were unaffected by CC9 digestion using any gRNA (**FIG. 10**, right panel).

Evaluating host signal reduction methods

18S V4 metabarcoding using DNA extracted from chimpanzee samples as input (n = 15) with PNA blocker, CC9 digest, both PNA and digest, and no host signal reduction demonstrated CC9 digest to be the most effective method for enriching target read abundance for all sample types (blood, liver, lung, colon, and fecal samples; **FIG. 11A**; **Table 15**). Fecal samples yielded consistently low levels of host reads and were therefore not analyzed further. In tissue samples (blood, liver, lung, and colon), the overall percentage change in target (non-host) reads compared to no treatment control was significantly higher for CC9 treatment (mean 58.7 % increase in target reads, SEM 3.6 %, range 37.2 % - 79.9 %) compared to PNA (mean 1.5 %, SEM 1.3 %, range -7.1 % - 12.6 %; paired t-test: t = 6.94, df = 3, P = .0061) or combination treatment (mean -0.2 %, SEM 0.7 %, range -5.6 % - 2.9 %; paired t-test: t = 8.89, df = 3, P = 0.0030; **FIG. 11B**).

Table 15. Descriptive statistics of read data obtained from 18S V4 metabarcoding with CRISPR-Cas9 digest, PNA mammal blocker, both CRISPR-Cas9 digest and PNA mammal blocker, or no treatment applied to nonhuman primate blood and tissue samples

			% host reads after quality filtering			
Sample	Treatment	n	Mean	SEM	Min	Max
Blood	None	3	0.8719	0.0470	0.8044	0.9864
	PNA	3	0.7918	0.0644	0.6983	0.9485
	CC9	3	0.4399	0.0249	0.3819	0.4851
	Both	3	0.8714	0.0413	0.8006	0.9693
Liver	None	3	0.9946	0.0043	0.9841	0.9999
	PNA	3	0.9894	0.0044	0.9806	0.9992

	CC9	3	0.3643	0.0327	0.2924	0.4306
	Both	3	0.9846	0.0032	0.9775	0.9909
Lung	None	3	0.9067	0.0230	0.8736	0.9627
	PNA	3	0.9081	0.0182	0.8746	0.9504
	CC9	3	0.1620	0.0096	0.1406	0.1811
	Both	3	0.9116	0.0246	0.8669	0.9689
Colon	None	3	0.7223	0.0363	0.6752	0.8112
	PNA	3	0.7463	0.0314	0.6769	0.8099
	CC9	3	0.1805	0.0052	0.1688	0.1907
	Both	3	0.7353	0.0210	0.6926	0.7814
Fecal	None	3	0.0224	0.0051	0.0143	0.0347
	PNA	3	0.0242	0.0055	0.0166	0.0376
	CC9	3	0.0040	0.0018	0.0007	0.0083
	Both	3	0.0239	0.0043	0.0162	0.0339

Optimization of CRISPR-Cas9 digest

We optimized parameters of the CC9 digest by varying at the ratio of ribonucleoprotein complex to target DNA PAM sequence and found that a ratio of 1:1 was most effective at lowering host signal (**FIG. 12A**). To confirm the identity of the low molecular weight (MW) bands resulting from CC9 digest of mixed samples (containing both host and parasite DNA), we compared host read abundance in the higher- and lower- MW bands to show that the cleaved products are indeed of host origin (**FIG. 12B**). We also evaluated the application of the CC9 digest before and after indexing PCR. There was no significant difference in digest efficiency for CC9 treatment applied to each individual amplicon prior to library preparation compared to CC9 applied to a library pool (paired t-test: t = .38, df = 30, $P = 0.18$; **FIG. 12C**). Because application of the digest after indexing is simpler and cheaper, we used this variation of the HSR protocol for all subsequent metabarcoding experiments.

18S V4 metabarcoding using a panel of all six newly designed gRNAs demonstrated all gRNAs to reduce host signal compared to mock-treated controls, with vertebrate gRNA PT7.1 having the lowest abundance and mammal gRNA arb321 having the highest (**FIG. 12D**; **Table 16**). Further testing using the three top-performing gRNAs (arb326, CA149, and PT7.1) showed that digestion with any of the three gRNAs significantly reduced host reads compared to no-treatment controls (arb326 compared to none, paired t-test: t = 282.2, df = 30, $P < 0.0001$; CA149 compared to none, paired t-test: t = 123.6, df = 30, $P < 0.0001$; PT7.1 compared to non,

paired t-test: t = 370.3, df = 30, $P < 0.001$). There was also a small, but significant difference in signal reduction among the three gRNAs, with CA149 being most effective (CA149 compared to arb326, paired t-test: t = 2.10, df = 30, $P = 0.049$; CA149 compared to PT7.1, paired t-test: t = 2.52, df = 30, $P = 0.021$; **FIG. 12E**; **Table 16**).

Table 16. Descriptive statistics of read data obtained from 18S V4 metabarcoding with CRISPR-Cas9 digest or no treatment applied to nonhuman primate blood samples

		% host reads after quality filtering			
gRNA	n	Mean	SEM	Min	Max
PT7.1	3	0.2040	0.0095	0.1905	0.2174
CA149	3	0.2792	0.0046	0.2726	0.2857
arb326	3	0.2829	0.0233	0.2500	0.3158
arb615	3	0.4129	0.0059	0.4045	0.4212
arb321	3	0.4663	0.0366	0.4146	0.5180
CA172	3	0.4718	0.0122	0.4545	0.4891
NONE	3	0.9037	0.0070	0.8937	0.9136
Arb326	31	0.1917	0.0038	0.0974	0.2433
CA149	31	0.1744	0.0080	0.0587	0.2211
PT7.1	31	0.1886	0.0043	0.1027	0.2568
NONE	31	0.9926	0.0033	0.9097	1.0000

CRISPR-Cas9 digest validation using known parasite infections of mammals

Dirofilaria immitis in experimentally infected dogs. 18S V4 metabarcoding of experimentally infected dog blood samples containing *Dirofilaria immitis* microfilariae (mean 57.8 microfilariae per 20 µl whole blood) demonstrated CC9 digestion to be more effective at host signal reduction than PNA blocking oligo or mock treatment (**FIG. 13A**). Specifically, CC9-digested samples yielded a higher abundance of *Dirofilaria immitis* reads (mean of 6 gRNAs = 37.24 %, SEM = 4.38 %, range: 23.66 % - 54.59 %) than did PNA blocking oligo treatment (92.77 %) or mock control (88.96 %). Intriguingly, CC9-digested samples also recovered reads from fungi and dietary items that were not detected by the other methods (**FIG. 13B**; **Table 17**).

Table 17. Descriptive statistics of read data obtained from 18S V4 metabarcoding with CRISPR-

Cas9 digest or no treatment applied to dog blood samples with known *Dirofilaria immitis* infection

	% reads after quality filtering				
Treatment	Host	*Dirofilaria immitis*	Fungi	Plant	Bird
None	0.8896	0.0977	0.0037	0.0074	0.0016
PNA	0.9277	0.0608	0.0010	0.0065	0.0039
PT7.1	0.3308	0.5684	0.0780	0.0193	0.0036
CA149	0.2366	0.5999	0.1505	0.0128	0.0002
arb326	0.2634	0.6281	0.0664	0.0155	0.0266
arb615	0.4473	0.4763	0.0461	0.0233	0.0070
arb321	0.4104	0.4716	0.0725	0.0114	0.0339
CA172	0.5460	0.4006	0.0455	0.0030	0.0049
CC9 Mean	0.3724	0.5241	0.0765	0.0142	0.0127

Hepatocystis in naturally infected red colobus. Data from wild red colobus blood samples demonstrated that, in untreated libraries, almost all reads were of host origin (mean = 99.9 %) and no hemoparasites were detected. By contrast, CC9 treated libraries from the same samples had, on average, only 42.6 % host reads, and hemoparasites were detected in 17 of 19 samples (**FIG. 14**; **Table 18**). These findings mirrored previous results from *Hepatocystis*-specific PCR of these same samples (32), in which the same two species/lineages of *Hepatocystis* were detected: species A in 13 of the 17 infected samples and species B in 5 of the 17 infected samples (**Table 19**). Two samples were positive by metabarcoding that were negative by PCR. Percent agreement was low between PCR and metabarcoding without HSR treatment (Cohen's Kappa test: $\kappa = 0.0$, 95 % CI from 0.0 to 0.0) and high between PCR and metabarcoding with CC9 digest (Cohen's Kappa test: $\kappa = 0.855$, 95 % CI from 0.581 to 1.000). Overall application of CC9 digest increased agreement with PCR 6-fold compared to no treatment (**Table 20**).

Table 18. Descriptive statistics of read data obtained from 18S V4 metabarcoding with CRISPR-Cas9 digest or no treatment applied to red colobus blood samples

	No treatment				CRISPR-Cas9 digest				No treatment vs CC9
	% host	% other	% *Hepatocystis* sp. A	% *Hepatocystis* sp. B	% host	% other	% *Hepatocystis* sp. A	% *Hepatocystis* sp. B	% change host reads
1	1.0000	0.0000	0.0000	0.0000	0.5322	0.4634	0.0022	0.0000	0.4678
2	1.0000	0.0000	0.0000	0.0000	0.4455	0.5522	0.0000	0.0000	0.5545
3	1.0000	0.0000	0.0000	0.0000	0.3363	0.6637	0.0000	0.0000	0.6637
4	1.0000	0.0000	0.0000	0.0000	0.7154	0.1028	0.1818	0.0000	0.2846
5	1.0000	0.0000	0.0000	0.0000	0.5820	0.2827	0.1353	0.0000	0.4180
6	1.0000	0.0000	0.0000	0.0000	0.5712	0.3793	0.0494	0.0000	0.4288
7	1.0000	0.0000	0.0000	0.0000	0.5185	0.2420	0.2349	0.0046	0.4815
8	0.9999	0.0001	0.0000	0.0000	0.4639	0.3209	0.2152	0.0000	0.5360
9	0.9999	0.0001	0.0000	0.0000	0.3971	0.4385	0.1643	0.0000	0.6028
10	0.9996	0.0004	0.0000	0.0000	0.3966	0.5205	0.0829	0.0000	0.6030
11	0.9994	0.0006	0.0000	0.0000	0.3810	0.3174	0.3017	0.0000	0.6184
12	0.9994	0.0006	0.0000	0.0000	0.3668	0.5100	0.1232	0.0000	0.6326
13	0.9985	0.0015	0.0000	0.0000	0.2880	0.4337	0.2783	0.0000	0.7105
14	0.9981	0.0019	0.0000	0.0000	0.2604	0.3788	0.3599	0.0000	0.7377
15	0.9966	0.0034	0.0000	0.0000	0.2402	0.7125	0.0473	0.0000	0.7564
16	1.0000	0.0000	0.0000	0.0000	0.7654	0.1586	0.0000	0.0759	0.2346
17	1.0000	0.0000	0.0000	0.0000	0.3494	0.3589	0.0000	0.2912	0.6506
18	0.9998	0.0002	0.0000	0.0000	0.2534	0.4870	0.0000	0.2595	0.7464
19	0.9988	0.0012	0.0000	0.0000	0.2445	0.3058	0.0000	0.4497	0.7543

Table 19. *Hepatocystis* detection by PCR versus metabarcoding with and without CRISPR-Cas9 digestion

	PCR Positive/Negative		Metabarcoding, no treatment % reads post quality filtering		Metabarcoding, CC9 digest % reads post quality filtering	
ID #	*Hepatocystis* sp. A	*Hepatocystis* sp. B	*Hepatocystis* sp. A	*Hepatocystis* sp. B	*Hepatocystis* sp. A	*Hepatocystis* sp. B
1	Negative	Negative	0	0	0.002	0
2	Negative	Negative	0	0	0	0
3	Negative	Negative	0	0	0	0
4	Positive	Negative	0	0	0.182	0
5	Positive	Negative	0	0	0.135	0
6	Positive	Negative	0	0	0.049	0
7	Positive	Negative	0	0	0.235	0.005
8	Positive	Negative	0	0	0.215	0
9	Positive	Negative	0	0	0.164	0
10	Positive	Negative	0	0	0.083	0
11	Positive	Negative	0	0	0.302	0
12	Positive	Negative	0	0	0.123	0
13	Positive	Negative	0	0	0.278	0
14	Positive	Negative	0	0	0.36	0
15	Positive	Negative	0	0	0.047	0
16	Negative	Positive	0	0	0	0.076
17	Negative	Positive	0	0	0	0.291
18	Negative	Positive	0	0	0	0.26
19	Negative	Positive	0	0	0	0.45

Table 20. Percentage agreement statistics using Cohen's Kappa test of read data obtained from 18S V4 metabarcoding with CRISPR-Cas9 digest or no treatment applied to red colobus blood samples

		PCR	
		Negative	Positive
Metabarcoding, No HSR	Negative	3	16
	Positive	0	0

# observed agreements	3
% observed agreements	15.79%
Kappa	0
SE of Kappa	0

95% CI	0 to 0

		PCR	
		Negative	Positive
Metabarcoding, CC9 digest	Negative	2	0
	Positive	1	16

# observed agreements	18
% observed agreements	94.74%
Kappa	0.855
SE of Kappa	0.14
95% CI	0.581 to 1.000

Discussion:

Here we show that a newly designed method using CRISPR-Cas9 and vertebrate host-targeted guide RNAs was more effective at host signal reduction than PNA blocking or no treatment. Furthermore, in samples known from prior analyses to contain parasites, eukaryotic endosymbiont reads were rare or not detectable in samples treated with a PNA blocking primer or not treated with any HSR method. However, when the new CC9 method was applied to these same samples, the parasites were detected at high read intensities. The new CC9 method also yielded reads matching two lineages of *Hepatocystis* previously characterized in red colobus using genus specific PCR (32).

The utility of the CC9 HSR method depends on the specificity of gRNAs (36, 43). We attempted to maximize specificity by designing gRNAs using several complementary approaches and screening a large pool of 100 candidate oligos to identify six final gRNA sequences. We then rigorously evaluated these six oligos *in silico* and in laboratory experiments using gDNA from individual eukaryotic organisms and from clinical samples infected with eukaryotic parasites. The consistency of our results across these conditions strongly suggests that the CC9 method is specific, effective, and robust. We note, however, that 8 % - 23 % of sequences from the nematode parasite *Trichinella pseudospiralis* were highly similar to the mammalian 18S V4 region CC9 recognition sites, reducing specificity in the case of this genus. If *Trichinella* is suspected, we recommend the use of gRNAs CA 149 and CA 172, which have the lowest cross-

reactivity. We also recommend *in silico* analysis to verify host complementarity prior to choosing a particular gRNA.

A distinct advantage of our method is that it does not depend on the PCR primers used to amplify the 18S V4 region, as long as those primers flank the site of gRNA complementarity. Therefore, any amplicon including the 18S V4 region is compatible with all gRNA oligos presented here. As is described in Example 1, we recently developed a new set of eukaryotic endosymbiont metabarcoding primers that out-performs all other published primer sets in terms of taxonomic breath, on-target amplification, and unbiased reconstruction of eukaryotic communities. We have examined this primer set in conjunction with the CC9 protocol described herein, and in combination the two methods achieve a similar reduction of host signal as this study (82 % less host reads compared to no treatment and 74 % compared to PNA clamp in blood samples; unpublished data). Also, because 18S V4 has the highest entropy of the hypervariable regions constituting 18S (44, 45), and thus the highest taxonomic resolution, we expect our gRNA designs to stay relevant for as long as this locus remains the industry standard for eukaryotic endosymbiont metabarcoding.

Overall, we have shown that CRISPR-Cas9 digestion of amplicons reduces host signal sufficiently to allow for detection of rare eukaryotic endosymbionts and thus to increase the sensitivity and efficiency of eukaryotic endosymbiont metabarcoding. Our new method should help advance the fields of parasitology and eukaryotic community ecology, similar to how 16S prokaryote metabarcoding has facilitated the study the microbiome.

Materials and Methods:

Sample collection and characterization

We used archived blood, tissue, and fecal samples from wild nonhuman primates, including western chimpanzees (*Pan troglodytes verus*) from Sierra Leone and red colobus (*Procolobus rufomitratus*) from Uganda that had been collected as part of previous studies (31, 32). Appropriate permits and approvals were obtained by each research team prior to collection and shipping of samples. Blood and tissue samples from chimpanzees had been assessed for pathogenic organisms as described in Owens, et al (31). Blood samples from red colobus had been assessed for *Hepatocystis* parasites as described in Thurber, et al (32). Blood from domestic dogs (*Canis lupis familiaris*) experimentally infected with *Dirofilaria immitis* strain "Missouri"

was obtained via BEI resources (Catalog # NR-48907; Manassas, VA, USA), 20 µl was added to a glass slide and combined with two drops of 2 % formalin, and microfilaria were enumerated using phase optics at x 10 magnification. Samples were examined in triplicate and load was expressed as number of microfilariae per 20 µl of blood averaged across the three replicates. Genomic DNA (gDNA) from single hosts and parasites were obtained from in-house sample archives retained from prior studies (Owens VESPA).

DNA extraction and 18S V4 metabarcoding

Fecal samples were thawed on ice and homogenized by vortexing prior to transferring 0.2 g of homogenate to bead beating tubes for DNA extraction using the DNeasy PowerLyzer PowerSoil Kit (Qiagen, Hilden, Germany), with gDNA eluted in C6 buffer and stored at -20 °C. Whole blood, serum, and plasma were thawed on ice and solid tissue samples were subsampled with a sterile 3 mm biopsy punch (Integra Life Sciences, Princeton, NJ, USA) while still frozen. gDNA was extracted from blood products and tissue samples using the Qiagen DNeasy Blood and Tissue kit following manufacturer's instructions, eluted in buffer AE, and stored at -20 °C.

Primers used to amplify the hypervariable 4 region (V4) of the 18S small subunit (SSU) ribosomal RNA (rRNA) gene (18S V4 hereafter) were based on published pan-eukaryotic sequences E572F and E1009R (33), which were modified to replace individual barcodes with overhang adapters (underlined) compatible with the Nextera library preparation system (Illumina, San Diego, CA, USA): F 5′-TCGTCGGCAGCGTCAGATGTGTATAAGAGACAG-CYGCGGTAATTCCAGCTC-3′ (SEQ ID NO: 66 - SEQ ID NO: 15) and R 5′-GTCTCGTGGGCTCGGAGATGTGTATAAGAGACAG-AYGGTATCTRATCRTCTTYG-3′ (SEQ ID NO: 67 - SEQ ID NO: 16). The most commonly published HSR method (host amplification blocking), which we used in this study, was a peptide nucleic acid (PNA) mammal blocking primer (PNA Bio, Thousand Oaks, CA, USA): 5′-TCTTAATCATGGCCTCAGTT-3′ (SE ID NO: 17) (24). Conditions for amplicon PCR with and without blocking primer were based on those described in Mann et al. (24). Resulting PCR products were cleaned using AMPure XP beads (Agencourt, Beverley, MA, USA) according to manufacturer's instructions and 5 µl was used as template in a 25-µl PCR with the Illumina Nextera XT Index Kit v2 and limited-cycle PCR with an annealing temperature of 55 °C for 10 cycles. Indexed libraries were cleaned using Agencourt AMPure XP beads and quantified using a Qubit fluorometer

(ThermoFisher Scientific, Waltham, MA, USA). Libraries were sequenced on an Illumina MiSeq instrument using paired-end 300 ×300 cycle V3 chemistry.

Guide RNA design and in silico screening

We used two concurrent approaches to design gRNA sequences to target vertebrate host 18S V4: 1) the ARB 7.0 software package (34) with the SILVA SSU rRNA 132 Non-redundant Reference (RefNR) database (35), and 2) The Broad Institute's online CRISPick tool (portals.broadinstitute.org/gppx/crispick/public) (36) using human (*Homo sapiens*, NCBI RefSeq GCF_000001405.40), house mouse (*Mus musculus*, NCBI RefSeq GCF_000001635.26), domestic dog (*Canis lupus familiaris*, NCBI RefSeq GCF_000002285.5), and chimpanzee (*Pan troglodytes*, NCBI RefSeq GCF_002880755.1) genomes as input. We screened 50 candidate gRNA sequences generated from each of these tools (n = 100 total) using SILVA TestProbe (37) *in silico* hybridization to the SILVA 138.1 RefNR database with maximum stringency (no mismatches between gRNA sequence and DNA target) or allowing for a single mismatch outside of the 6-base pair "seed sequence" (**Table 13**). Resulting coverage metrics were used to choose the six gRNA sequences that targeted the highest number of vertebrates and lowest number of eukaryotic endosymbionts for further testing: arb321, arb326, arb615 were designed in the arb software suite, and CA149, CA172, PT7.1 were designed using CRISPick. Alignments of gRNAs with host sequences and digest maps were visualized using CLC Genomics Workbench v.20.2.4 (Qiagen, Hilden, Germany).

CRISPR-Cas9 in vitro digestion of representative organisms

All reagents for CC9 treatment of amplicons were components of the Alt-R CRISPR-Cas9 system (Integrated DNA Technologies, Coralville, IA, USA), based on recombinant *Streptococcus pyogenes* Cas9 nuclease, including Alt-R® S.p. Cas9 Nuclease V3, Alt-R® CRISPR-Cas9 tracrRNA, and Alt-R® CRISPR-Cas9 crRNA. crRNA is the component containing the specific targeting sequence that, when complexed with tracrRNA, forms the functional gRNA (see **Table 13** for sequences). Digest reactions were performed following the IDT "Alt-R CRISPR-Cas9 system – *in vitro* cleavage of target DNA with RNP complex" protocol version 2.2 using recommendations for PCR product templates of 500 – 2000 base pair lengths and 2 – 5 nM final DNA concentration per reaction.

CC9 cleavage and gRNA specificity were initially assessed *in vitro* using a panel of genomic DNA samples extracted from single representative vertebrate hosts (n = 5) and eukaryotic endosymbionts (n = 6). Representative host organisms included: Mammal- *Ursus maritimus* (polar bear), Amphibian- *Lithobates chiricahuensis* (leopard frog), Bird- *Gallus gallus* (chicken), Reptile- *Varanus varius* (monitor lizard), and Fish- *Salmo trutta* (brown trout). Representative eukaryotic endosymbiont organisms included: Protozoan- *Entamoeba histolytica* (amoeba), Protozoan- *Trypanosoma brucei* (flagellate), Microsporidian- *Encephalitozoon cuniculi,* Acanthocephalan- *Echinorhynchus salmonis* (spiny-headed worm), Platyhelminth- *Schistosoma mansoni* (fluke), and Nematode- *Ascaris suum* (roundworm). 18S V4 amplicon PCR was performed as described above, and resulting amplicons were used in Alt-R CRISPR-Cas9 digest reactions. Cleavage products were separated by gel electrophoresis on 1.5% agarose gels containing .02 µg/ml ethidium bromide, visualized under ultraviolet light, and documented using a GelDoc XR imager (BioRad, Hercules, CA, USA). Successful cleavage was indicated by the presence of bands of between approximately 150 - 500 base pairs, which were discernably smaller than the full 18S V4 amplicon of approximately 700 base pairs.

Comparison of host signal reduction methods

We compared the efficacy of HSR for improving eukaryotic endosymbiont metabarcoding by performing 18S V4 library preparation in conjunction with 4 different protocols 1) CC9 digestion of amplicons using gRNA arb321, 2) published V4 PNA mammal-blocking oligo described above [23] added to the amplicon PCR, 3) both CC9 digestion and PNA mammal-blocking oligo, and 4) mock-treated control (no CRISPR-Cas9 or PNA reagents added). PCR templates consisted of gDNA extracted from chimpanzee blood, liver, lung, colon, and fecal samples (n = 3 each). 18S V4 library preparation and CC9 digests were performed as described above. For CC9 digested amplicons, uncleaved products (bands corresponding to undigested target amplicons) were excised from agarose gels using sterile razor blades and DNA was extracted from the gel matrix using a the ZymoClean Gel DNA Recovery Kit (Zymo, Irvine, CA, USA) according to manufacturer's instructions.

Optimization of CRISPR-Cas9 digest

We tested various ratios of ribonucleoprotein complex (RNP) to host target DNA of 0.75:1, 1:1, and 1.25:1 in our CRISPR-Cas9 digest. CC9 treatment was also tested at two steps in

the metabarcoding protocol: 1) after initial amplification and cleanup, prior to indexing PCR (requiring one digest reaction per sample) or 2) after indexing PCR, clean up and pooling of libraries (requiring one digest reaction total for the combined pool of samples). For evaluation of the effect of gRNA targeting sequence on CC9 digest efficiency, we performed metabarcoding on chimpanzee blood samples (n = 3) using a panel of all 6 newly designed gRNAs. We amplified 18S V4 from each sample and divided the PCR products into seven equal parts (one for each gRNA and one for a no-treatment control) prior to library preparation followed by sequencing and quantification of host read abundance under each condition. The top three gRNAs (arb326, CA149, PT7.1) were then tested in the same manner on a larger set of chimpanzee blood samples (n = 31).

Detection of known parasite infections in mammal blood samples

To test the effect of HSR and CC9 on detection of eukaryotic parasites in a verified infection, we performed eukaryotic endosymbiont metabarcoding on dog blood samples containing a mean of 57.8 *Dirofilaria immitis* microfilariae per 20 µl whole blood. We prepared sequencing libraries using CC9 digestion with a panel of all 6 newly designed gRNAs, amplification with a PNA blocking oligo or mock-treated control prior to sequencing, and quantified host read abundance under each condition.

For metabarcoding of naturally infected hosts, we used whole blood samples from wild red colobus that were characterized by microscopic investigation and PCR as part of a concluded study (32). Most samples (n = 16 of 19) had been found to contain one of two distinct lineages of the apicomplexan parasite *Hepatocystis*: species A in 12 of 16 infected hosts, and species B in 4 of 16 infected hosts (32). We used aliquots of these same blood samples for gDNA extraction, 18S amplicon library preparation, treatment with CC9 digest or mock control, sequencing, and quantification of host read abundances.

Sequence data processing and analyses

Raw sequence reads were processed using QIIME2 v.1.9.1 (38). Forward and reverse reads were assembled into paired contigs using the command multiple_join_paired_ends.py and quality filtered using the command multiple_split_libraries_fastq.py with default parameters, except for setting the Phred threshold to 30 or higher (-q 29) and minimum length to 100 bp (-l 100). Chimeras were identified with Usearch v.6.1 (39) and removed. Reads were then assigned

to OTUs using the QIIME protocol for open reference OTU picking with the command pick_open_reference_otus.py and the default UCLUST tool (v.0.2.0) (40), and taxonomy was assigned to OTUs using default settings with the command assign_taxonomy.py against the SILVA database v. 132 (35). Still-undetermined OTUs were assigned using BLAST within QIIME2 (-m blast) against the full GenBank nucleotide database (41). OTUs constituting < 0.5 % of the total data set were removed from further analyses. Prism v.8.4.3 (GraphPad Software, Inc.) was used for plotting data and conducting statistical analyses.

References:

1. Forsman AM, Savage AE, Hoenig BD, Gaither MR. DNA Metabarcoding Across Disciplines: Sequencing Our Way to Greater Understanding Across Scales of Biological Organization. Integr Comp Biol. 2022;62(2):191-8.

2. Hamady M, Knight R. Microbial community profiling for human microbiome projects: Tools, techniques, and challenges. Genome Res. 2009;19(7):1141-52.

3. Tedersoo L, Bahram M, Zinger L, Nilsson RH, Kennedy PG, Yang T, et al. Best practices in metabarcoding of fungi: From experimental design to results. Mol Ecol. 2022;31(10):2769-95.

4. Laforest-Lapointe I, Arrieta MC. Microbial Eukaryotes: a Missing Link in Gut Microbiome Studies. mSystems. 2018;3(2).

5. Lundberg DS, Yourstone S, Mieczkowski P, Jones CD, Dangl JL. Practical innovations for high-throughput amplicon sequencing. Nat Methods. 2013;10(10):999-1002.

6. Sakai M, Ikenaga M. Application of peptide nucleic acid (PNA)-PCR clamping technique to investigate the community structures of rhizobacteria associated with plant roots. J Microbiol Methods. 2013;92(3):281-8.

7. Vestheim H, Jarman SN. Blocking primers to enhance PCR amplification of rare sequences in mixed samples - a case study on prey DNA in Antarctic krill stomachs. Front Zool. 2008;5:12.

8. Belda E, Coulibaly B, Fofana A, Beavogui AH, Traore SF, Gohl DM, et al. Preferential suppression of *Anopheles gambiae* host sequences allows detection of the mosquito eukaryotic microbiome. Sci Rep. 2017;7(1):3241.

9. Sow A, Brevault T, Benoit L, Chapuis MP, Galan M, Coeur d'acier A, et al. Deciphering host-parasitoid interactions and parasitism rates of crop pests using DNA metabarcoding. Sci Rep. 2019;9(1):3646.

10. Nicolas L, Prina E, Lang T, Milon G. Real-time PCR for detection and quantitation of leishmania in mouse tissues. J Clin Microbiol. 2002;40(5):1666-9.

11. Titus RG, Marchand M, Boon T, Louis JA. A limiting dilution assay for quantifying Leishmania major in tissues of infected mice. Parasite Immunol. 1985;7(5):545-55.

12. Alberdi A, Aizpurua O, Gilbert MTP, Bohmann K. Scrutinizing key steps for reliable metabarcoding of environmental samples. Methods Ecol Evol. 2018;9(1):134-47.

13. Jiang P, Lai S, Wu S, Zhao XM, Chen WH. Host DNA contents in fecal metagenomics as a biomarker for intestinal diseases and effective treatment. BMC Genomics. 2020;21(1):348.

14. Feehery GR, Yigit E, Oyola SO, Langhorst BW, Schmidt VT, Stewart FJ, et al. A method for selectively enriching microbial DNA from contaminating vertebrate host DNA. PLoS One. 2013;8(10):e76096.

15. O'Rorke R, Lavery S, Jeffs A. PCR enrichment techniques to identify the diet of predators. Mol Ecol Resour. 2012;12(1):5-17.

16. Flaherty BR, Talundzic E, Barratt J, Kines KJ, Olsen C, Lane M, et al. Restriction enzyme digestion of host DNA enhances universal detection of parasitic pathogens in blood via targeted amplicon deep sequencing. Microbiome. 2018;6(1):164.

17. Terahara T, Chow S, Kurogi H, Lee SH, Tsukamoto K, Mochioka N, et al. Efficiency of peptide nucleic acid-directed PCR clamping and its application in the investigation of natural diets of the Japanese eel leptocephali. PLoS One. 2011;6(11):e25715.

18. Vestheim H, Deagle BE, Jarman SN. Application of blocking oligonucleotides to improve signal-to-noise ratio in a PCR. Methods Mol Biol. 2011;687:265-74.

19. Mayer T, Mari A, Almario J, Murillo-Roos M, Abdullah M, Dombrowski N, et al. Obtaining deeper insights into microbiome diversity using a simple method to block host and non-targets in amplicon sequencing. bioRxiv. 2020.

20. Flaherty BR, Barratt J, Lane M, Talundzic E, Bradbury RS. Sensitive universal detection of blood parasites by selective pathogen-DNA enrichment and deep amplicon sequencing. Microbiome. 2021;9(1):1.

21. Mamanova L, Coffey AJ, Scott CE, Kozarewa I, Turner EH, Kumar A, et al. Target-enrichment strategies for next-generation sequencing. Nat Methods. 2010;7(2):111-8.

22. von Wintzingerode F, Landt O, Ehrlich A, Göbel UB. Peptide nucleic acid-mediated PCR clamping as a useful supplement in the determination of microbial diversity. Appl Environ Microbiol. 2000;66(2):549-57.

23. Troedsson C, Lee RF, Stokes V, Walters TL, Simonelli P, Frischer ME. Development of a denaturing high-performance liquid chromatography method for detection of protist parasites of metazoans. Appl Environ Microbiol. 2008;74(14):4336-45.

24. Mann AE, Mazel F, Lemay MA, Morien E, Billy V, Kowalewski M, et al. Biodiversity of protists and nematodes in the wild nonhuman primate gut. Isme J. 2020;14(2):609-22.

25. Hino A, Maruyama H, Kikuchi T. A novel method to assess the biodiversity of parasites using 18S rDNA Illumina sequencing; parasitome analysis method. Parasitol Int. 2016;65(5):572-5.

26. Lappan R, Classon C, Kumar S, Singh OP, de Almeida RV, Chakravarty J, et al. Meta-taxonomic analysis of prokaryotic and eukaryotic gut flora in stool samples from visceral leishmaniasis cases and endemic controls in Bihar State India. PLoS Negl Trop Dis. 2019;13(9):e0007444.

27. Wu J, Huang B, Chen H, Yin Q, Liu Y, Xiang Y, et al. The landscape of accessible chromatin in mammalian preimplantation embryos. Nature. 2016;534(7609):652-7.

28. Gu W, Crawford ED, O'Donovan BD, Wilson MR, Chow ED, Retallack H, et al. Depletion of Abundant Sequences by Hybridization (DASH): using Cas9 to remove unwanted high-abundance species in sequencing libraries and molecular counting applications. Genome Biol. 2016;17:41.

29. Song L, Xie K. Engineering CRISPR/Cas9 to mitigate abundant host contamination for 16S rRNA gene-based amplicon sequencing. Microbiome. 2020;8(1):80.

30. Wu X, Kriz AJ, Sharp PA. Target specificity of the CRISPR-Cas9 system. Quant Biol. 2014;2(2):59-70.

31. Owens LA, Colitti B, Hirji I, Pizarro A, Jaffe JE, Moittie S, et al. A *Sarcina* bacterium linked to lethal disease in sanctuary chimpanzees in Sierra Leone. Nature communications. 2021;12(1):763.

32. Thurber MI, Ghai RR, Hyeroba D, Weny G, Tumukunde A, Chapman CA, et al. Co-infection and cross-species transmission of divergent Hepatocystis lineages in a wild African primate community. Int J Parasitol. 2013;43(8):613-9.

33. Comeau AM, Li WK, Tremblay JE, Carmack EC, Lovejoy C. Arctic Ocean microbial community structure before and after the 2007 record sea ice minimum. PLoS One. 2011;6(11):e27492.

34. Ludwig W, Strunk O, Westram R, Richter L, Meier H, Yadhukumar, et al. ARB: a software environment for sequence data. Nucleic Acids Res. 2004;32(4):1363-71.

35. Quast C, Pruesse E, Yilmaz P, Gerken J, Schweer T, Yarza P, et al. The SILVA ribosomal RNA gene database project: improved data processing and web-based tools. Nucleic Acids Res. 2013;41(Database issue):D590-6.

36. Doench JG, Fusi N, Sullender M, Hegde M, Vaimberg EW, Donovan KF, et al. Optimized gRNA design to maximize activity and minimize off-target effects of CRISPR-Cas9. Nat Biotechnol. 2016;34(2):184-91.

37. Klindworth A, Pruesse E, Schweer T, Peplies J, Quast C, Horn M, et al. Evaluation of general 16S ribosomal RNA gene PCR primers for classical and next-generation sequencing-based diversity studies. Nucleic Acids Res. 2013;41(1):e1.

38. Caporaso JG, Kuczynski J, Stombaugh J, Bittinger K, Bushman FD, Costello EK, et al. QIIME allows analysis of high-throughput community sequencing data. Nat Methods. 2010;7(5):335-6.

39. Edgar RC, Haas BJ, Clemente JC, Quince C, Knight R. UCHIME improves sensitivity and speed of chimera detection. Bioinformatics. 2011;27(16):2194-200.

40. Edgar RC. Search and clustering orders of magnitude faster than BLAST. Bioinformatics. 2010;26(19):2460-1.

41. Sayers EW, Cavanaugh M, Clark K, Pruitt KD, Schoch CL, Sherry ST, et al. GenBank. Nucleic Acids Res. 2021;49(D1):D92-D6.

42. Comeau AM, Douglas GM, Langille MG. Microbiome Helper: a Custom and Streamlined Workflow for Microbiome Research. mSystems. 2017;2(1).

43. Cho SW, Kim S, Kim Y, Kweon J, Kim HS, Bae S, et al. Analysis of off-target effects of CRISPR/Cas-derived RNA-guided endonucleases and nickases. Genome Res. 2014;24(1):132-41.

44. Bradley IM, Pinto AJ, Guest JS. Design and Evaluation of Illumina MiSeq-Compatible, 18S rRNA Gene-Specific Primers for Improved Characterization of Mixed Phototrophic Communities. Appl Environ Microbiol. 2016;82(19):5878-91.

45. Pinol J, Senar MA, Symondson WOC. The choice of universal primers and the characteristics of the species mixture determine when DNA metabarcoding can be quantitative. Mol Ecol. 2019;28(2):407-19.

CLAIMS

What is claimed:

1. A primer set comprising a forward primer comprising a sequence selected from SEQ ID NOs: 1-4 and a reverse primer comprising a sequence selected from SEQ ID NOs: 5-8.

2. The primer set of claim 1, wherein the forward primer comprises SEQ ID NO: 3.

3. The primer set of claim 1 or 2, wherein the reverse primer comprises SEQ ID NO: 6.

4. A guide RNA (gRNA) selected from SEQ ID NOs: 9-14.

5. The gRNA of claim 4, wherein the gRNA hybridizes to 18S rRNA gene amplicons from vertebrates but does not hybridize to 18S rRNA gene amplicons from eukaryotic endosymbionts.

6. A mock community of eukaryotic endosymbionts comprising 18S rRNA genes, or portions thereof, from a plurality of eukaryotic endosymbionts in equimolar quantities, wherein the plurality of eukaryotic endosymbionts comprises two or more eukaryotic endosymbionts selected from the group consisting of: *Echinorhynchus salmonis* (ES201), *Hymenolopis diminuta* (HD1), *Ascaris suum* (AS1), *Dirofilaria immitis* (DI8), *Trichinella spiralis* (TS3), *Encephalitozoon cuniculi* (EC2), *Entamoeba histolytica* (EH3), *Balamuthia mandrillaris* (BM2), *Naegleria fowleri* (NF12), *Leishmania major* (LM4), *Giardia intestinalis* (GI405), *Plasmodium falciparum* (PF115), *Babesia* sp. (Bab10), *Toxoplasma gondii* (TG3), *Cryptosporidium hominis* (CH109), and *Blastocystis hominis* 1 (ATCC 50177) (BH1).

7. The mock community of claim 6, wherein the plurality of eukaryotic endosymbionts comprises ES201, HD1, AS1, DI8, TS3, EC2, EH3, BM2, NF12, LM4, GI405, PF115, Bab10, TG3, CH109, and BH1.

8. A method for assessing the ability of a primer set to detect one or more eukaryotic endosymbionts, the method comprising:

a) amplifying the mock community of claim 6 or 7 using the primer set; and

b) detecting any resulting amplicons;

wherein detection of an amplicon associated with a particular eukaryotic endosymbiont indicates that the primer set is able to detect that particular eukaryotic endosymbiont.

9. A method for detecting one or more eukaryotic endosymbionts in a sample, the method comprising:

a) extracting DNA from the sample;

b) amplifying the DNA using the primer set of any one of claims 1-3 to generate amplicons;

c) sequencing the amplicons to generate sequencing reads; and

d) analyzing the sequencing reads;

wherein the presence of sequencing reads associated with a particular eukaryotic endosymbiont indicates that the eukaryotic endosymbiont is present in the sample.

10. The method of claim 9, further comprising: adding an RNA-guided nuclease and the gRNA of claim 4 or 5 to the amplicons generated in step (b) to digest amplicons generated from host DNA prior to step (c).

11. A method for diagnosing and treating a subject with a parasitic infection, the method comprising:

a) obtaining a sample from the subject;

b) extracting DNA from the sample;

c) amplifying the DNA using the primer set of any one of claims 1-3 to generate amplicons;

d) sequencing the amplicons to generate sequencing reads;

e) analyzing the sequencing reads to detect the presence of a parasite in the sample; and

f) treating the subject for the detected parasite.

12. The method of claim 11, wherein the subject is a human.

13. The method of claim 11 or 12, further comprising: adding an RNA-guided nuclease and the gRNA of claim 4 or 5 to the amplicons generated in step (c) to digest amplicons generated from host DNA prior to step (d).

14. The method of any one of claims 9-13, further comprising amplifying the mock community of claim 6 or 7 in step (c) as a positive control.

15. The method of any one of claims 9-14, wherein the sample is a blood sample or fecal sample.

16. The method of claim 15, wherein the primer set comprises the forward primer of SEQ ID NO: 3 and the reverse primer of SEQ ID NO: 6.

17. The method of any one of claims 9-16, wherein the method is capable of detecting parasites from 24 clinically relevant clades.

18. The method of any one of claims 9-17, wherein less than 50% of the sequencing reads are off-target reads.

19. A kit comprising the primer set of any one of claims 1-3 and instructions for use.

20. The kit of claim 19, further comprising the gRNA of claim 4 or 5.

21. The kit of claim 19 or 20, further comprising the mock community of claim 6 or 7.

22. The kit of any one of claims 19-21, further comprising adapters.

23. The kit of claim 22, wherein the forward primer further comprises a first adapter and the reverse primer further comprises a second adapter.

FIG. 1A

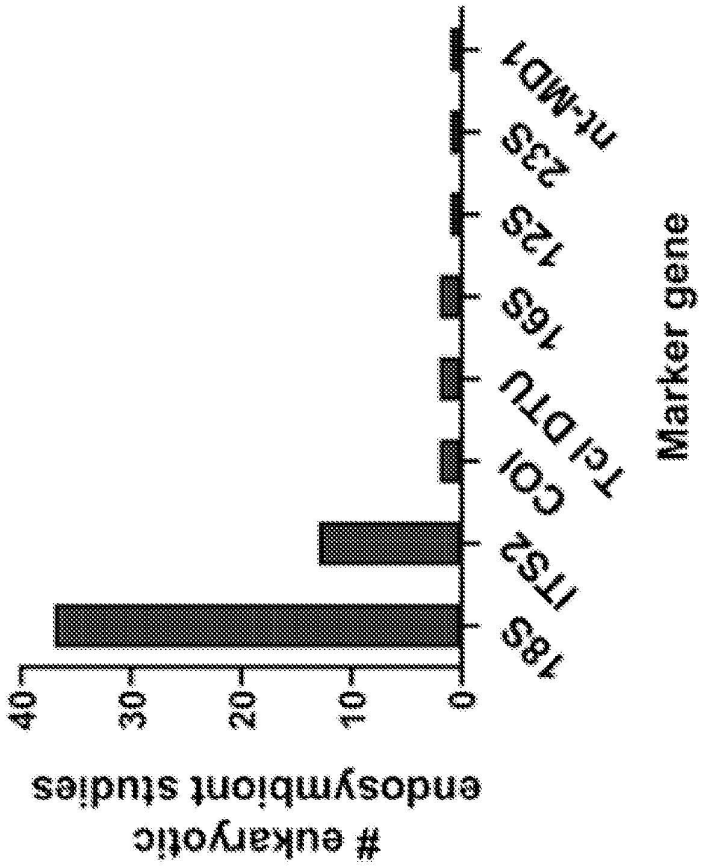
eukaryotic endosymbiont studies
0
10
20
30
40
18S
ITS2
Tci CO1
Tci DTU
16S
12S
23S
nt-MD1
Marker gene

FIG. 1B

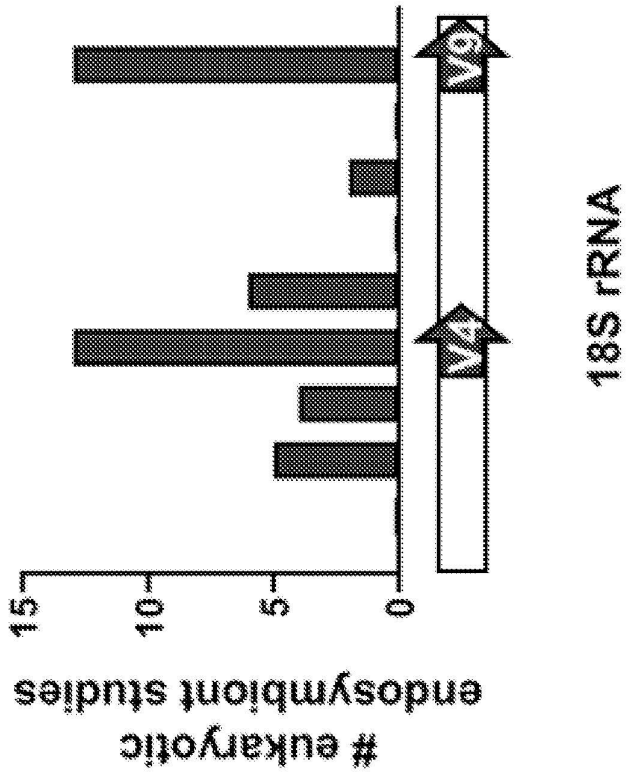
eukaryotic endosymbiont studies
0
5
10
15
V4
V9
18S rRNA

FIG. 1C

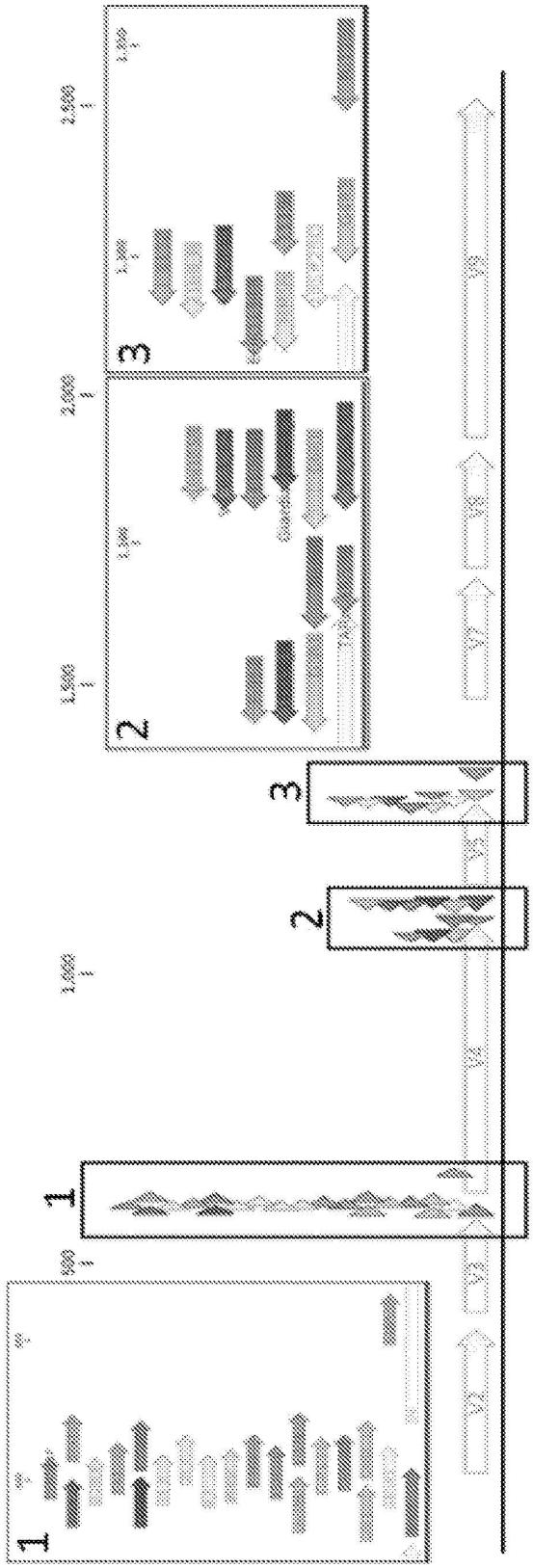

FIG. 1D

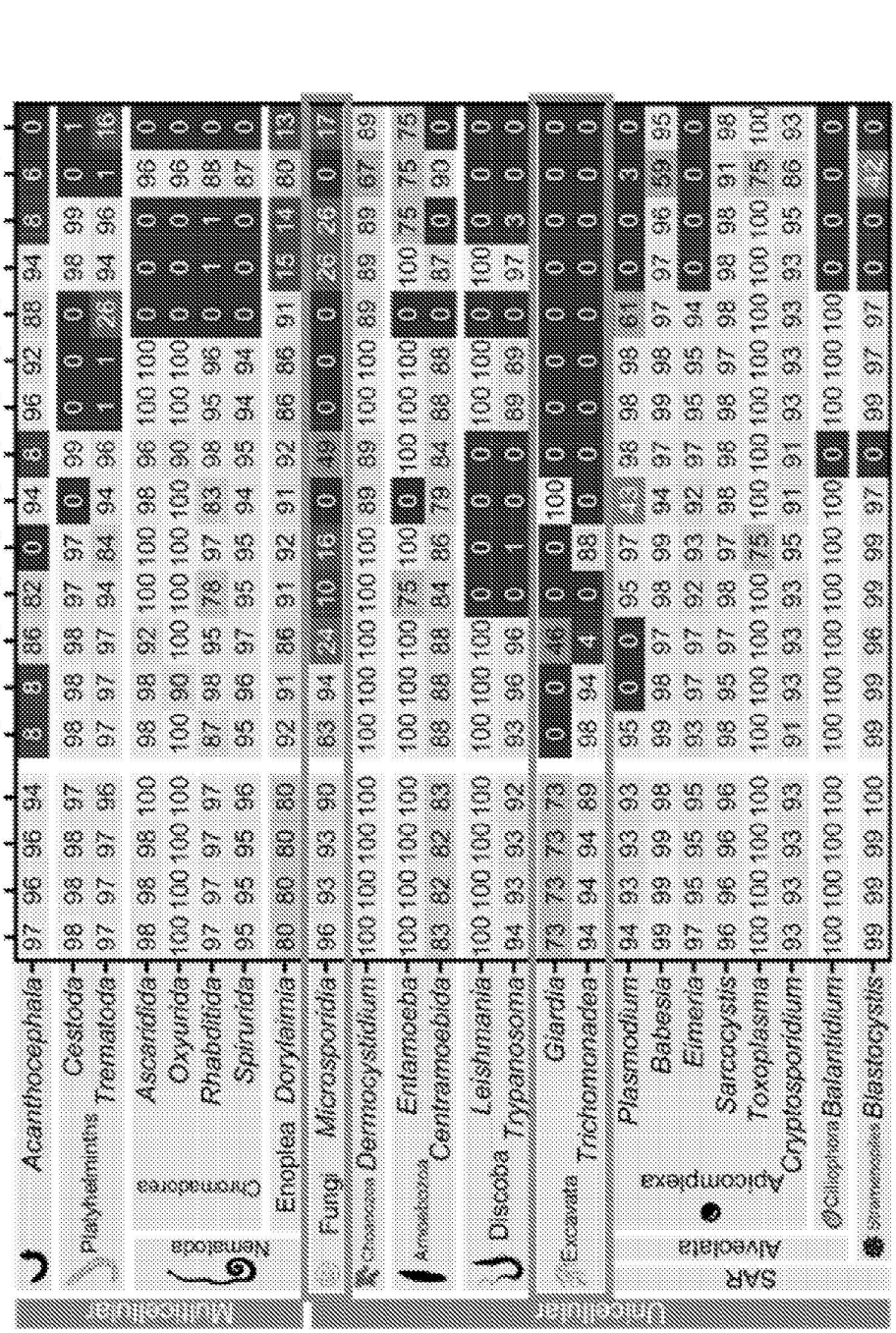
Owens-29F
Owens-2-2bF
Owens-13F
Owens-9F
Bates
C-S/Oelsen
Hugerth
Krogsgaard
Hadziavdic-566
DeMone
Machida
Stoeck
Bradley
Hadziavdic-574
Comeau
C-S/Brate-2
Wood
C-S/Brate-1
Helminths
Platyhelminths
Nematoda
Arthropoda
Fungi
Chlorophyta
Amoebozoa
Discoba
Excavata
SAR
Alveolata
Apicomplexa
Chromerida
Acanthocephala
Cestoda
Trematoda
Ascaridida
Oxyurida
Rhabditida
Spirurida
Enoplea
Dorylaimia
Microsporidia
Dermocystidium
Entamoeba
Centramoebida
Leishmania
Trypanosoma
Giardia
Trichomonadea
Plasmodium
Babesia
Eimeria
Sarcocystis
Toxoplasma
Cryptosporidium
Balantidium
Blastocystis
0
20
40
60
80
100

FIG. 1E

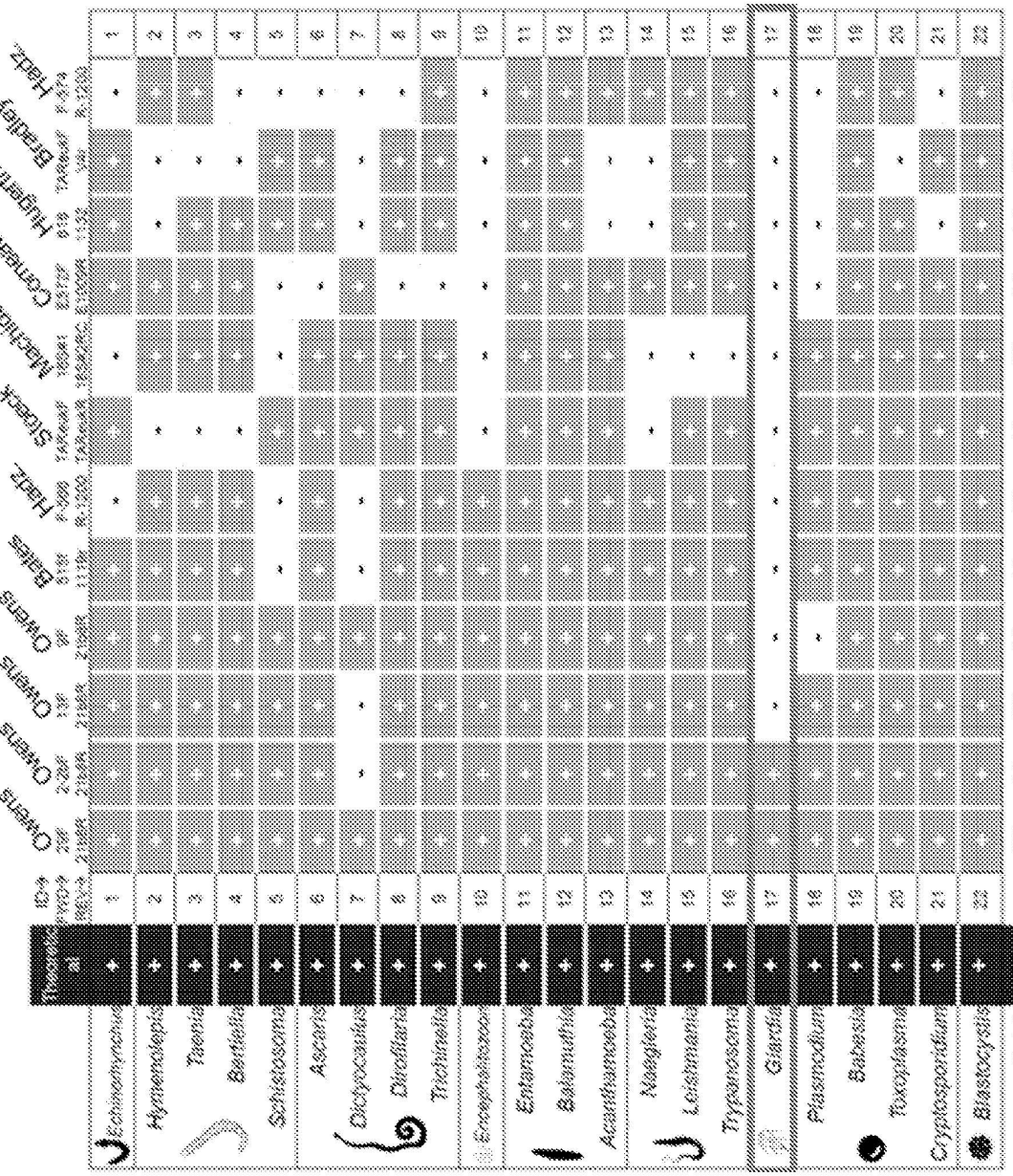

FIG. 2A

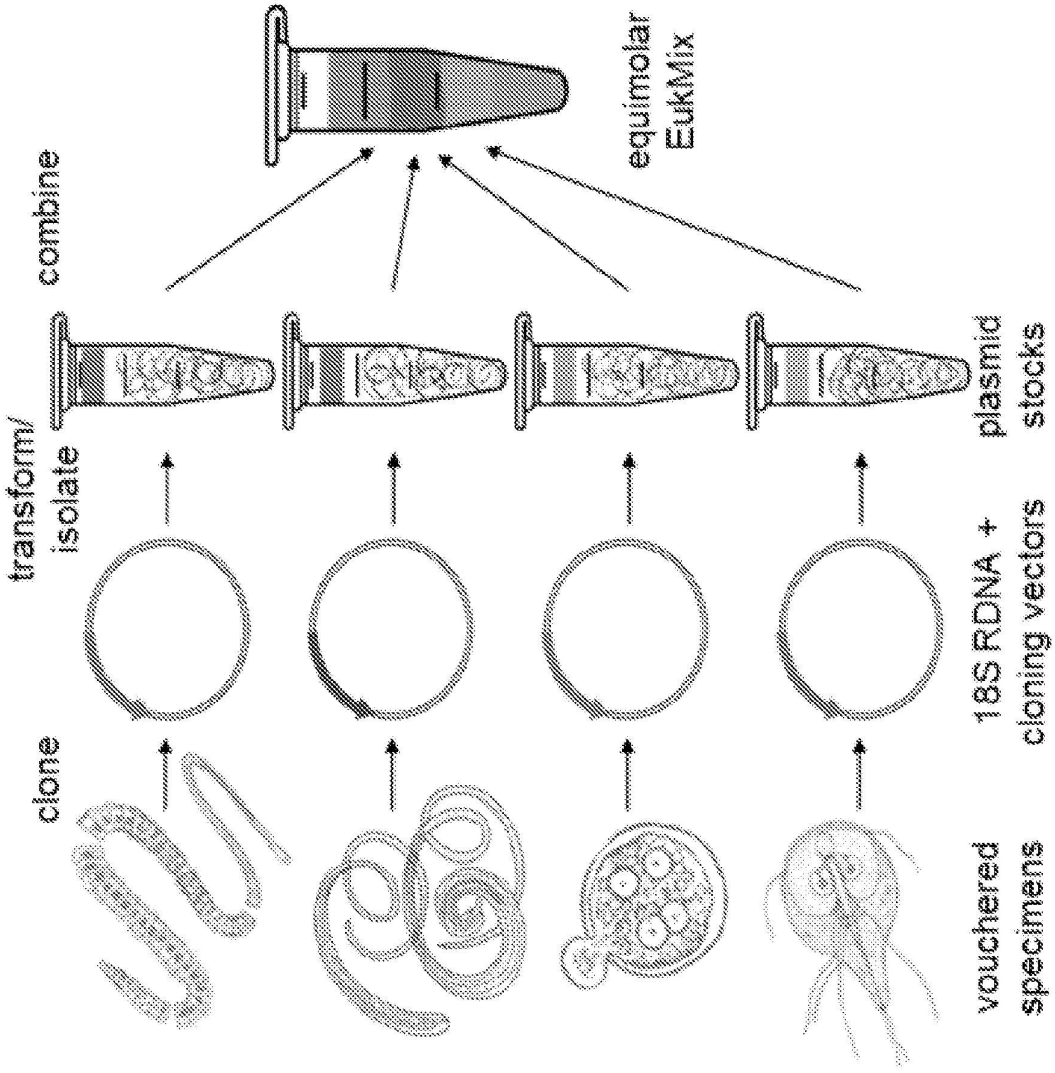
vouchered specimens
clone
18S RDNA + cloning vectors
transform/ isolate
plasmid stocks
combine
equimolar EukMix

FIG. 2B

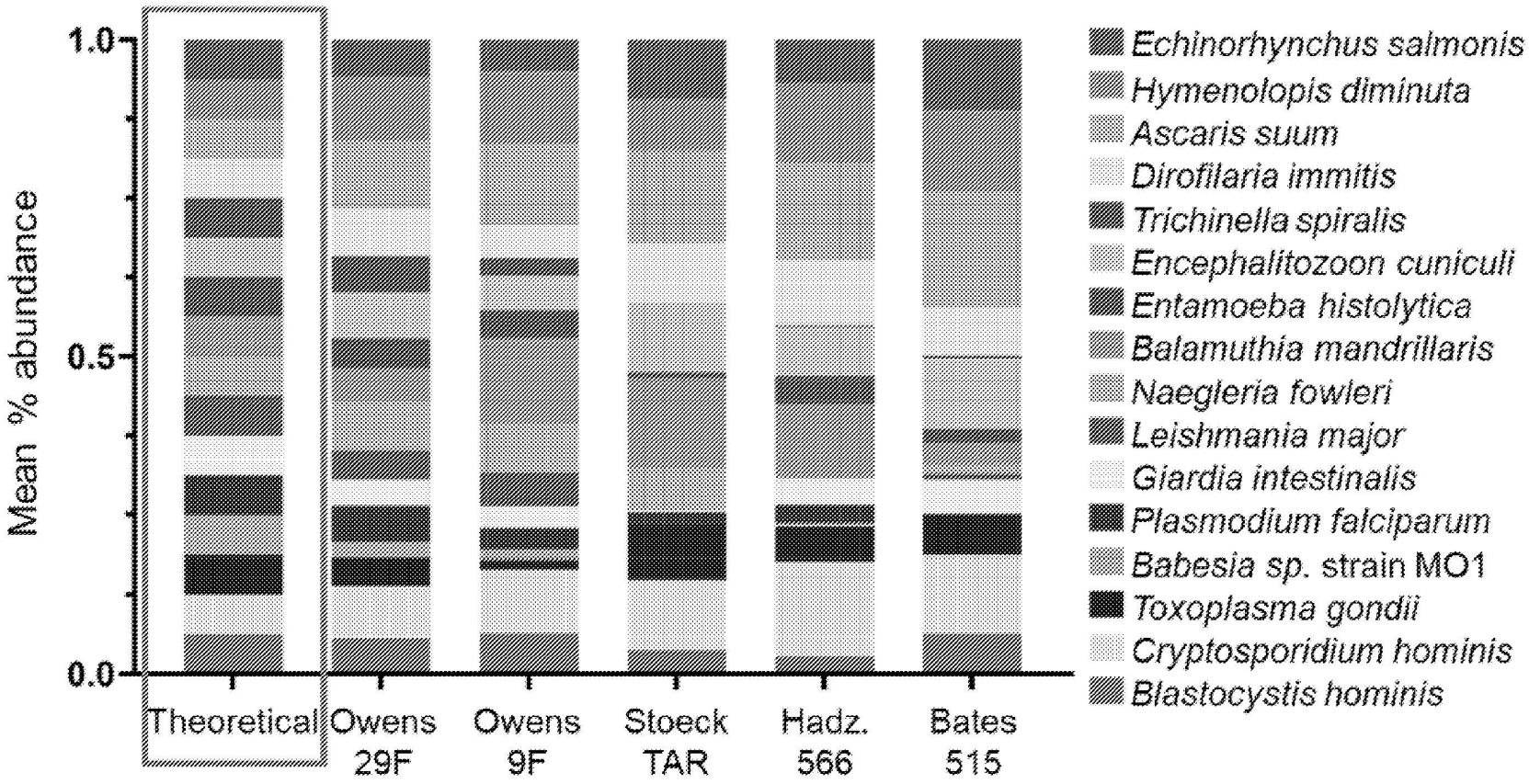
Mean % abundance
1.0
0.5
0.0
Theoretical
Owens 29F
Owens 9F
Stoeck TAR
Hadz. 566
Bates 515
Echinorhynchus salmonis
Hymenolopis diminuta
Ascaris suum
Dirofilaria immitis
Trichinella spiralis
Encephalitozoon cuniculi
Entamoeba histolytica
Balamuthia mandrillaris
Naegleria fowleri
Leishmania major
Giardia intestinalis
Plasmodium falciparum
Babesia sp. strain MO1
Toxoplasma gondii
Cryptosporidium hominis
Blastocystis hominis

FIG. 2C

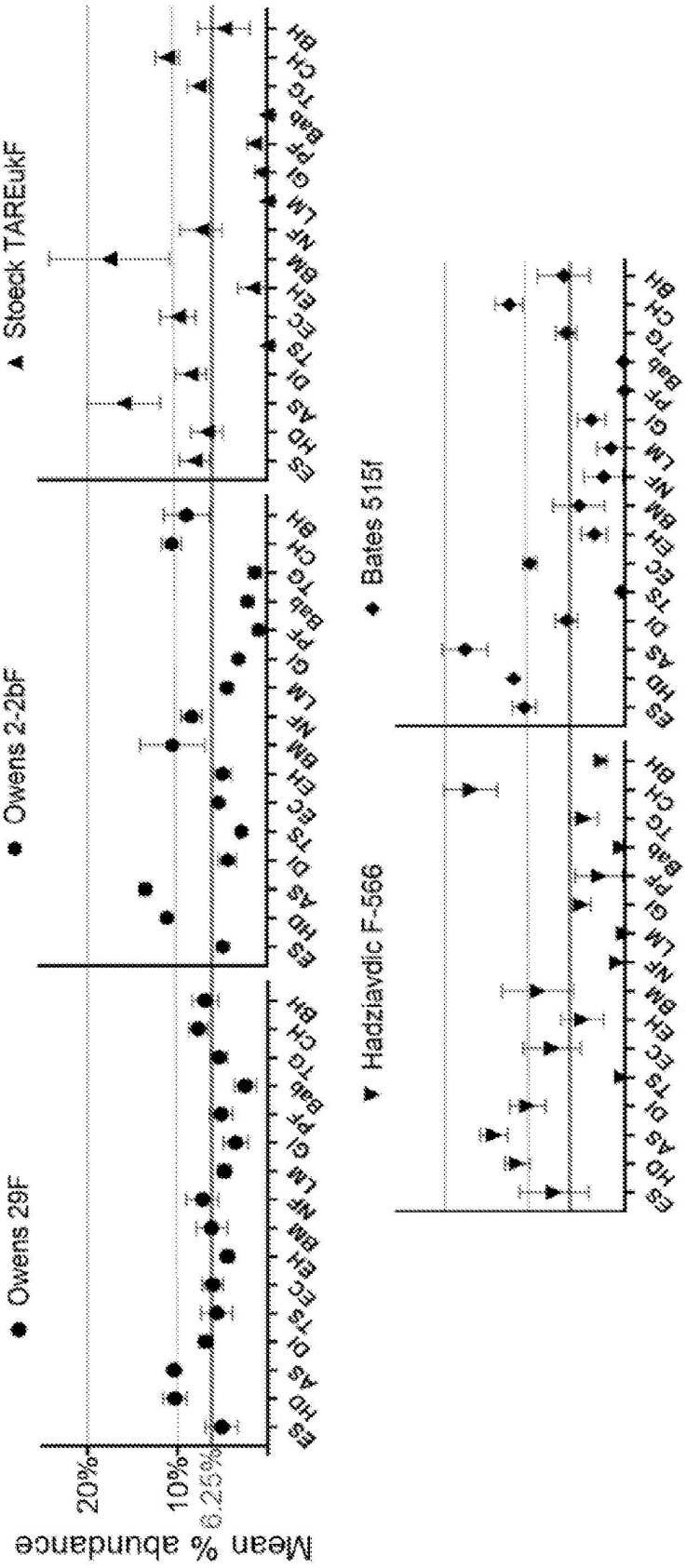
Mean % abundance
20%
10%
6.25%
Owens 29F
Owens 2-2bF
Stoeck TAREukF
Hadziavdic F-566
Bates 515f
ES HD AS OI TS EC EH BM NF LM GI PF BabTG CH BH

FIG. 2D

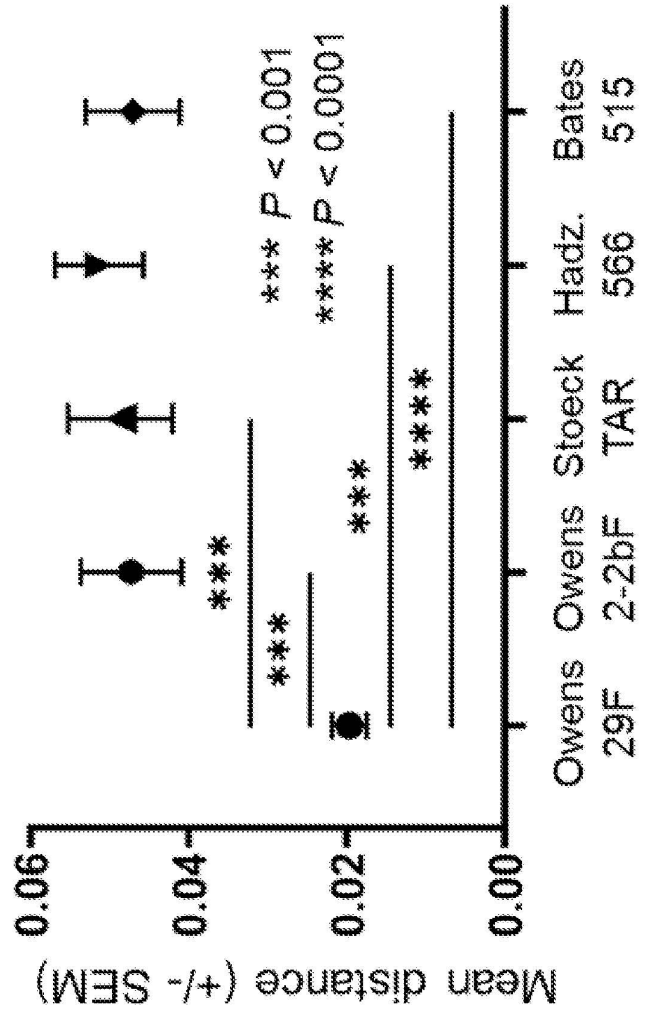
Mean distance (+/- SEM)
0.06
0.04
0.02
0.00
***
***
***
****
*** P < 0.001
**** P < 0.0001
Owens 29F
Owens 2-2bF
Stoeck TAR
Hadz. 566
Bates 515

FIG. 2E

	Pielou's species evenness		Simpson's diversity index		Shannon diversity	
	Mean	SEM	Mean	SEM	Mean	SEM
Theoretical	1.000	0.000	1.000	0.003	2.500	0.000
29F	**0.901**	**0.007**	**0.928**	**0.003**	**2.498**	**0.020**
9F	0.775	0.020	0.891	0.005	2.148	0.055
TAREuk	0.721	0.036	0.874	0.026	2.000	0.100
F-566	0.713	0.024	0.882	0.007	1.977	0.067
515f	0.745	0.023	0.889	0.003	2.064	0.063

FIG. 3A

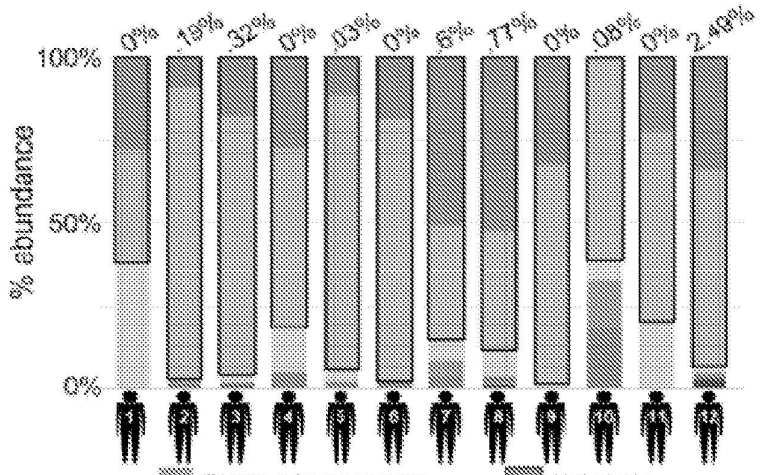

FIG. 3B

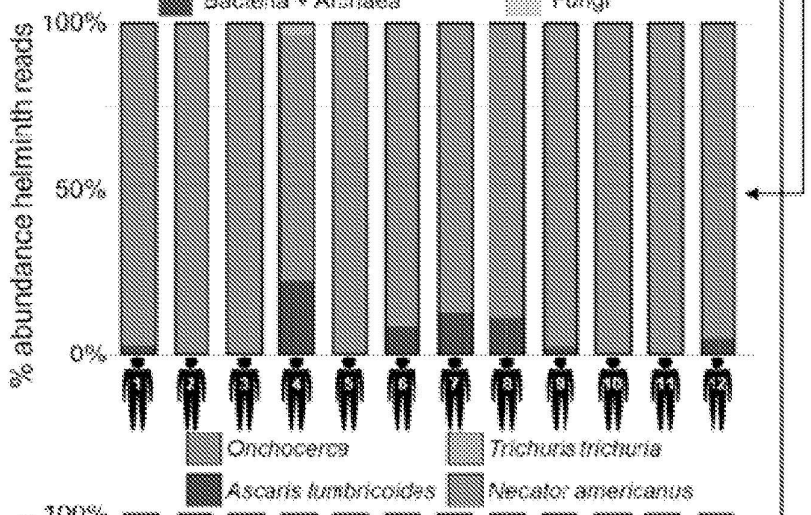

FIG. 3C

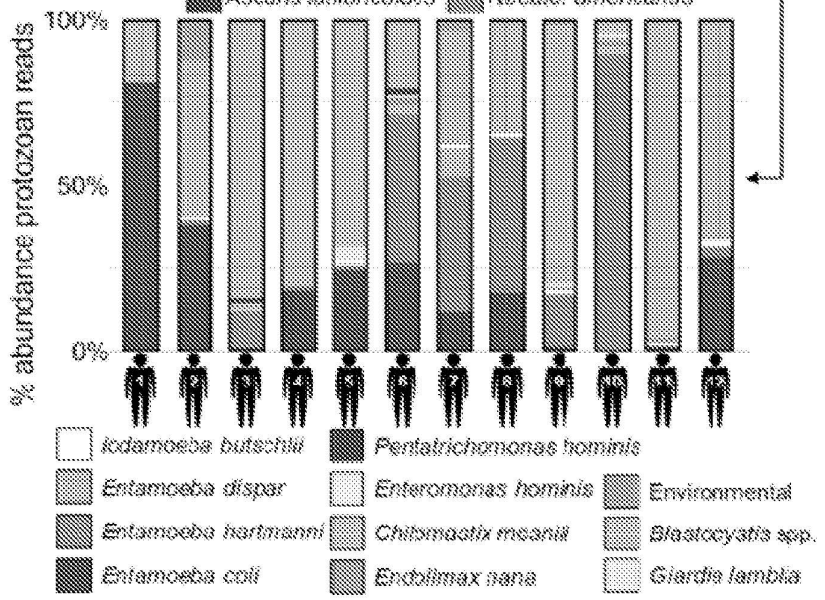

FIG. 3D

Microscopy only
VESPA only
Both methods

		1		2		3		4		5		6		7		8		9		10		11		12		Prevalence	
		M	MB	M	MB	M	MB	M	MB	M	MB	M	MB	M	MB	M	MB	M	MB	M	MB	M	MB	M	MB	M	MB
Protozoa	*Entamoeba coli*	Y	28	Y	34	N	0.2	N	10	N	13	N	21	N	4	Y	7	N	0.5	N	0	N	1	Y	18	**0.33**	**0.92**
	Entamoeba hartmanni	N	0	N	1	N	2	N	0.5	N	1	N	36	N	14	N	0.2	N	9	N	55	N	0	N	2	**0**	**0.83**
	Entamoeba dispar	Y	1	N	0	Y	0.1	Y	0.4	N	0.4	Y	2	Y	3	N	0	N	0	Y	2	N	0	N	0	**0.50**	**0.58**
	Iodamoeba butschlii	N	0	N	0	N	0.1	N	0	Y	1	N	0	N	0	N	0.4	N	0.3	N	0	Y	0.3	Y	2	**0.25**	**0.58**
	Endolimax nana	N	0	Y	0.1	Y	0.1	N	0	N	0	N	1	N	0	N	0	N	0	Y	1	Y	0.4	Y	1	**0.42**	**0.50**
	Chilomastix mesnili	N	0	N	0	Y	0.2	N	0	N	0	N	0	N	0	N	1	Y	0.1	Y	1	Y	0.1	Y	3	**0.42**	**0.50**
	Enteromonas hominis	N	0	N	0.2	N	0	N	0	N	0	N	0.1	N	0	N	0	N	0	N	0.3	N	0	N	0	**0**	**0.25**
	Pentatrichomonas hominis	N	0	N	0	N	0.2	N	0	N	0	N	0	N	0	N	0	N	0	N	0	N	0	N	0	**0**	**0.08**
	Giardia lamblia	N	0	N	0	N	0	N	0	Y	2	N	0	N	0	N	0	N	0	N	0	N	0	N	0	**0.08**	**0.17**
	Blastocystis sp.	N	6	N	42	N	76	N	44	N	68	Y	17	N	12	Y	12	Y	56	N	3	N	54	Y	39	**0.33**	**1.00**
Helminths	*Ascaris lumbricoides*	Y	1	N	0	N	0	N	6	N	0	N	2	N	6	N	6	Y	0.4	N	0	N	0	N	2	**0.17**	**0.58**
	*Onchocerca	NA	0	NA	0	NA	0	Y	0.4	N	0	Y	2	Y	0.2	NA	0	NA	0	NA	0	NA	0	NA	0	**0.75**	**0.75**
	Necator americanus	N	27	N	9	N	18	N	20	N	11	N	16	N	45	N	47	Y	32	N	1	N	22	N	31	**0.08**	**1.00**
	Trichuris trichiura	N	0	N	0	N	0	N	0.2	N	0	N	0	N	0	N	0	N	0	N	0	N	0	N	0	**0**	**0.08**
	Protozoan richness	**2**	**3**	**2**	**5**	**3**	**8**	**1**	**4**	**2**	**6**	**2**	**7**	**1**	**6**	**2**	**6**	**2**	**6**	**3**	**6**	**3**	**5**	**5**	**6**		
	Helminth richness	**1**	**2**	**0**	**1**	**0**	**1**	**1**	**4**	**0**	**1**	**1**	**3**	**1**	**3**	**0**	**2**	**2**	**2**	**0**	**1**	**0**	**1**	**0**	**2**		

M: Microscopy, MB: VESPA

FIG. 3E

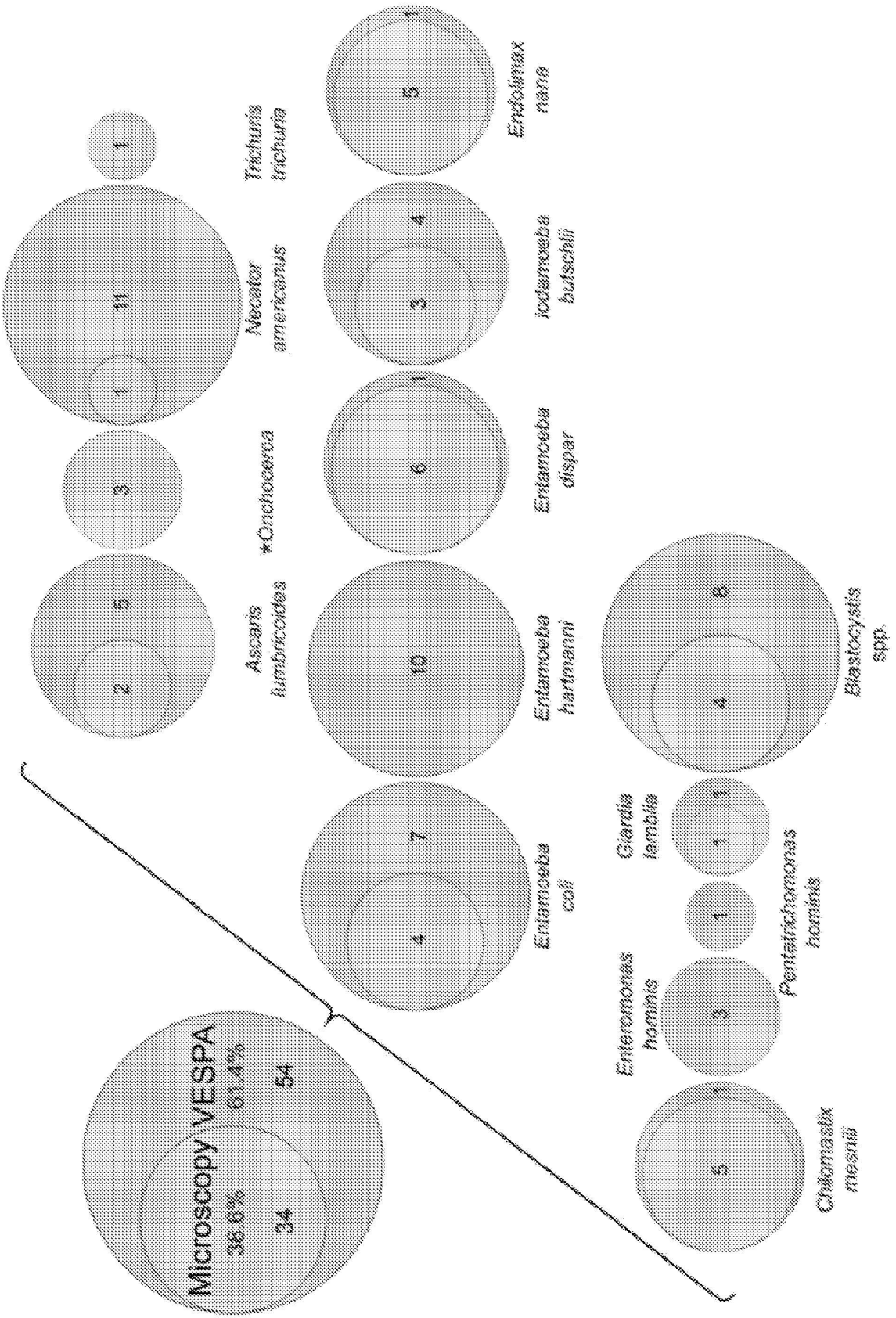
Microscopy/VESPA
38.6%
61.4%
34
54
Ascaris lumbricoides
*Onchocerca
Necator americanus
Trichuris trichuria
Entamoeba coli
Entamoeba hartmanni
Entamoeba dispar
Iodamoeba butschlii
Endolimax nana
Enteromonas hominis
Giardia lamblia
Pentatrichomonas hominis
Blastocystis spp.
Chilomastix mesnili

FIG. 3F

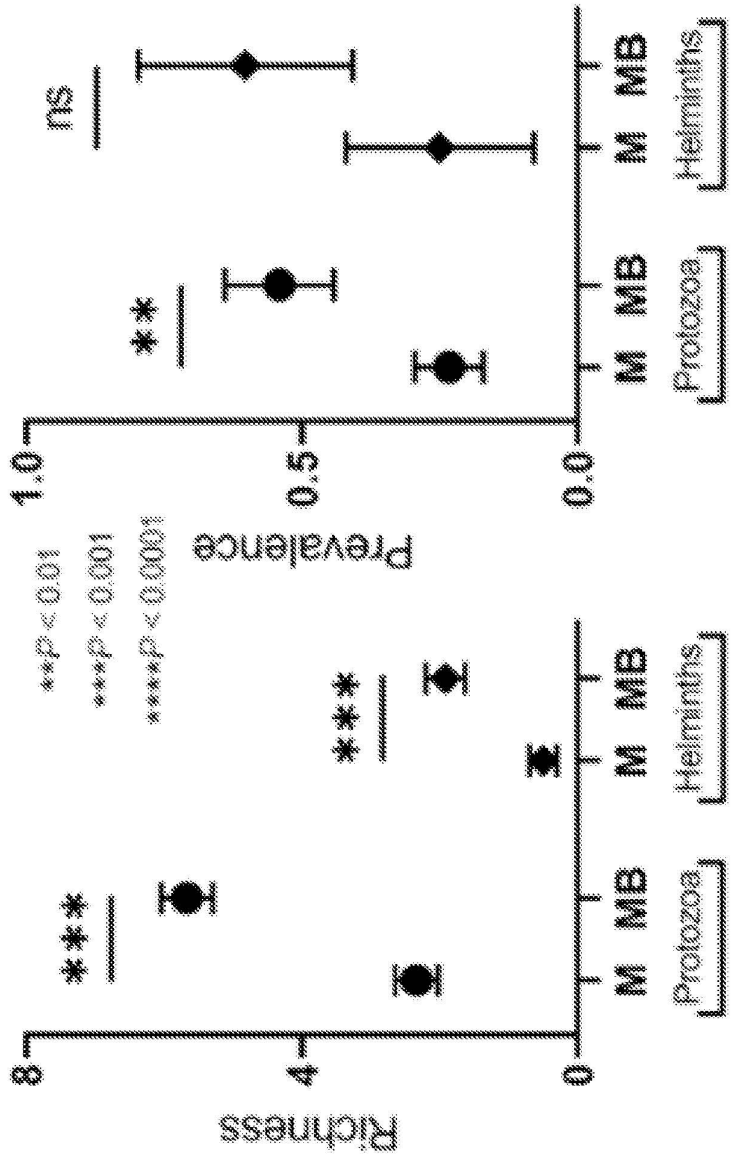
Richness
8
4
0
Prevalence
1.0
0.5
0.0
M MB
Protozoa
Helminths
ns
**
***
****
**p < 0.01
***p < 0.001
****p < 0.0001

FIG. 4A

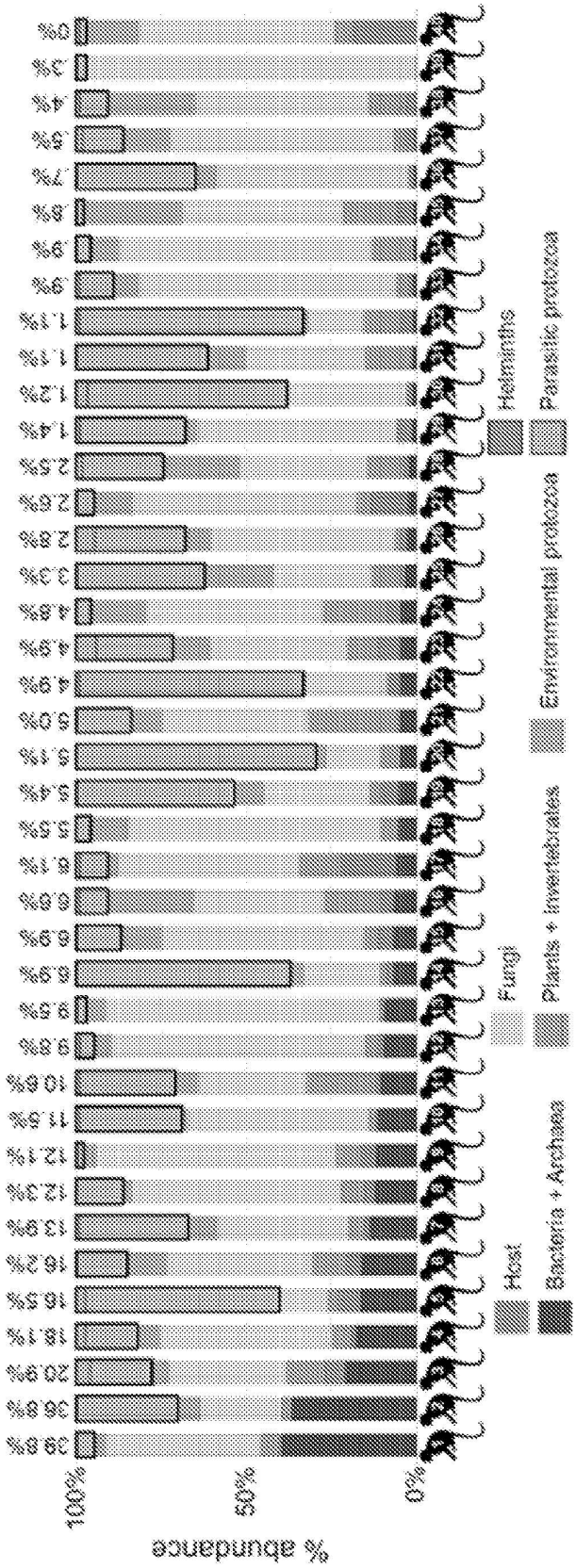
% abundance
100%
50%
0%
Bacteria + Archaea
Host
Fungi
Plants + Invertebrates
Environmental protozoa
Helminths
Parasitic protozoa

FIG. 4B

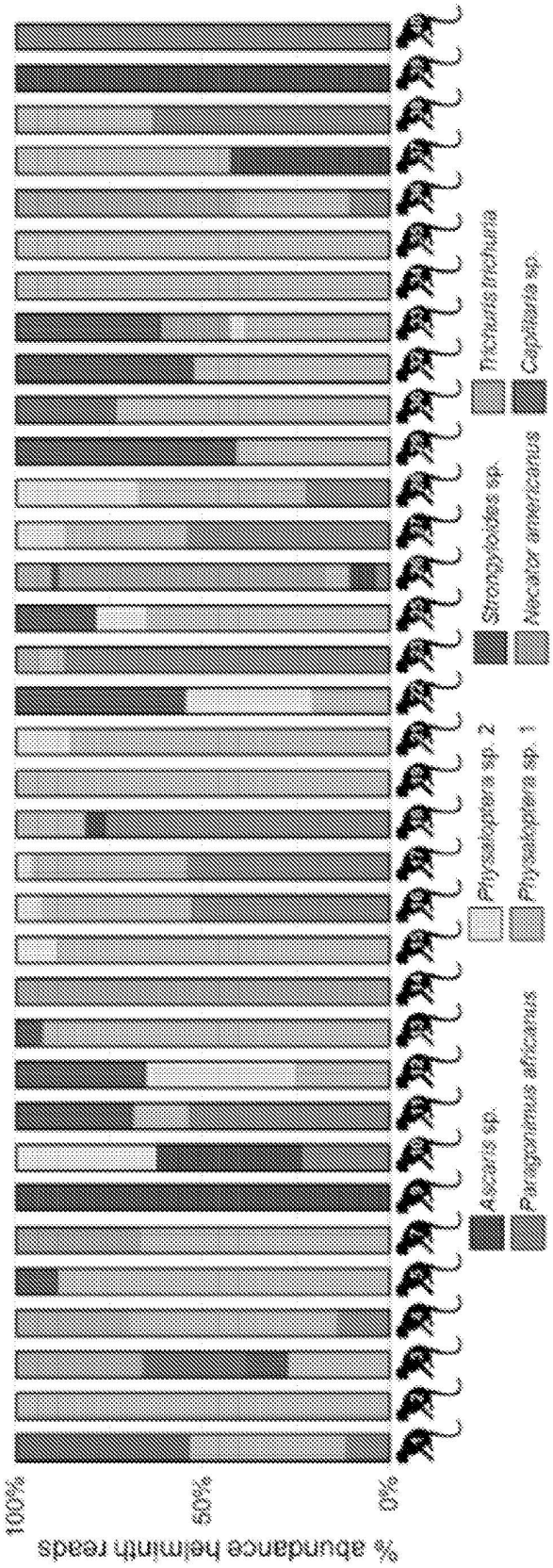
% abundance helminth reads
100%
50%
0%
Ascaris sp.
Physaloptera sp. 2
Strongyloides sp.
Trichuris trichiura
Parapharyngodon africanus
Physaloptera sp. 1
Necator americanus
Capillaria sp.

FIG. 4C

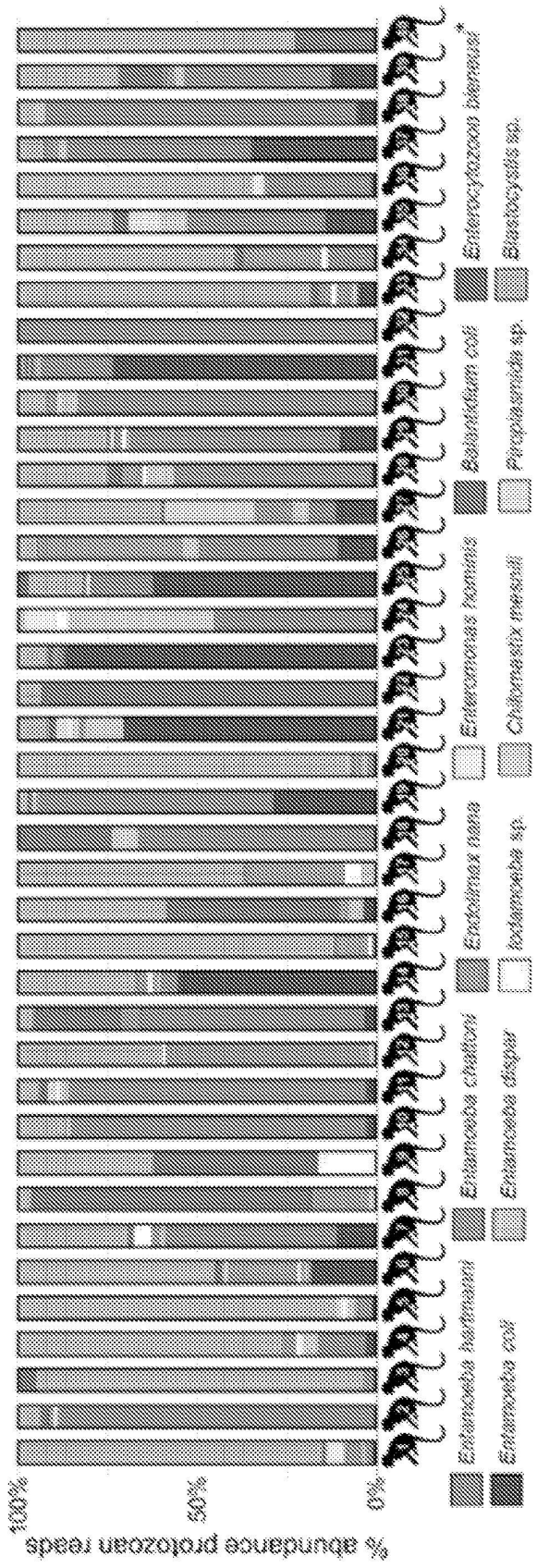
% abundance protozoan reads
100%
50%
0%
Entamoeba hartmanni
Entamoeba coli
Entamoeba chattoni
Entamoeba dispar
Endolimax nana
Iodamoeba sp.
Enteromonas hominis
Chilomastix mesnili
Balantidium coli
Pinoplasmida sp.
Entamoeba histolytica*
Blastocystis sp.

FIG. 4D

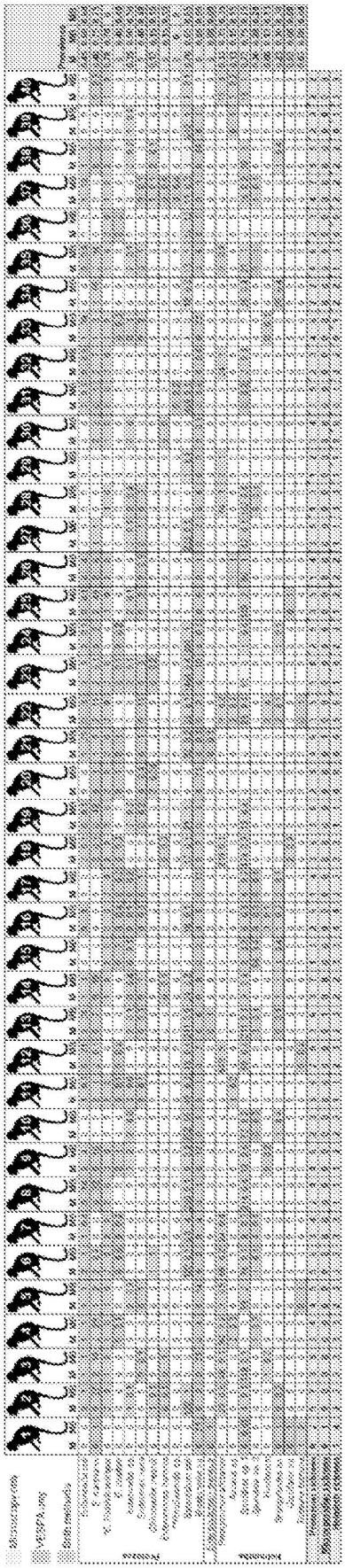
M: Microscopy, MB: VESPA

FIG. 4E

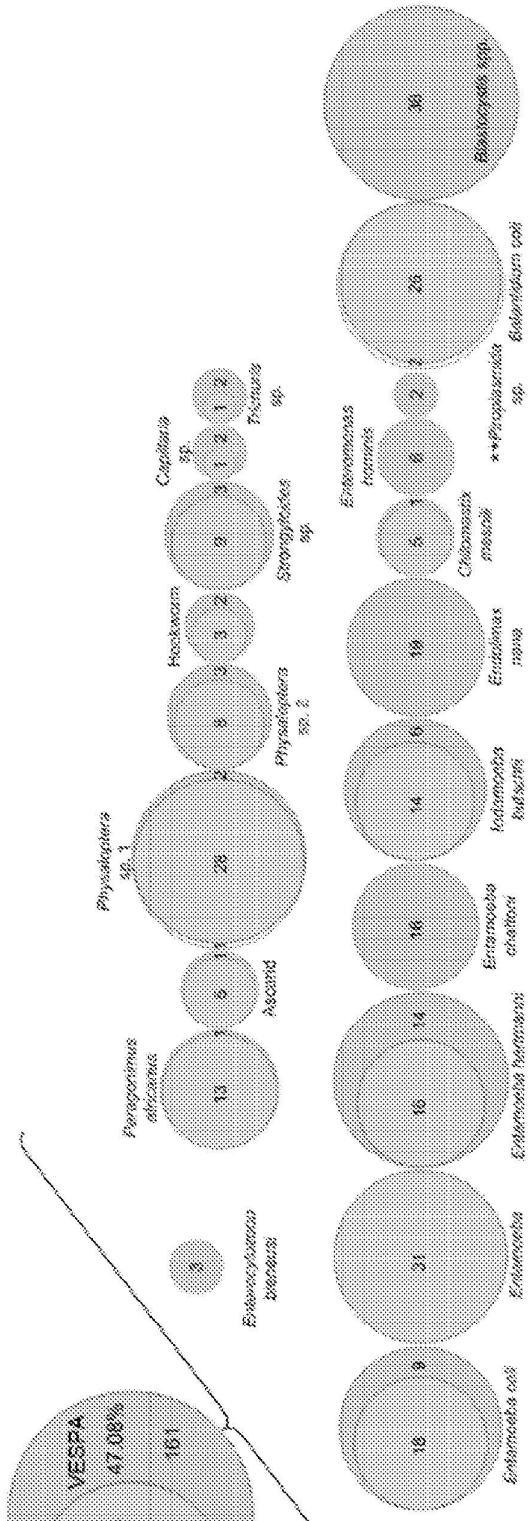
Microscopy
VESPA
9.04%
42.98%
47.08%
34
147
161
Entamoeba coli
Endolimax nana
Entamoeba hartmanni
Entamoeba chattoni
Iodamoeba bütschlii
Entamoeba histolytica
Chilomastix mesnili
**Propionibacterium spp.
Balantidium coli
Blastocystis spp.
Pentatrichomonas hominis
Retortamonas intestinalis
Pygoplasmus africanus
Necator
Physaloptera sp. 1
Physaloptera sp. 2
Hookworm
Strongyloides spp.
Capillaria spp.
Trichuris spp.

FIG. 4F

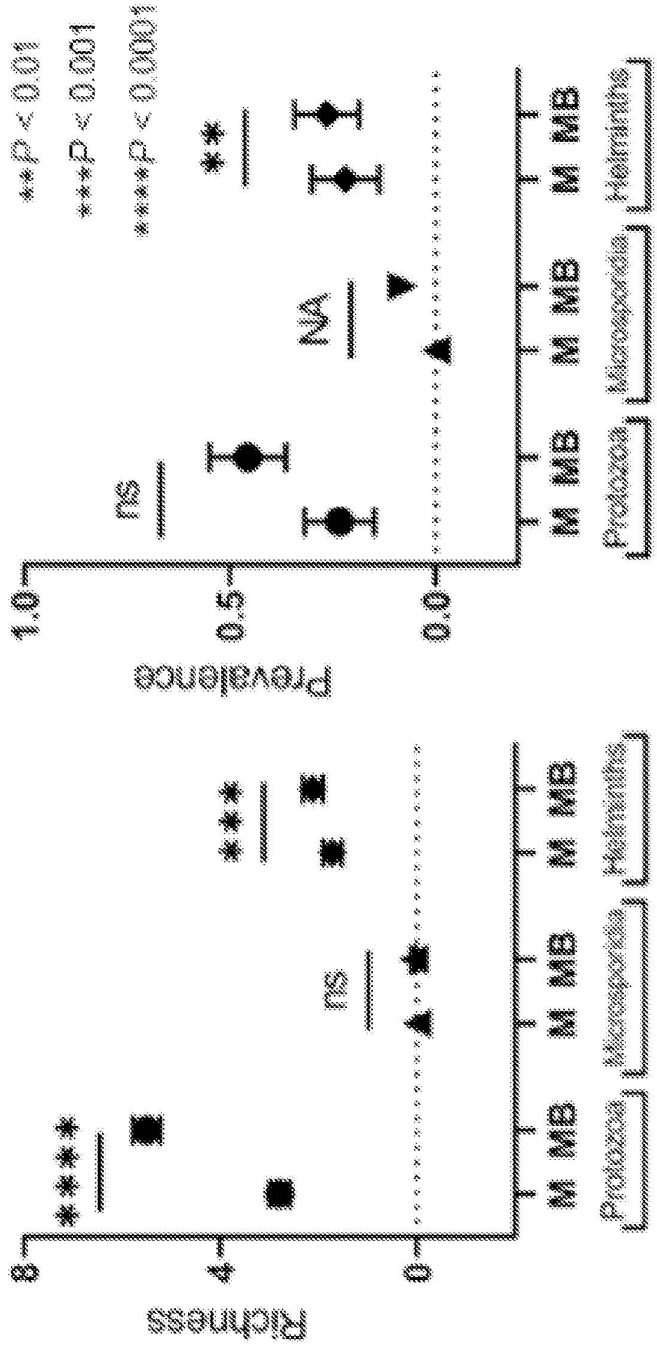
**P < 0.01
***P < 0.001
****P < 0.0001
Prevalence
1.0
0.5
0.0
ns
NA
**
M MB M MB M MB
Protozoa
Microsporidia
Helminths
Richness
8
4
0
****
ns
***
M MB M MB M MB
Protozoa
Microsporidia
Helminths

FIG. 5

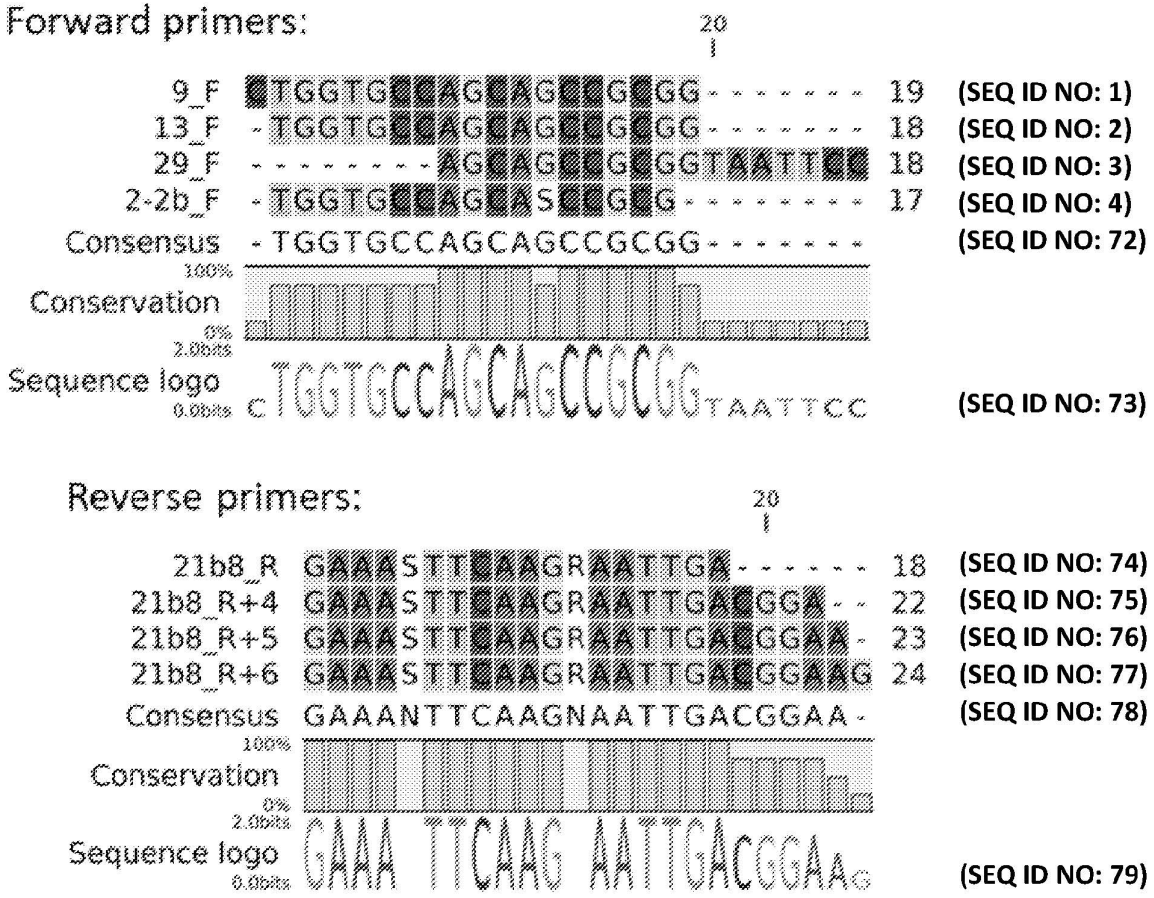
Forward primers:
20
9_F 19 (SEQ ID NO: 1)
13_F 18 (SEQ ID NO: 2)
29_F 18 (SEQ ID NO: 3)
2-2b_F 17 (SEQ ID NO: 4)
Consensus (SEQ ID NO: 72)
100%
Conservation
0%
2.0bits
Sequence logo
0.0bits
(SEQ ID NO: 73)
Reverse primers:
20
21b8_R 18 (SEQ ID NO: 74)
21b8_R+4 22 (SEQ ID NO: 75)
21b8_R+5 23 (SEQ ID NO: 76)
21b8_R+6 24 (SEQ ID NO: 77)
Consensus (SEQ ID NO: 78)
100%
Conservation
0%
2.0bits
Sequence logo
0.0bits
(SEQ ID NO: 79)

FIG. 6

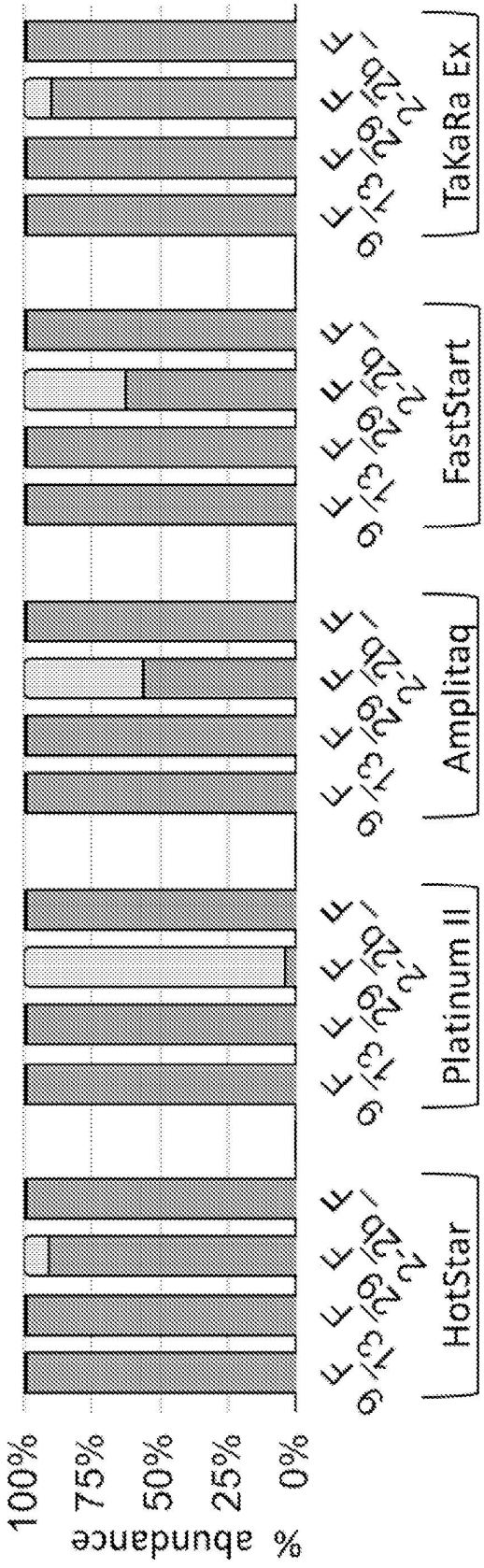
Target
Off-target
% abundance
100%
75%
50%
25%
0%
T6/T13/T29/T-29
HotStar
Platinum II
Amplitaq
FastStart
TaKaRa Ex

FIG. 7A

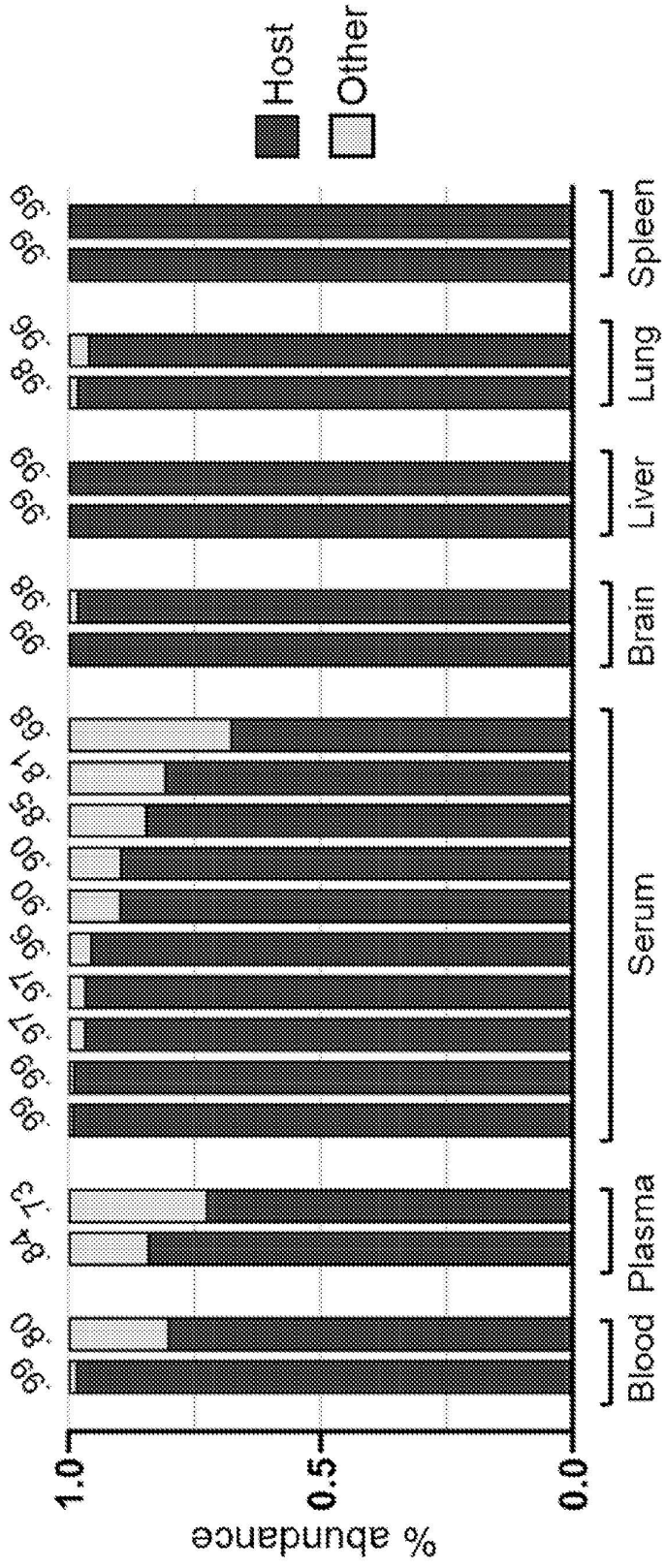
Host
Other
% abundance
1.0
0.5
0.0
99, 80
84, 73
99, 99
97, 97
96, 96
90, 90
93, 85
91, 89
98, 99
99, 99
99, 99
99, 99
Blood Plasma
Serum
Brain
Liver
Lung
Spleen

FIG. 7B

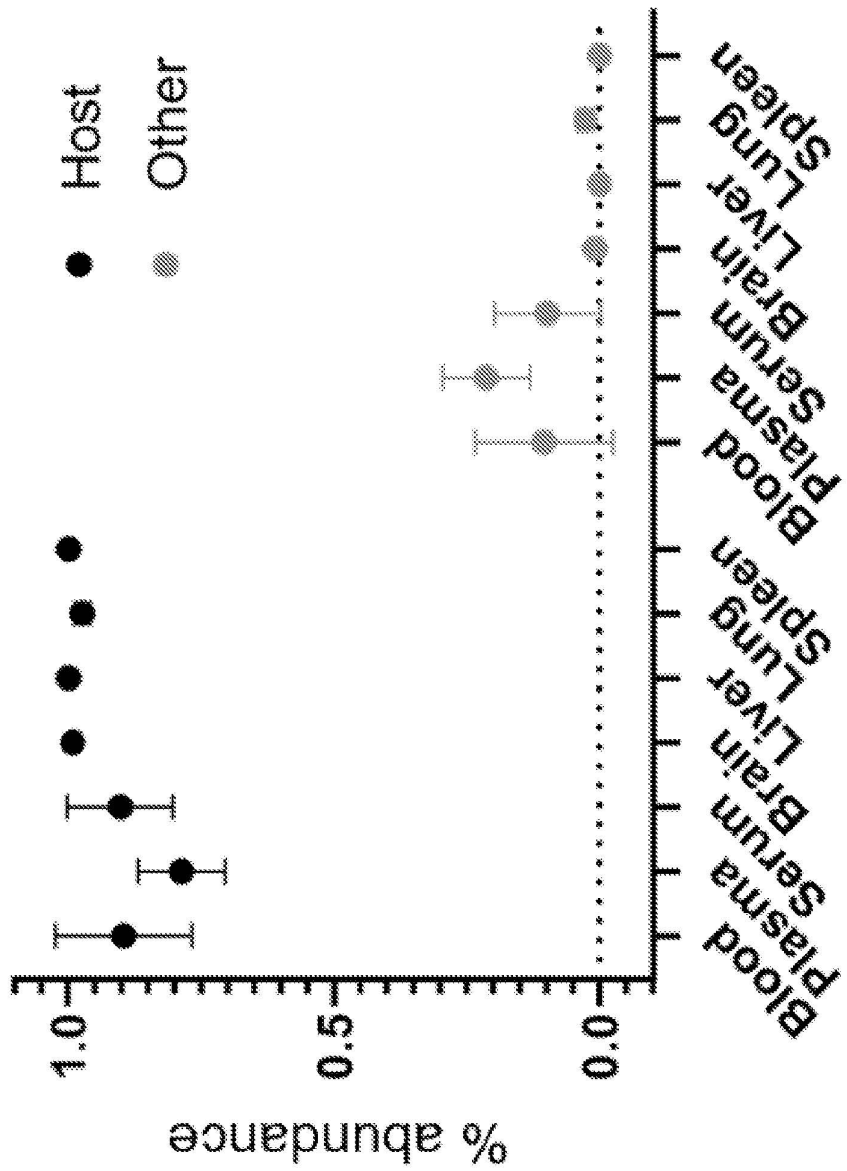
Host
Other
% abundance
1.0
0.5
0.0
Blood
Plasma
Serum
Brain
Liver
Lung
Spleen
Blood
Plasma
Serum
Brain
Liver
Lung
Spleen

FIG. 8A

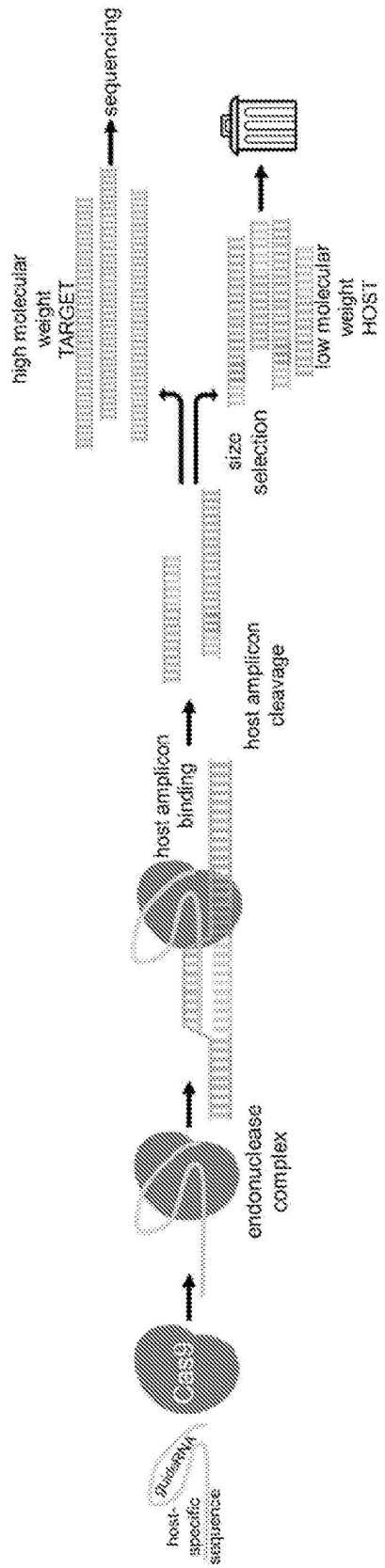
host-specific sequence
guideRNA
Cas9
endonuclease complex
host amplicon binding
host amplicon cleavage
size selection
high molecular weight TARGET
low molecular weight HOST
sequencing

FIG. 8B

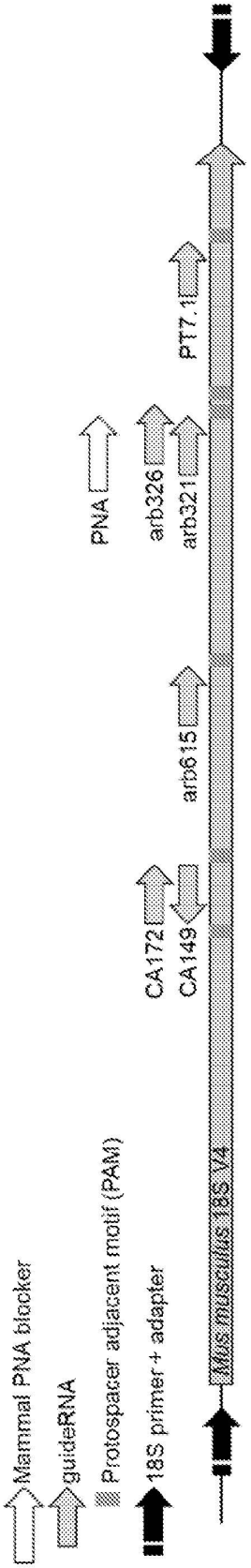
Mammal PNA blocker
guideRNA
Protospacer adjacent motif (PAM)
18S primer + adapter
CA172
CA149
arb615
PNA
arb326
arb321
PT7.1
Mus musculus 18S V4

FIG. 8C

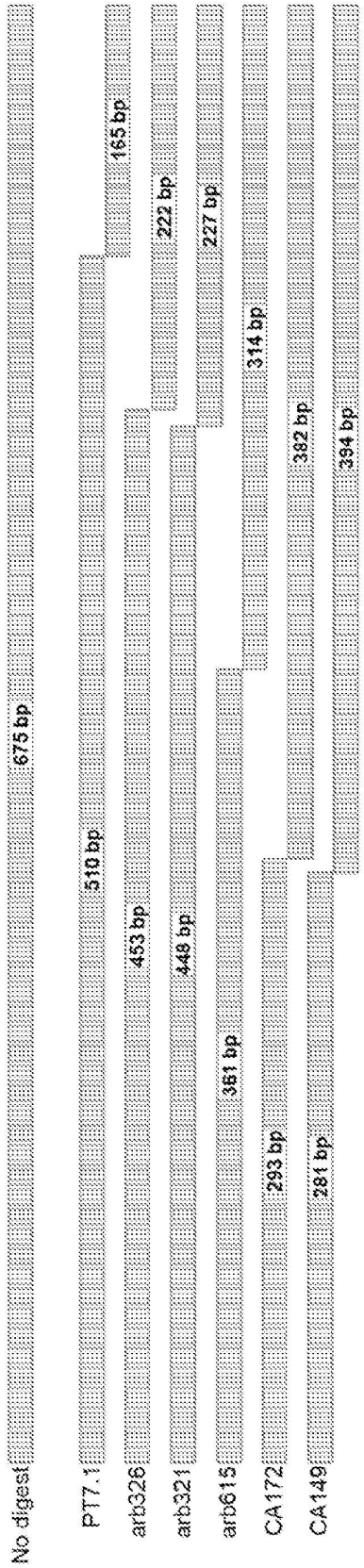
No digest
675 bp
PT7.1
510 bp
165 bp
arb326
453 bp
222 bp
arb321
448 bp
227 bp
arb615
361 bp
314 bp
CA172
293 bp
382 bp
CA149
281 bp
394 bp

FIG. 9

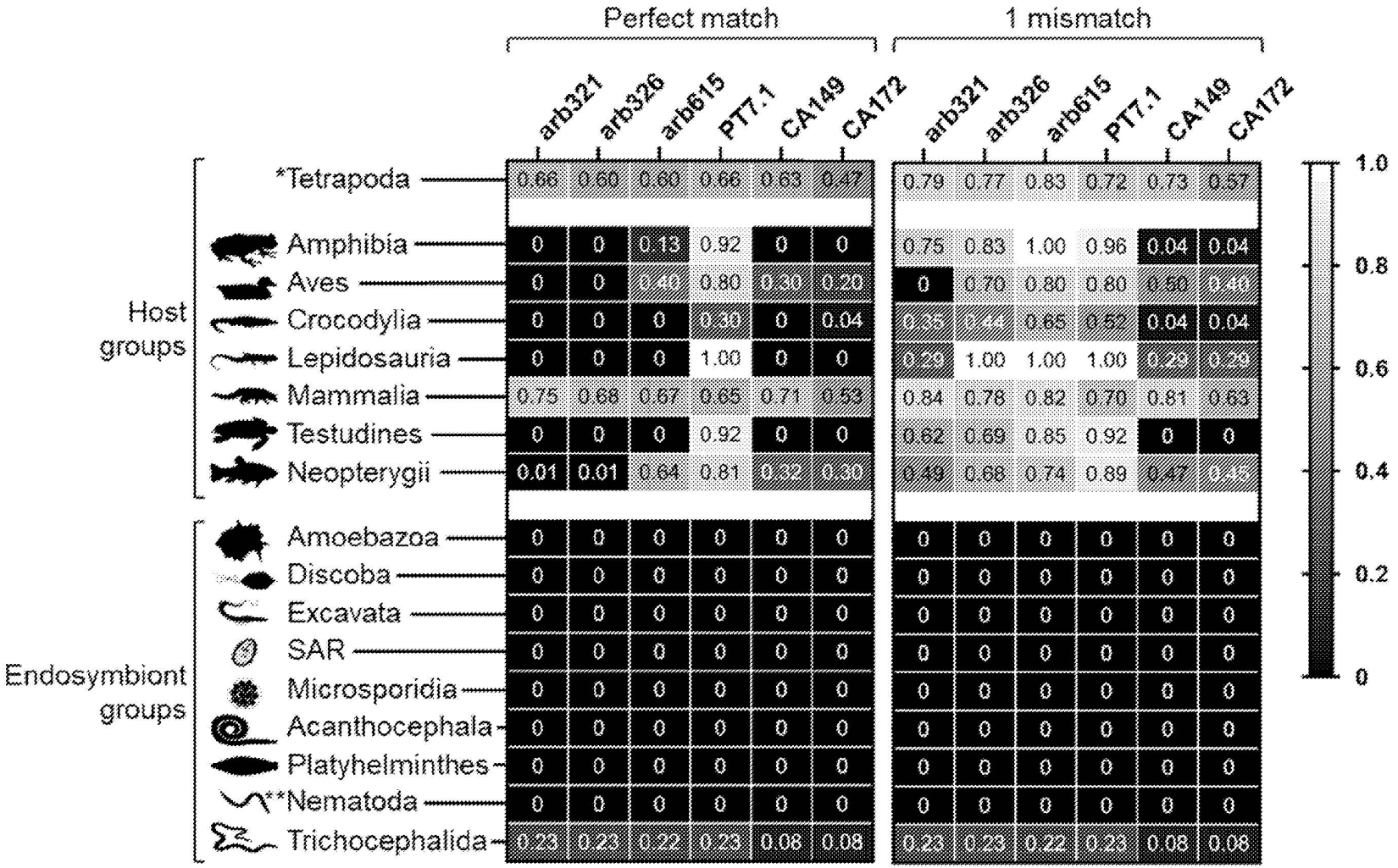
Perfect match
1 mismatch
arb321
arb326
arb615
PT7.1
CA149
CA172
Host groups
Endosymbiont groups
*Tetrapoda
Amphibia
Aves
Crocodylia
Lepidosauria
Mammalia
Testudines
Neopterygii
Amoebazoa
Discoba
Excavata
SAR
Microsporidia
Acanthocephala
Platyhelminthes
**Nematoda
Trichocephalida
1.0
0.8
0.6
0.4
0.2
0

FIG. 10

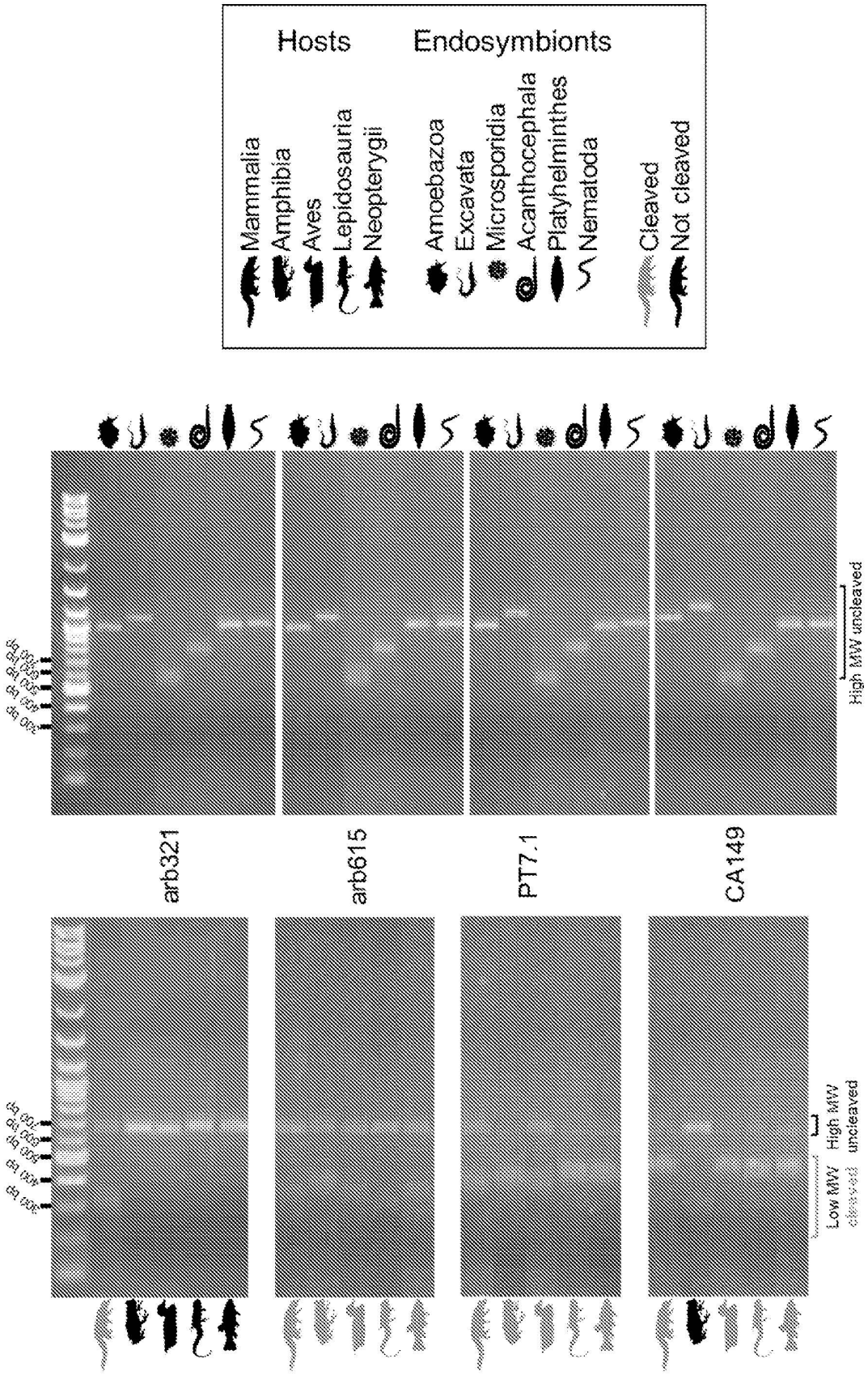
Hosts
Endosymbionts
Mammalia
Amphibia
Aves
Lepidosauria
Neopterygii
Amoebazoa
Excavata
Microsporidia
Acanthocephala
Platyhelminthes
Nematoda
Cleaved
Not cleaved
arb321
arb615
PT7.1
CA149
High MW uncleaved
Low MW cleaved
High MW uncleaved

FIG. 11A

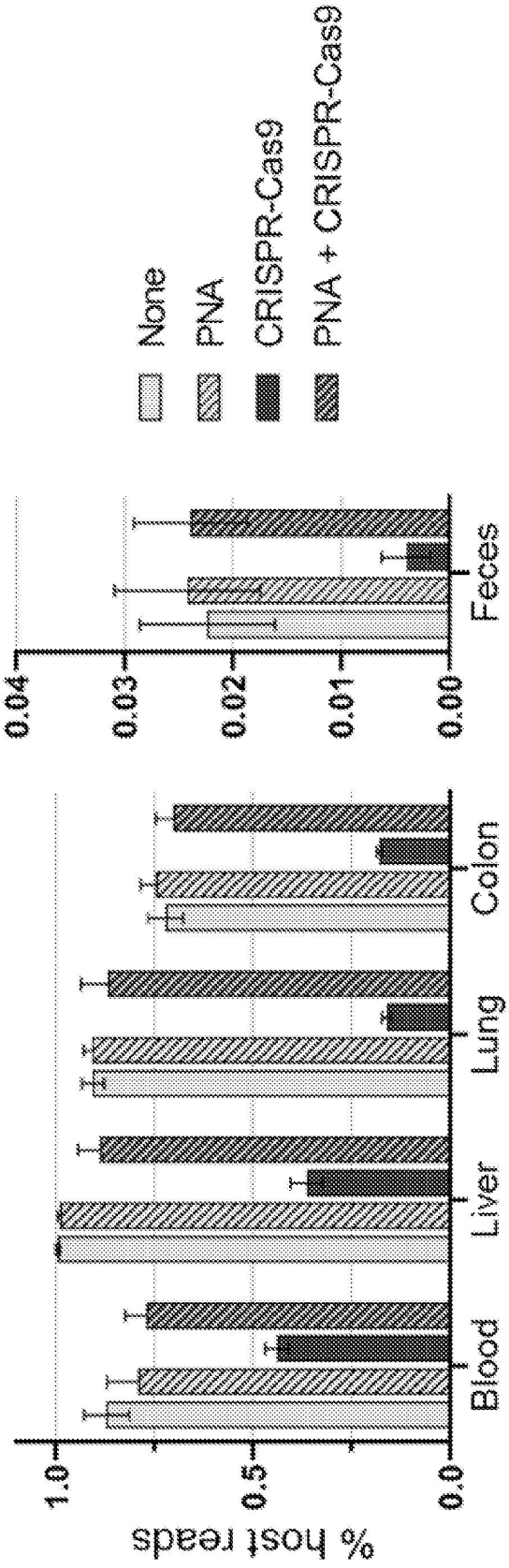
None
PNA
CRISPR-Cas9
PNA + CRISPR-Cas9
% host reads
1.0
0.5
0.0
Blood
Liver
Lung
Colon
0.04
0.03
0.02
0.01
0.00
Feces

FIG. 11B

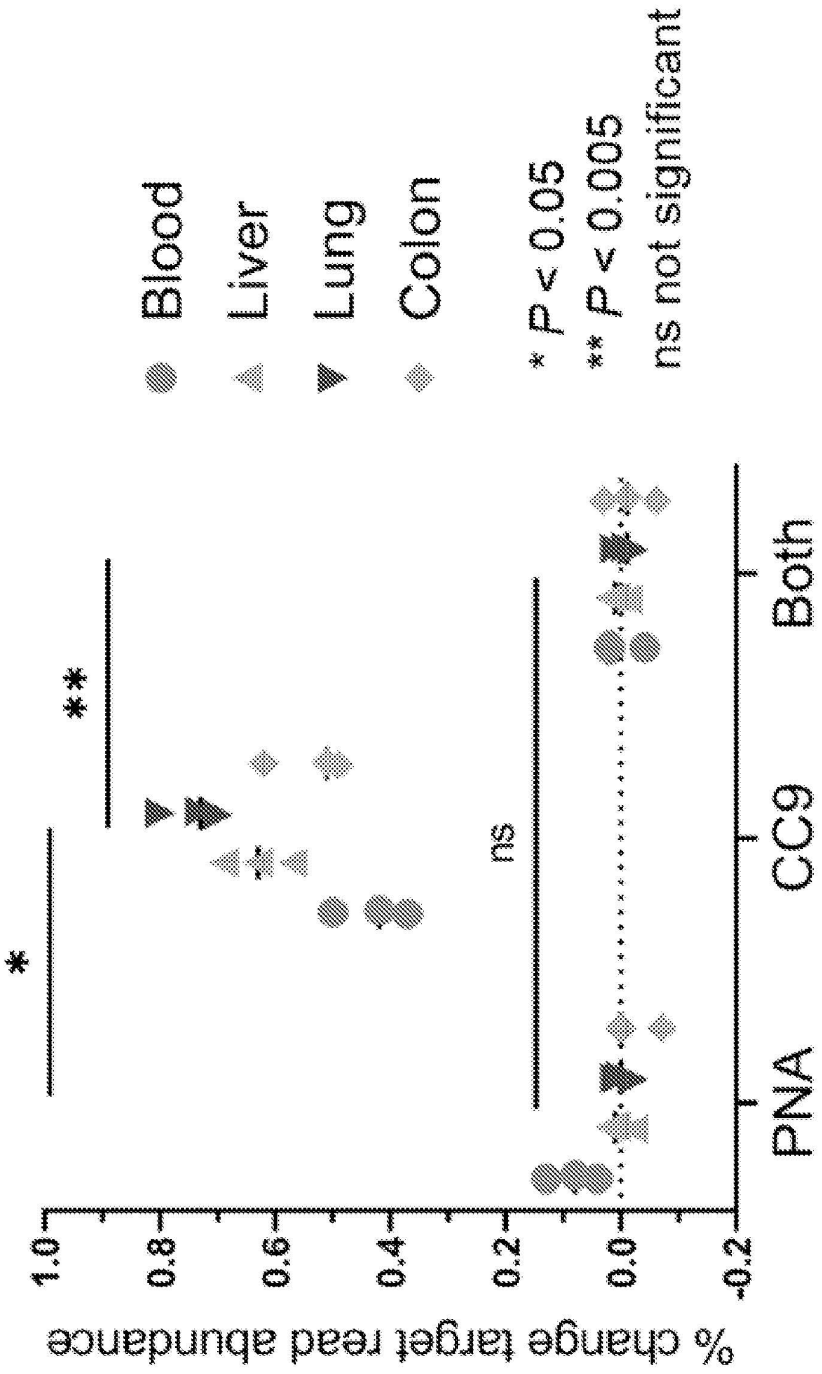
% change target read abundance
1.0
0.8
0.6
0.4
0.2
0.0
-0.2
PNA
CC9
Both
*
**
ns
Blood
Liver
Lung
Colon
* P < 0.05
** P < 0.005
ns not significant

FIG. 12A

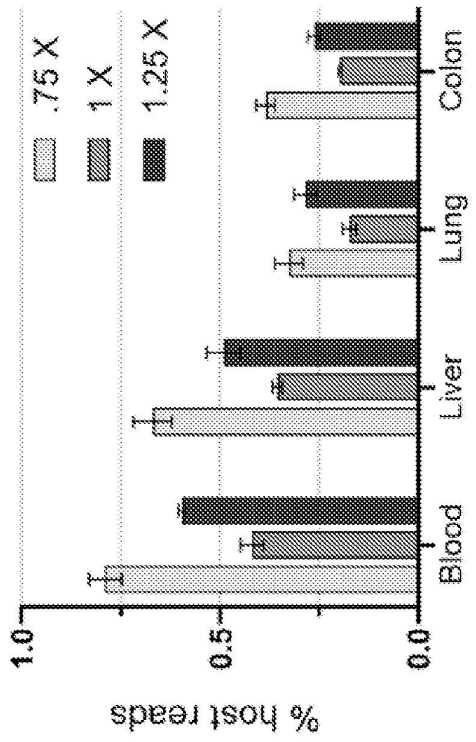

FIG. 12B

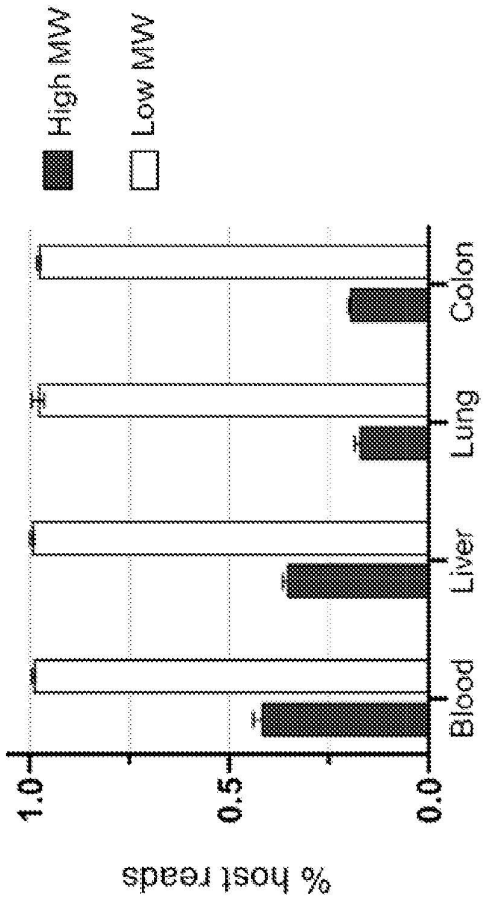

FIG. 12D

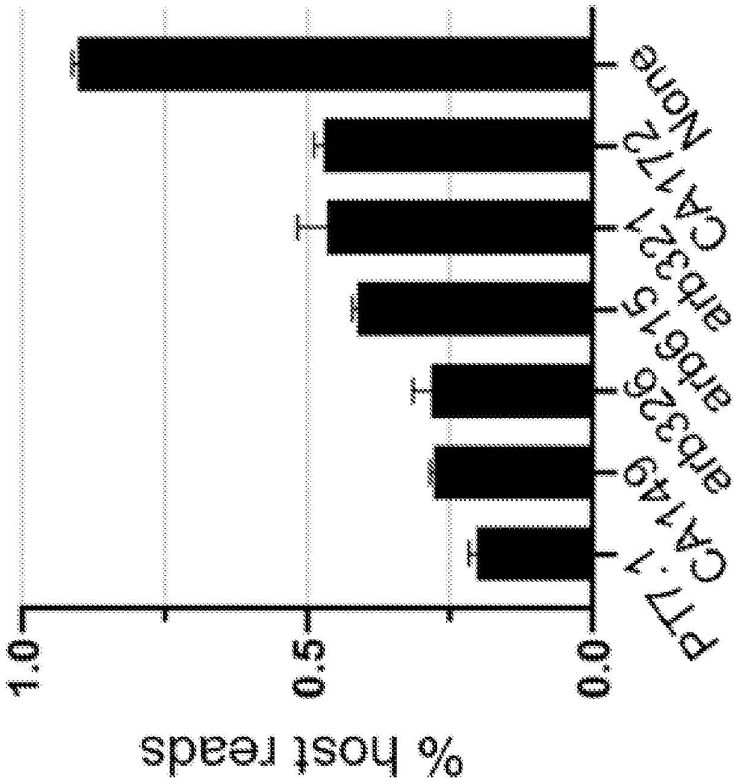

FIG. 12C

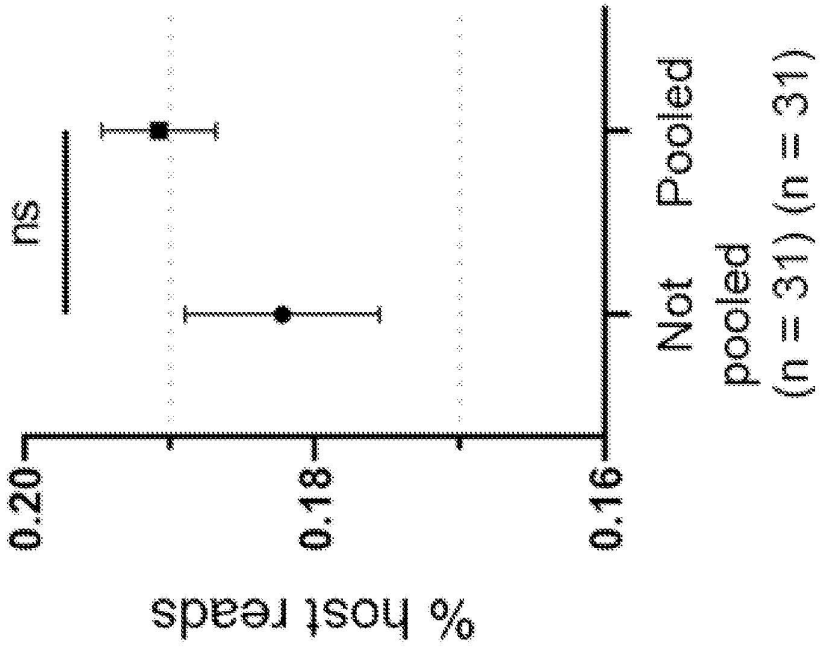

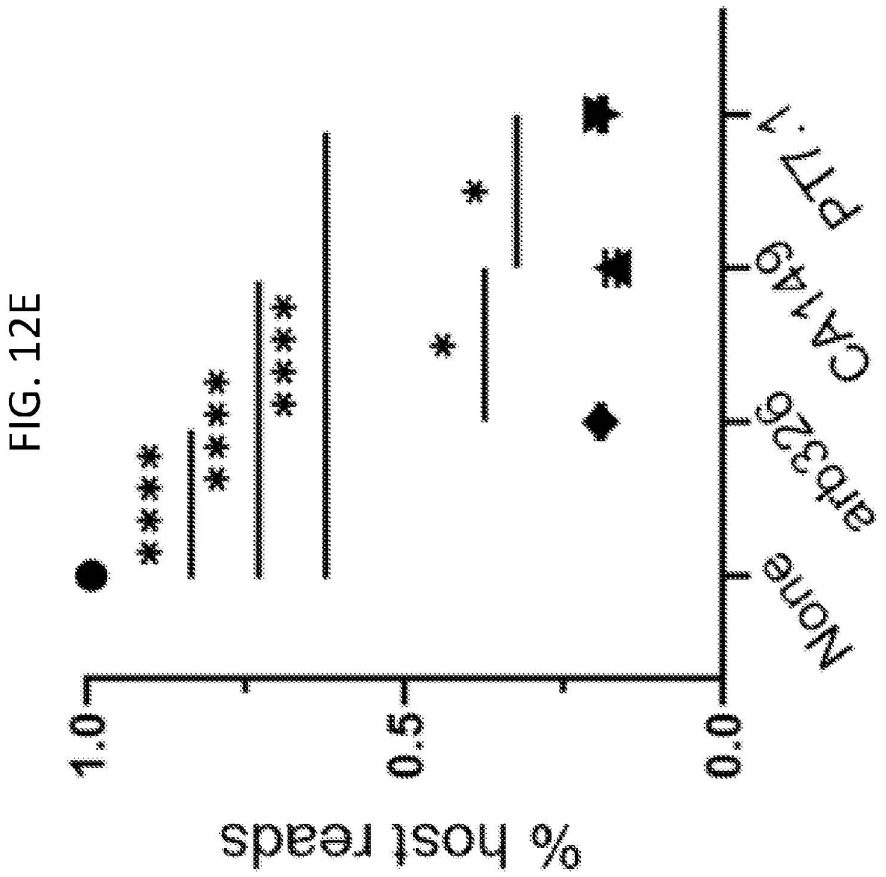

FIG. 12E

FIG. 13A

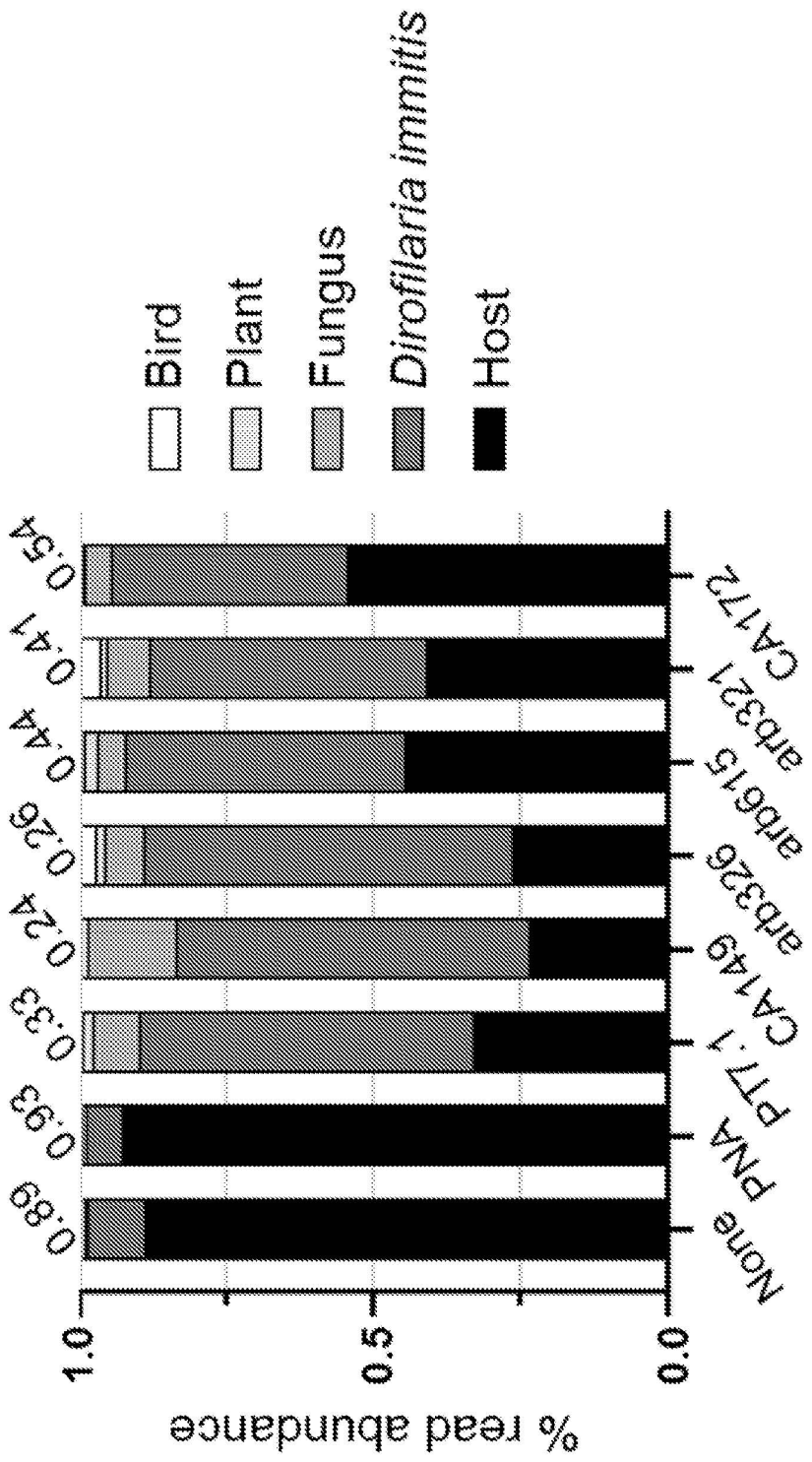
Bird
Plant
Fungus
Dirofilaria immitis
Host
% read abundance
1.0
0.5
0.0
None
PNA
PT7.1
CA149
ab328
ab615
ab321
CA172
0.89
0.93
0.33
0.24
0.26
0.44
0.41
0.64

FIG. 13B

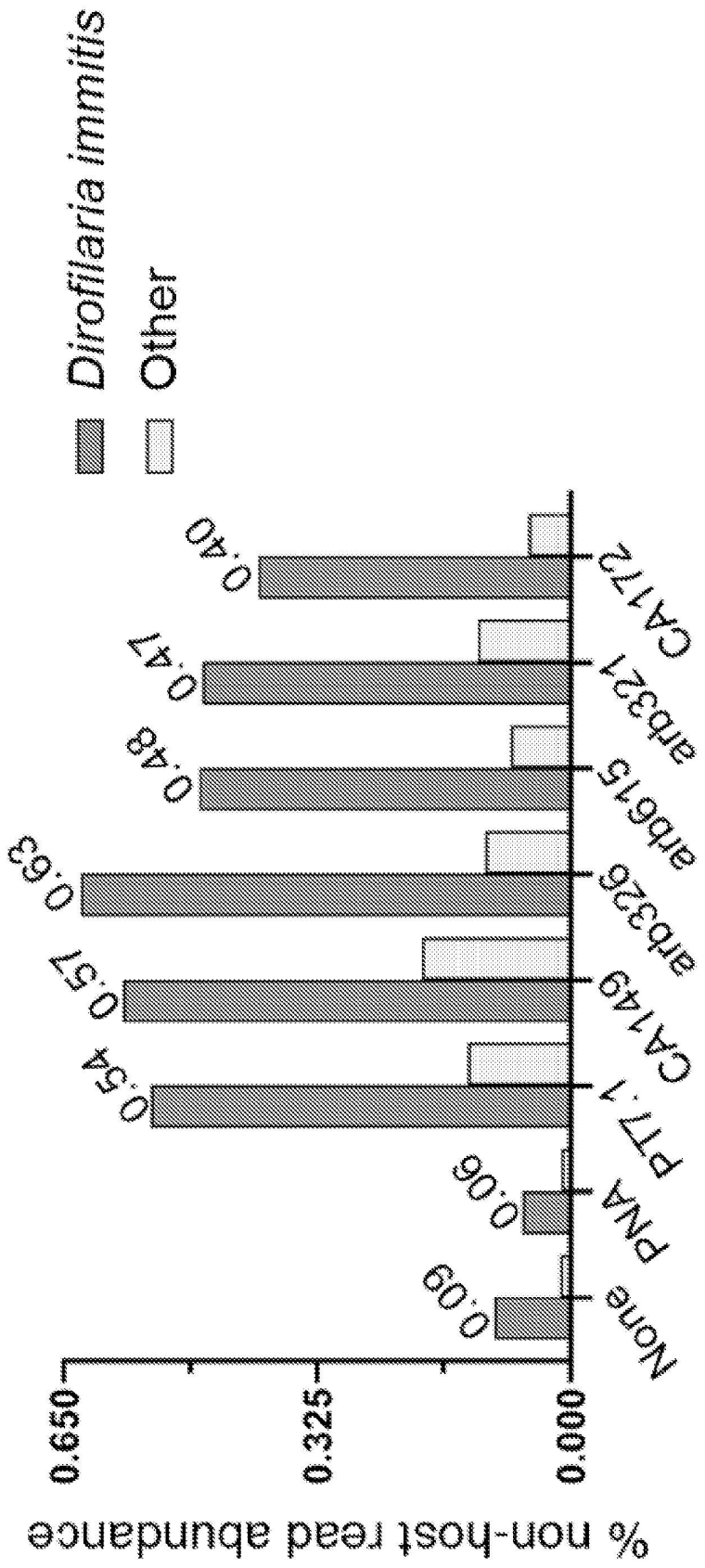
Dirofilaria immitis
Other
% non-host read abundance
0.650
0.325
0.000
None
PNA
PT7.1
CA149
ab326
ab615
ab321
CA172
0.09
0.06
0.54
0.57
0.63
0.48
0.47
0.40

FIG. 14

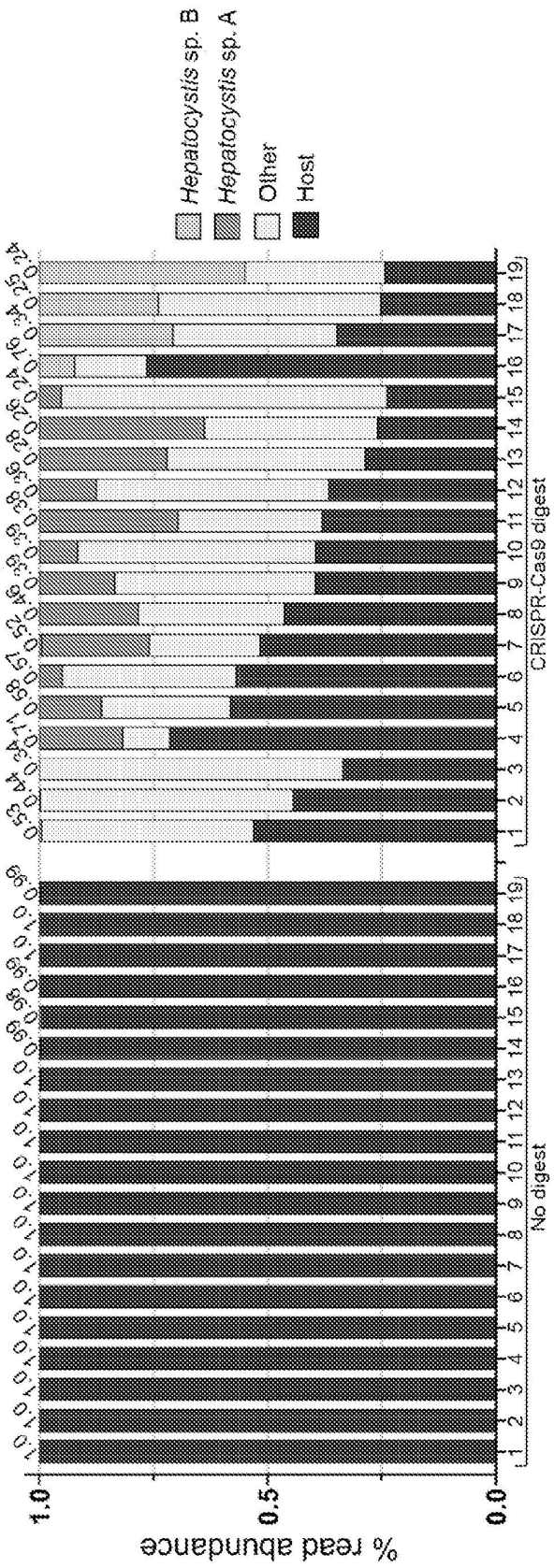
Hepatocystis sp. B
Hepatocystis sp. A
Other
Host
% read abundance
1.0
0.5
0.0
No digest
CRISPR-Cas9 digest

FIG. 15A

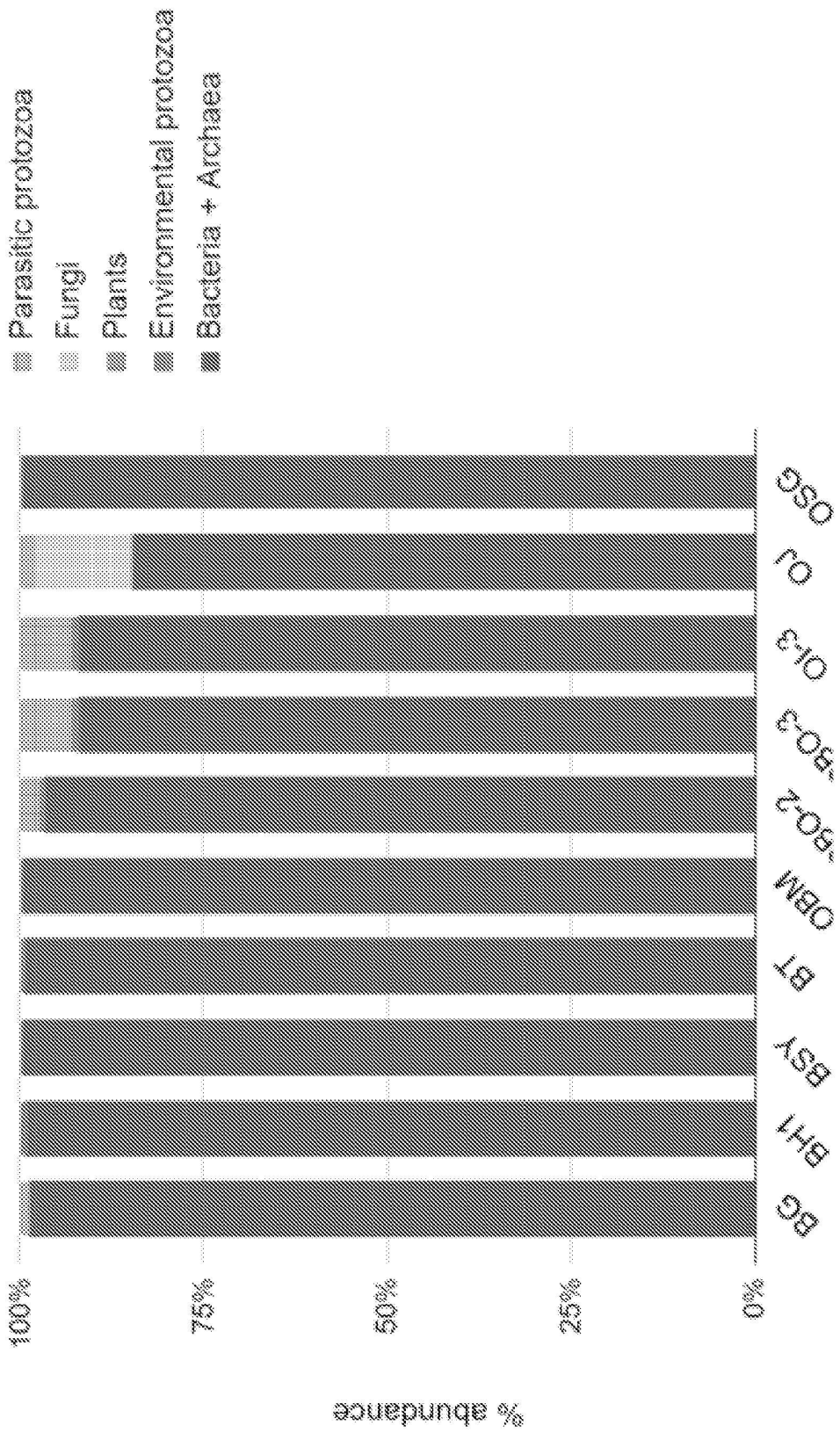
Parasitic protozoa
Fungi
Plants
Environmental protozoa
Bacteria + Archaea
100%
75%
50%
25%
0%
% abundance
BG
BH1
BSY
BT
OBM
OP2
OP3
OJ3
OJ
OSG

FIG. 15B

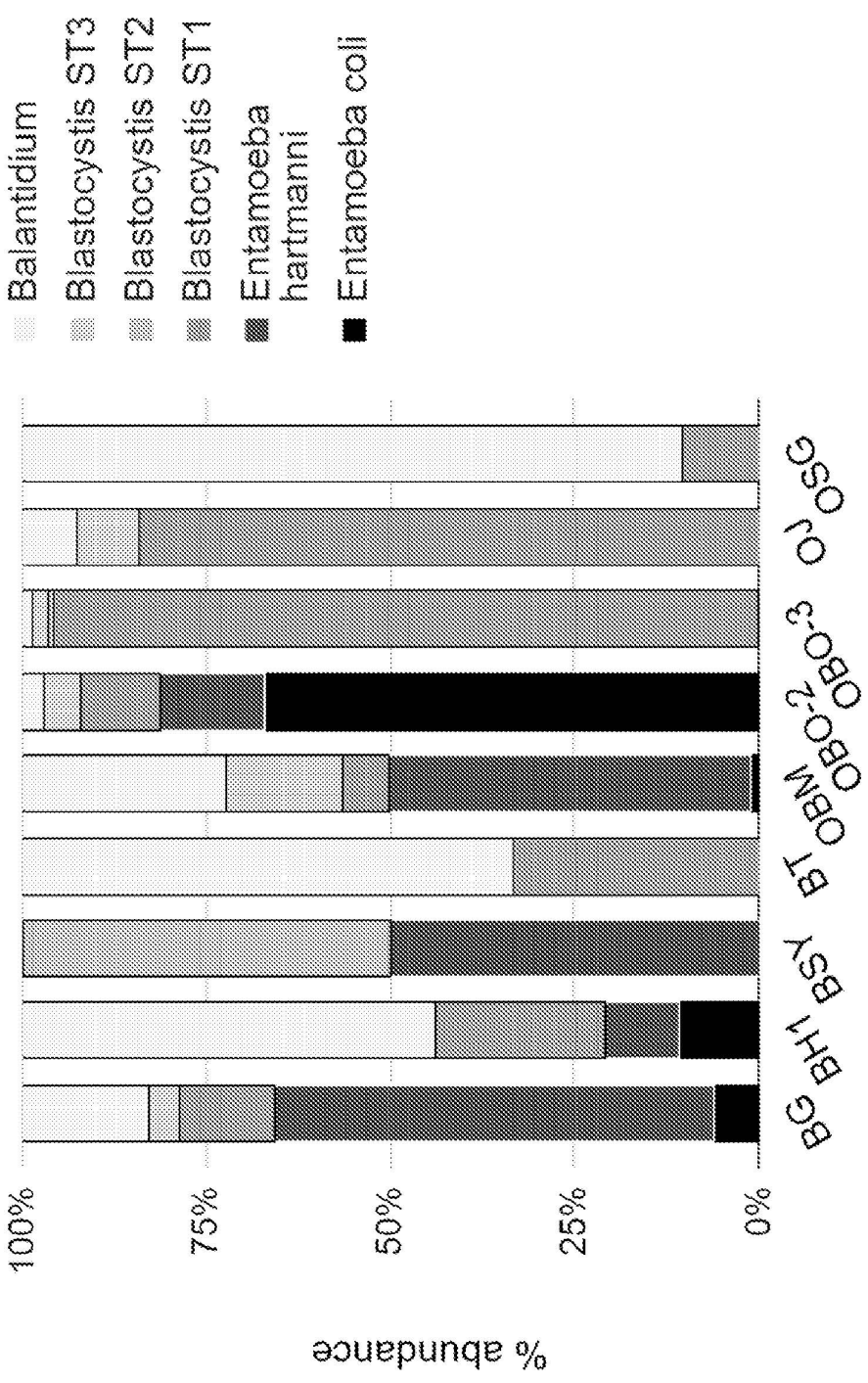
Balantidium
Blastocystis ST3
Blastocystis ST2
Blastocystis ST1
Entamoeba hartmanni
Entamoeba coli
100%
75%
50%
25%
0%
% abundance
BG
BH1
BSY
BT
OBWM
OBO-2
OBO
OBO-3
OJ
OSG

FIG. 16

		BG		BH		BSY		BT		OBM		OBO-2		OBO-3		OI		OJ		OSG	
		M	MB	M	MB	M	MB	M	MB	M	MB	M	MB	M	MB	M	MB	M	MB	M	MB
Protozoa	*Entamoeba coli*	**1**	**0.06%**	**1**	**0.02%**	0	0%	2	0%	0	0.03%	**1**	**1.63%**	0	0%	0	0%	**3**	**0.02%**	0	0%
	Entamoeba hartmanni	**2**	**0.54%**	**1**	**0.02%**	**2**	**0.13%**	2	0%	0	0.14%	**1**	**0.35%**	**2**	**0.02%**	0	0.02%	**2**	**0.02%**	2	0%
	Entamoeba histolytica	1	0%	1	0%	0	0%	2	0%	3	0%	2	0%	0	0%	0	0%	2	0.00%	2	0%
	Iodamoeba butschlii	0	0%	2	0%	0	0%	2	0%	2	0%	0	0%	0	0%	0	0%	0	0%	2	0%
	Balantidium coli	0	0.33%	0	0.10%	1	0%	**1**	**0.12%**	**2**	**0.08%**	**2**	**0.07%**	0	0.08%	**1**	**0.08%**	**2**	**0.12%**	**1**	**0.16%**
	Blastocystis hominis	0	0.17%	0	0.01%	0	0.13%	0	0.16%	0	0.16%	0	0.13%	0	0.43%	0	0.48%	0	1.57%	0	0.03%
Helminths	*Paragonimus africanus*	90	0%	3	0%	0	0%	0	0%	0	0%	0	0%	0	0%	17	0%	0	0%	0	0%
	Bertiella	0	0%	0	0%	0	0%	0	0%	0	0%	0	0%	93	0%	0	0%	0	0%	0	0%
	Abbreviata	1	0%	59	0%	0	0%	10	0%	18	0%	0	0%	0	0%	0	0%	56	0%	21	0%
	Ascarid	2	0%	0	0%	0	0%	0	0%	0	0%	0	0%	0	0%	0	0%	0	0%	0	0%
	Enterobius vermicularis	0	0%	0	0%	0	0%	0	0%	0	0%	0	0%	0	0%	0	0%	0	0%	2	0%
	Hookworm	0	0%	0	0%	0	0%	0	0%	0	0%	0	0%	0	0%	0	0%	1	0%	0	0%
	Strongyloides	0	0%	0	0%	0	0%	0	0%	0	0%	0	0%	0	0%	0	0%	1	0%	0	0%
	Capillaria	0	0%	0	0%	1	0%	0	0%	0	0%	0	0%	0	0%	0	0%	0	0%	0	0%
	Protozoan richness	3	4	4	4	2	2	5	2	3	4	4	4	1	3	1	3	3	4	4	2
	Helminth richness	3	0	2	0	1	0	1	0	1	0	0	0	1	0	1	0	3	0	2	0

Detected by microscopy only

Detected by metabarcoding only

Detected by microscopy and metabarcoding

Not detected

FIG. 17

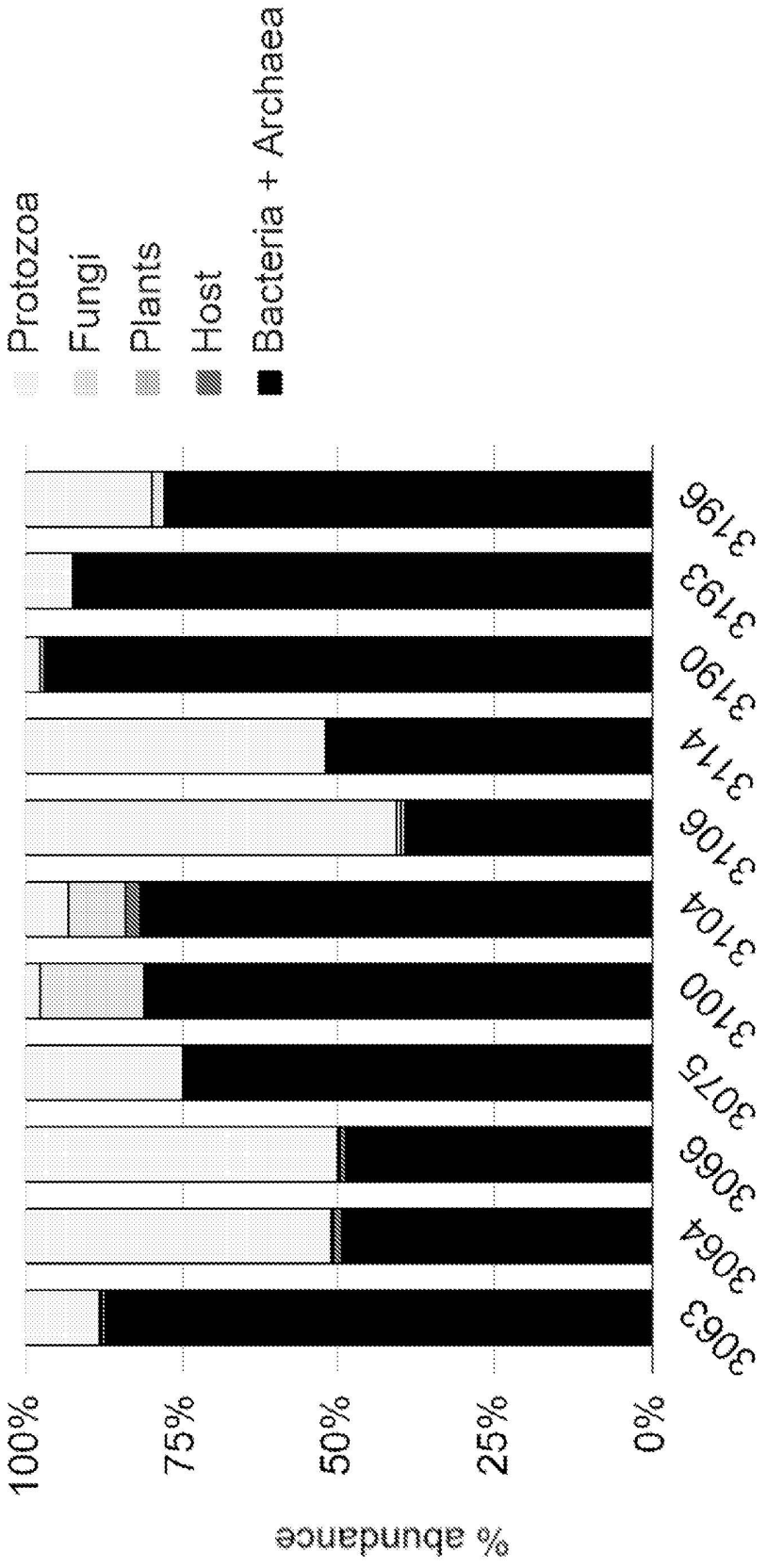
Protozoa
Fungi
Plants
Host
Bacteria + Archaea
100%
75%
50%
25%
0%
% abundance
3063
3064
3066
3075
3100
3104
3106
3114
3190
3193
3196

FIG. 18

		3063		3064		3066		3075		3100		3104		3106		3114		3190		3193		3196	
		M	MB	M	MB	M	MB	M	MB	M	MB	M	MB	M	MB	M	MB	M	MB	M	MB	M	MB
Helminths	*Oesophogostomum*	0	0%	1	0%	0	0%	0	0%	2	0%	0	0%	2	0%	0	0%	0	0%	0	0%	0	0%
	Ascarid	54	0%	81	0%	0	0%	0	0%	0	0%	0	0%	0	0%	0	0%	0	0%	0	0%	0	0%
	Trichuris	0	0%	17	0%	0	0%	0	0%	7	0%	0	0%	17	0%	16	0%	26	0%	0	0%	0	0%
	Hookworm	16	0%	0	0%	0	0%	0	0%	11	0%	1	0%	0	0%	0	0%	0	0%	0	0%	0	0%
	Strongyloides	0	0%	0	0%	0	0%	0	0%	0	0%	9	0%	1	0%	0	0%	0	0%	0	0%	0	0%
	Helminth richness	2	0	3	0	0	0	0	0	3	0	1	0	3	0	1	0	1	0	0	0	0	0

Detected by microscopy only Not detected

FIG. 19A

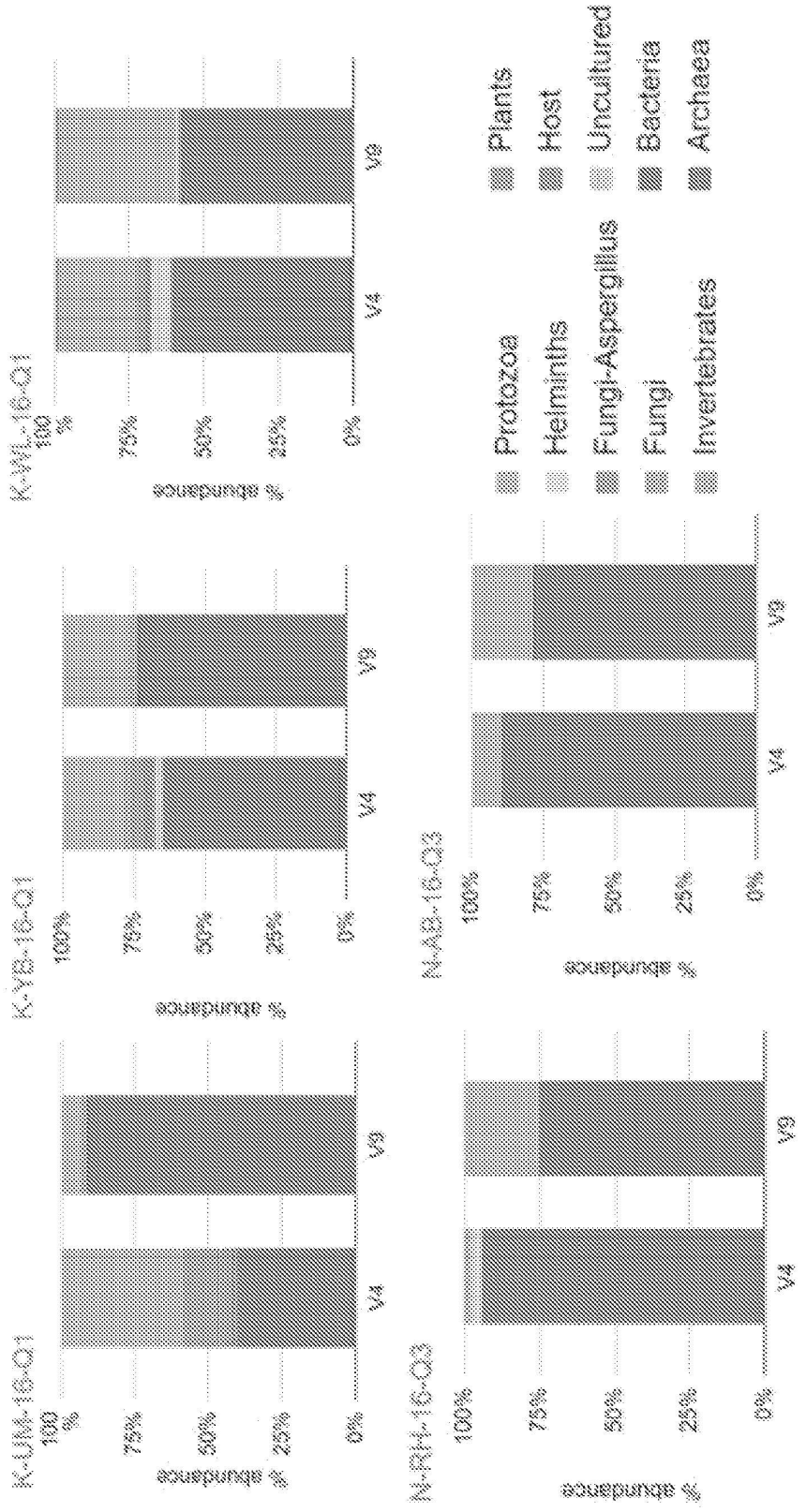
K-WL-16-Q1
K-YB-16-Q1
K-UM-16-Q1
N-AB-16-Q3
N-RH-16-Q3
% abundance
100%
75%
50%
25%
0%
V4
V9
Protozoa
Helminths
Fungi-Aspergillus
Fungi
Invertebrates
Plants
Host
Uncultured
Bacteria
Archaea

FIG. 19B

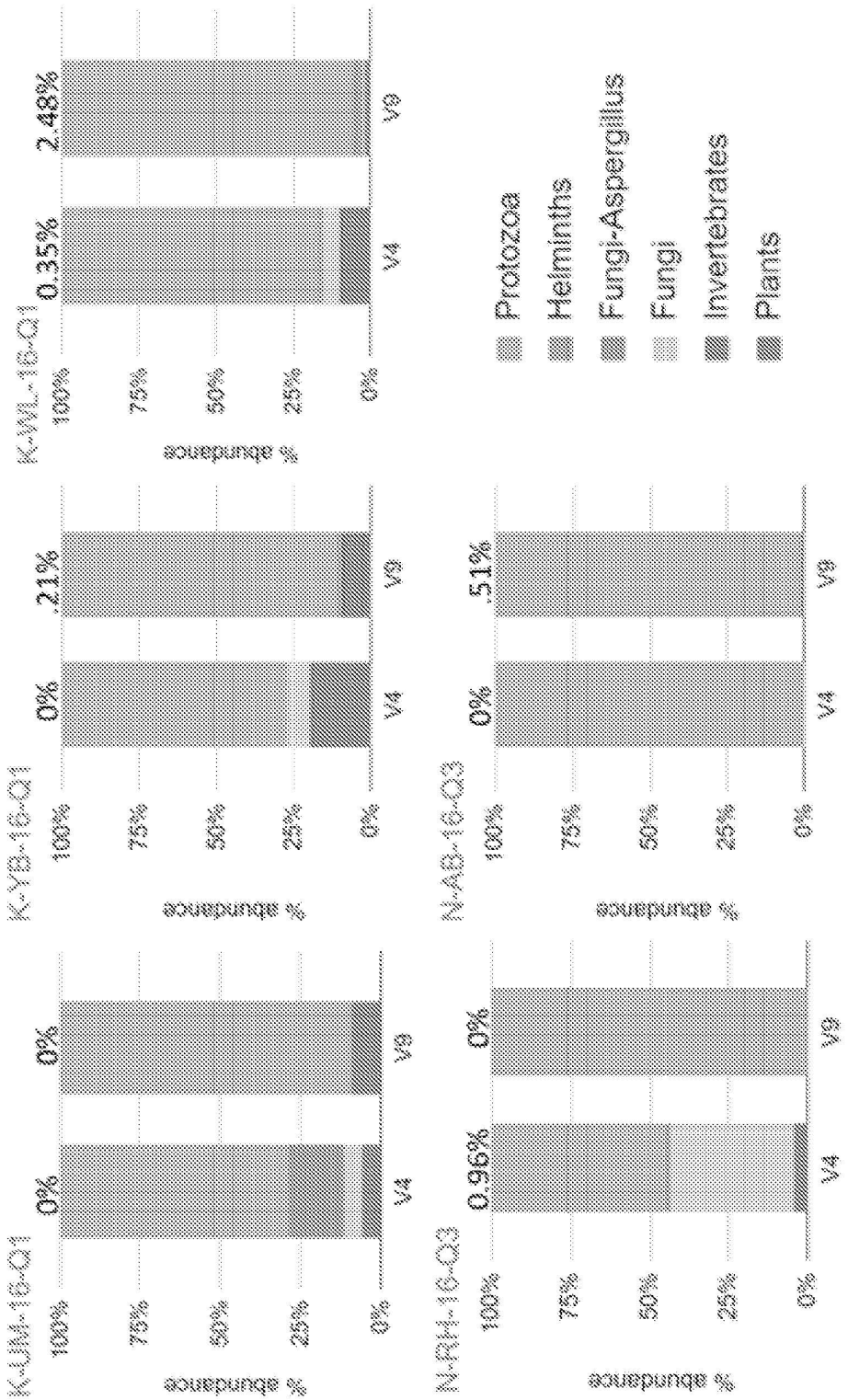
K-WL-16-Q1
0.35%
2.48%
V4
V9
% abundance
100%
75%
50%
25%
0%
Protozoa
Helminths
Fungi-Aspergillus
Fungi
Invertebrates
Plants
K-YB-16-Q1
0%
.21%
N-AB-16-Q3
0%
.51%
K-UM-16-Q1
0%
0%
N-RH-16-Q3
0.96%
0%